University of Ulm
Institute of Neurology
Prof. Dr. med. Albert C. Ludolph

Characterisation of Mutations in the Dynactin p150 Subunit in Primary Motor Neurons and Cell-lines

Dissertation
for obtaining the doctoral degree (Dr. med.)
of the Medical Faculty of the University of Ulm

submitted by
Marie Meyer-Ohlendorf
from Eckernförde, Schleswig Holstein
2011

Incumbent Dean	**: Prof. Dr. rer. nat. Thomas Wirth**
1st Correspondent	**: Prof. Dr. med. Albert C. Ludolph**
2nd Correspondent	**: Prof. Dr. med. Tobias M. Böckers**
Day of the Dissertation	**: 08.02.2013**

This thesis is dedicated to my beloved grandmother Gisela Meyer-Ohlendorf, who passed away when I was fourteen years old, because she had suffered from ALS. Her tragic illness made me aware of this dreadful disease and showed me that so far the disease has not been understood and lots of work has to be done before someday maybe a cure will be found.

Table of contents

Table of contents I

Index of abbreviations III

1. Introduction 1

1.1. Amyotrophic lateral sclerosis ... 1

1.2. Dynactin and its function ... 2

1.3. Dynactin as a risk factor or disease causing gene ... 9

1.4. Clinical phenotypes of patients carrying chosen p150 mutations ... 12

1.5. Aim of the thesis ... 16

2. Material and Methods 17

2.1. Materials ... 17

2.2. Cell culture ... 19

2.3. Protein Biochemistry ... 24

2.4. Immunecytochemistry ... 30

2.5. Microbiological methods ... 32

2.6. Molecular biological methods ... 34

3. Results 38

3.1. Establishment of primary motor neuron cultures ... 38

3.2. Morphological studies of the p150 mutations in cell lines ... 44

3.3. Over expression of mutated p150 in motor neurons ... 53

3.4. Impact of p150 mutations on other subcellular components in Cos-7 cells ... 58

3.5. Transgenic mouse models ... 82

4. Discussion 83

4.1. Establishment of primary motor neurons ... 83

4.2. Significance of four mutations in the p150 subunit of dynactin ... 83

4.3. Expression pattern of four mutations in p150 in cell lines ... 84

4.4. Comparability of the expression in primary motor neurons ... 90

4.5. The effect of p150 mutations on the cytoskeleton and important organelles ... 91

4.6. The effect of p150 mutations on the dynein/dynactin complex ... 94

4.7. The effect of p150 mutations on nuclear proteins ... 96

4.8. Transgenic mouse models ... 97

4.9. Conclusions 97
5. Summary **105**
6. References **107**
Acknowledgements **117**
Curriculum vitae **118**

Index of abbreviations

aa	amino acid
Acr-Bis-Sol.	Acrylamide-Bis-Solution
ALS	amyotrophic lateral sclerosis
ANG	angiogenin
APS	ammoniumperoxidisulfate
Arg	arginine
Arp	actin related protein
Asp	aspartic acid
BDNF	brain derived neurotrophic factor
BICD	bicaudal D
bidest H_2O	twice distilled water
bp	base pairs
BSA	albumin from bovine serum
Ca	calcium
Cra	Cramping
Cap-Gly	cytoskeleton-associated protein, glycine-rich
cDNA	coding deoxyribonucleic acid
ch	chicken
CLIP-170	cytoplasmic linker protein 170
Cos-7	*Cercopithecus aethiops, origin-defective SV-40,* kidney fibroblasts from African green monkey
Cys	cysteine
Dapi	4',6-diamidino-2-phenylindole
DCTN1	Dynactin gene 1
DIV	days in vitro
DMEM	Dulbecco's Modified Eagle Medium
DMSO	dimethylsulfoxid
DNA	deoxyribonucleic acid
DNAse	deoxyribonuclease
DSMZ	Deutsche Sammlung für Mikroorganismen und

	Zellkutur
DTT	DL-Dithiothreitol
E14	embryonic day 14
EB1	end binding 1
Eg5	kinesin family motor Eg5
ECL	enhanced chemiluminescent reagent
EDTA	ethylenediaminettraacetic acid
ER	endoplasmatic reticulum
Erk	extracellular signal-regulated kinase
FBS	fetal bovine serum
FTLD	fronto temporal lobar degeneration
FTD	fronto temporal dementia
FUS	fused in liposarcoma
GFAP	glial fibrillary associated protein
Gln	glutamine
Gly	glycine
gt	goat
h	hour
HBSS--	Hank's buffered salt solution without calcium and magnesium
HBSS++	Hank's buffered salt solution with calcium and magnesium
HC	heavy chain
HeLa	Henriette Lacks cells (Cell-line of a cervix carcinoma)
HEPES	(4-(2-hydroxyethyl)-1-piperazineethanesulfonic acid
HPV	human papillomavirus
HRP	horseradish peroxidase
IC	intermediate chain
Ile	isoleucine

kb	kilo bases
kDa	Kilodalton
Leu	leucine
Loa	Legs at odd angle
m	mouse
MAP	microtubule associated proteins
MEM	Modified Eagle Medium
Met	methionine
Mg	magnesium
min	minute
NaCl	sodium chloride
NEAA	non essential amino acids
NF-H	neurofilament heavy
NF-κB	nuclear factor kappa B
NGF	nerve growth factor
NT-3/4	neurotrophin 3/4
nt	nucleotide
OD	optical density
o.n.	over night
PAA	polyacrylamide
PAGE	polyacrylamide gel electrophoresis
PBP	progressive bulbar palsy
PBS	phosphate buffered saline
PBS--	phosphate buffered saline without calcium and magnesium
PBS++	phosphate buffered saline with calcium and magnesium
PCR	polymerase chain reaction
PFA	paraformaldehyd

PLS	primary lateral sclerosis
PMA	progressive muscle atrophy
Pro	proline
ProSAP	proline rich synapse associated protein
PSD	post synaptic density
PVDF	polyvinylidendifluorid
p50	dynamitin
rb	rabbit
RFP	red fluorescent protein
RNA	ribonucleic acid
rpm	rounds per minute
RT	room temperature
sALS	sporadic ALS
SDS	sodium dodecylsulfate
Ser	serine
shRNA	Short hairpin ribonucleic acid
SNP	single nucleotide polymorphism
SOD1	superoxide dismutase 1
TAE	tris-acetat-EDTA-buffer
TARDBP-43/TDP-43	transactive responsive (TAR) DNA binding protein
TEMED	N,N,N',N'-tetramethylethylendiamin
Thr	threonine
TLS	translated in liposarcoma
Tris	tris-hydroxymethyl-aminomethan
Trp	tryptophan
UV	ultra violet
V	volt
VAPB	vesical associated membrane protein B (VAMP-B)

1. Introduction

1.1. Amyotrophic lateral sclerosis

Motor neuron disease (MND), known in many countries as Amyotrophic lateral sclerosis (ALS), is the most common adult onset disorder of motor neurons with an incidence of 1-3 per 100,000 per year [82]. ALS is a progressive and fatal neurodegenerative disease. It is characterized by degeneration of lower motor neuron groups in the spinal cord and brain stem and of upper motor neurons in the motor cortex alike, which results in muscle paralysis [8, 82].

Patients suffering from MND typically develop a combination of upper and lower motor neuron signs, which starts with progressive muscle weakness and wasting with pathologically brisk reflexes, eventually involving the limb and bulbar muscles [82]. There are several clinically distinguishable variants, which are characterized by the initial site of symptoms. The progressive muscular atrophy variant (PMA) initially affects only the spinal lower motor neurons, whereas the primary lateral sclerosis variant (PLS) initially affects the upper motor neurons. Finally, the progressive bulbar palsy variant (PBP) primary impacts the bulbar musculature only [82].

ALS is a disease with an average onset between the fifth and the sixth decade of life [63], but very rare juvenile onset forms do exist [82]. Affected people usually die within three to five years from the onset of symptoms from suffocation and pneumonia because of respiratory failure [2]. Men are more commonly affected from MND than women with a male to female ratio of approximately 1.6/1 [82].

ALS is a clinically and genetically heterogeneous disease, that can be divided into sporadic ALS (sALS), which makes up 90 to 95 % of the cases, and familial ALS (fALS), which makes up the remaining 5-10 % of cases and usually presents with an autosomal dominant inheritance [67, 87].

The aetiology and the pathogenesis of most of the ALS cases remain unknown, but there are a number of proposed mechanisms including oxidative damage, aberrant RNA metabolism, viral mechanisms, glutamate excitotoxicity, autoimmune or metabolic defects, mitochondrial dysfunction, toxic, or apoptotic processes, protein misfolding, growth factor deficiency, glial cell pathology, or altered axonal transport [42, 78].

For the more uncommon familial form, several sequence changes in different candidate genes have been accounted for causing the disease. For instance, the

first example was the discovery of mutations in the superoxide dismutase1 (SOD1) gene [76], that account for 20-25 % of all familial cases and also for some of the sporadic cases [4, 34, 67]. Recent studies have also revealed a number of sequence changes in genes that cause autosomal dominantly inherited forms of clinically typical ALS, which include the TAR DNA binding protein-43 (TARDP/TDP 43) [64, 85], the angiogenin (ANG) [25], and the fused in sarcoma/ translated in liposarcoma protein (FUS/TLS) [43, 88], as well as the vesical associated membrane protein (VAMP-) associated protein B (VAPB) in atypical forms of ALS [63, 65].

TDP-43 is an ubiquitously expressed highly conserved nuclear protein that can also be found in ubiquitinated cytoplasmic and nuclear inclusions in ALS cases [64]. These features could not only be found in familial but also in sporadic ALS cases [37, 85]. FUS is described as functionally homologous to TDP43. Mutations in the FUS gene account for 4 % of all cases of familial ALS [13, 43, 63, 88].

Furthermore, in a family with slowly progressive autosomal dominant motor neuron disease without sensory symptoms, a missense mutation in the dynactin p150 subunit was found [70]. A mutation analysis showed a single base pair exchange, which lead to an amino acid substitution of serine for glycine at the position 59 (G59S). This base pair exchange was found in all affected family members. Missense mutations in the dynactin gene (DCTN1) encoding the p150 subunit of dynactin have been linked to both familial and sporadic ALS [47]. Subsequently, other mutations in the p150 subunit of dynactin have been detected [16, 62].

1.2. Dynactin and its function

Dynactin is a multi-subunit protein complex, that is required for most cytoplasmic dynein activity in eukaryotes and contributes to the activity of another microtubule-based motor, kinesin II [15, 81]. The dynactin molecule consists of eleven polypeptide subunits, that are assembled in a manner that an arm with two globular termini projects from a rod like structure, which makes up most of the mass of the molecule [81] *(Figure 01)*. This rod is composed of an octameric polymer of the Actin-related-protein 1 (Arp1), which resembles a short actin filament but is less dynamic than conventional actin [81]. As the Arp1 is capable of binding to beta III spectrin directly, which is a specialized isoform found as a component of the Golgi membrane [31], the association of Arp1 with the beta III

spectrin may be a general mechanism by which dynactin binds to sub cellular structures [81]. One end of the Arp1 rod terminates with another actin related protein, Arp11 [20] and the dynactin subunit p62 [80]. The Arp11 probably serves as a capping protein, that does not allow further subunit addition to the minus end of the Arp1 [81], whereas the p62, with a zinc-binding motif near the N-terminus, presumably participates in binding to Arp1, Arp11, other dynactin subunits, or to other sub cellular structures [81]. The opposite end of the Arp1 rod is capped by the conventional actin-capping protein, CapZ [80]. Moreover, the p62 subunit bears the two smallest dynactin subunits, p25 and p27, which also exist in a freely soluble pool in cells [81].

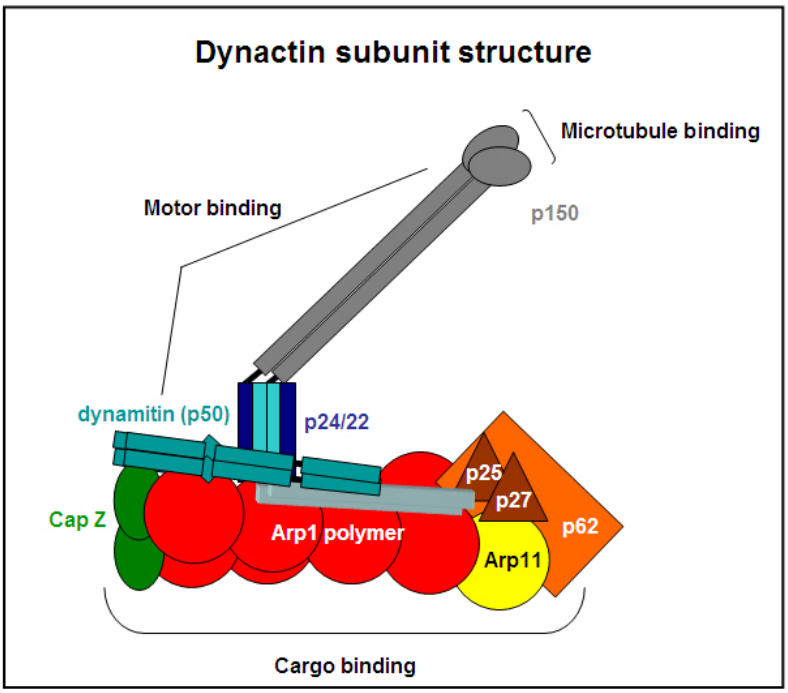

Fig. 01: Location and structural features of the dynactin subunits.

source: [81].
Arp: Actin related protein
The approximate location and structural features of the dynactin compound are shown in this illustration. It is consistent of eleven subunits that are depicted in various colours. The Arp1-polymer serves as a backbone of the whole structure and together with other subunits, which are further mentioned in the text, is responsible for the cargo binding. The p150 subunit is mainly responsible for the microtubule and the motor binding.

Projecting from the dynactin's Arp1 rod is an extending arm, which includes the three remaining dynactin subunits, the p150, dynamitin, and p24/22. Each dynactin molecule contains four copies of dynamitin and two copies of p150 and p24/22 [81]. The p150 subunit, which is the biggest of all dynactin subunits, provides the binding domains for microtubule binding and several others as well.

p150 contains three central coiled coil-domains, that are interspersed with regions of undefined structure [81]. There are two globular structures located at the very tip of the dynactin arm, that both contain a conserved cytoskeleton-associated protein, glycine rich (Cap-Gly) motif [75]. This Cap-Gly domain is located within the extreme N-terminus of the p150, expanding from amino acid 29-95 of the overall 1278 amino acids that make up the p150 subunit *(Figure 02 B)*.

A

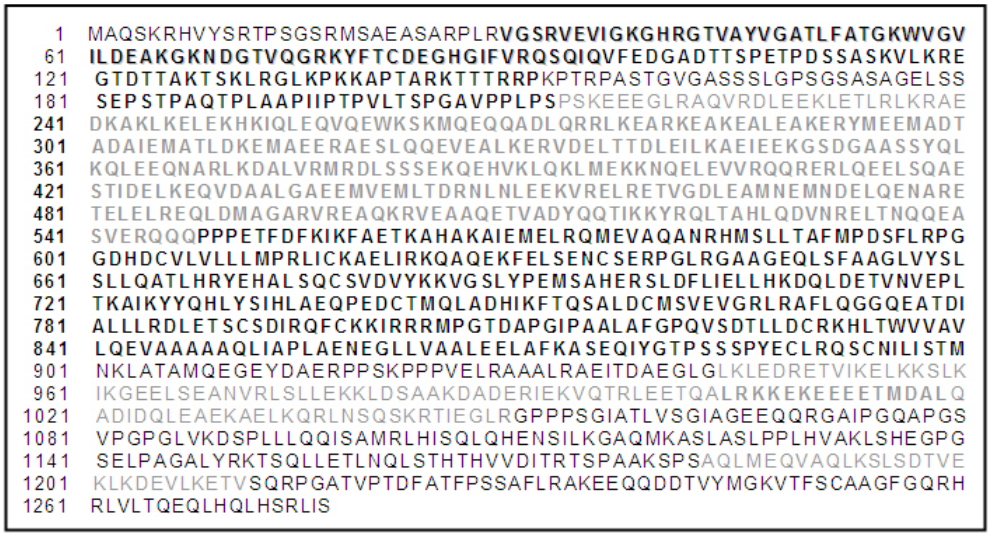

B

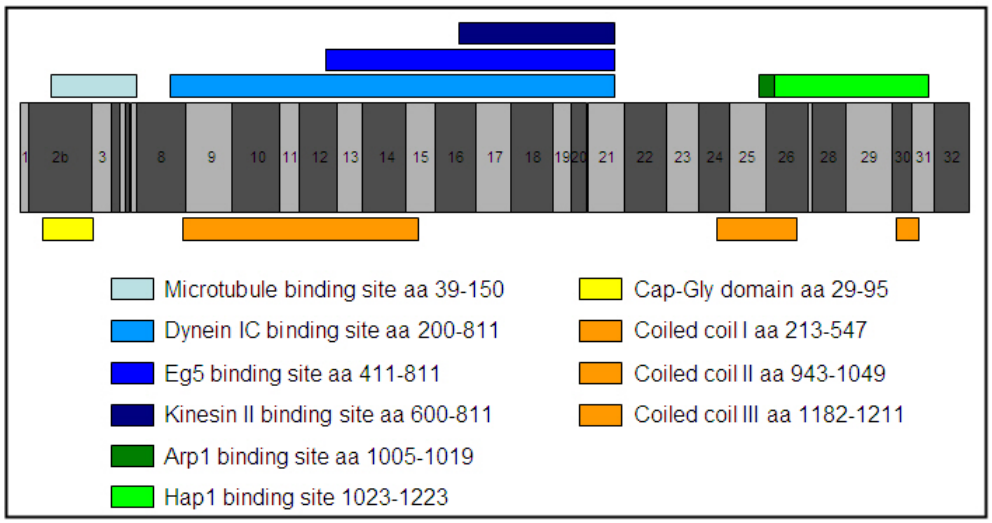

C

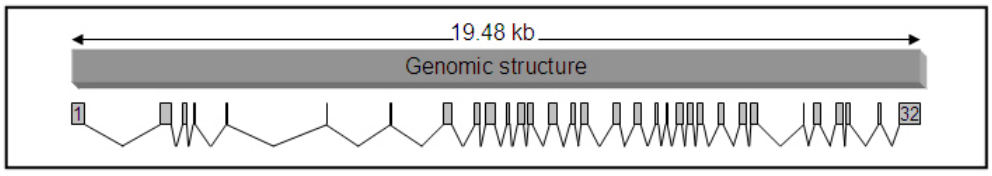

D

AGAGGCTAGCACGGTTCCTGACAAGTCTAGAGCAGCACTAGCGCAGAGTGAGACTCATCAGCTGGCAAGCAGGATTCTG
TGTCTCTGGGTTCAGGAATCCTCAGGCAGCAGAGGGGACTTGCTCCTCAGCCCCCATCACTGCCCCCACCCCTACCCGT
GTAGGCCACCGAGTGAGGCCCATGGACTGGGGAGGGCTGTGCCTGACGACTCCTGTGTCCCTCTATGAGGGCCCAGCG
CCCTGACCCTCCTGCCTAGGTTTCTACCTTTTCTCTCTGTCTTTGGCCAGCTGGGGGAGGGGGTAGAGGCCGGGTGAGC
AACATGGCACAGAGCAAGAGGCACGTGTACAGCCGGACGCCCAGCGGCAGCAGGATGAGTGCGGAGGCAAGCGCCCG
GCCTCTGCGGGTGGGCTCCCGTGTAGAGGTGATTGGAAAAGGCCACCGAGGCACTGTGGCCTATGTTGGAGCCACACTG
TTTGCCACTGGCAAATGGGTAGGCGTGATTCTGGATGAAGCAAAGGGCAAAAATGATGGAACTGTTCAAGGCAGGAAGTA
CTTCACTTGTGATGAAGGGCATGGCATCTTTGTGCGCCAGTCCCAGATCCAGGTATTTGAAGATGGAGCAGATACTACTTC
CCCAGAGACACCTGATTCTTCTGCTTCAAAAGTCCTCAAAAGAGAGGGAACTGATACAACTGCAAAGACTAGCAAACTGCG
GGGACTGAAGCCTAAGAAGGCACCGACAGCCCGAAAGACCACAACTCGGCGACCCAAGCCCACGCGCCCAGCCAGTAC
TGGGGTGGCTGGGGCCAGTAGCTCCCTGGGCCCCTCTGGCTCAGCGTCAGCAGGTGAGCTGAGCAGCAGTGAGCCCAG
CACCCCGGCTCAGACTCCGCTGGCAGCACCCATCATCCCCACGCCGGTCCTCACCTCTCCTGGAGCAGTCCCCCCGCTT
CCTTCCCCATCCAAGGAGGAGGAGGGACTAAGGGCTCAGGTGCGGGACCTGGAGGAGAAACTAGAGACCCTGAGACTG
AAACGGGCAGAAGACAAAGCAAAGCTAAAAGAGCTGGAGAAACACAAAATCCAGCTGGAGCAGGTGCAGGAATGGAAGA
GCAAAATGCAGGAGCAGCAGGCCGACCTGCAGCGGCGCCTCAAGGAGGCGAGAAAGGAAGCCAAGGAGGCGCTGGAG
GCAAAGGAACGCTATATGGAGGAGATGGCTGATACTGCTGATGCCATTGAGATGGCCACTTTGGACAAGGAGATGGCTGA
AGAGCGGGCTGAGTCCCTGCAGCAGGAGGTGGAGGCACTGAAGGAGCGGGTGGACGAGCTCACTACTGACTTAGAGAT
CCTCAAGGCTGAGATTGAAGAGAAGGGCTCAGATGGCGCTGCATCCAGTTATCAGCTCAAGCAGCTTGAGGAGCAGAAT
GCCCGCCTGAAGGATGCCCTGGTGAGGATGCGGGATCTTTCTTCCTCAGAGAAGCAGGAGCATGTGAAGCTCCAGAAGC
TCATGGAAAAGAAGAACCAAGAGCTGGAAGTTGTGAGGCAACAGCGGGAGCGTCTGCAGGAGGAGCTAAGCCAGGCAGA
GAGCACCATTGATGAGCTCAAGGAGCAGGTGGATGCTGCTCTGGGTGCTGAGGAGATGGTGGAGATGCTGACAGATCGG
AACCTGAATCTGGAAGAGAAAGTGCGCGAGTTGAGGGAGACTGTGGGAGACTTGGAAGCGATGAATGAGATGAACGATG
AGCTGCAGGAGAATGCACGTGAGACAGAACTGGAGCTGCGGGAGCAGCTGGACATGGCAGGCGCGCGGGTTCGTGAGG
CCCAGAAGCGTGTGGAGGCAGCCCAGGAGACGGTTGCAGACTACCAGCAGACCATCAAGAAGTACCGCCAGCTGACCG
CCCATCTACAGGATGTGAATCGGGAACTGACAAACCAGCAGGAAGCATCTGTGGAGAGGCAACAGCAGCCACCTCCAGA
GACCTTTGACTTCAAAATCAAGTTTGCTGAGACTAAGGCCCATGCCAAGGCAATTGAGATGGAATTGAGGCAGATGGAGG
TGGCCCAGGCCAATCGACACATGTCCCTGCTGACAGCCTTCATGCCTGACAGCTTCCTTCGGCCAGGTGGGGACCATGA
CTGCGTTCTGGTGCTGTTGCTCATGCCTCGTCTCATTTGCAAGGCAGAGCTGATCCGGAAGCAGGCCCAGGAGAAGTTTG
AACTAAGTGAGAACTGTTCAGAGCGGCCTGGGCTGCGAGGAGCTGCTGGGGAGCAACTCAGCTTTGCTGCTGGACTGGT
GTACTCGCTGAGCCTGCTGCAGGCCACGCTACACCGCTATGAGCATGCCCTCTCTCAGTGCAGTGTGGATGTGTATAAGA
AAGTGGGCAGCCTGTACCCTGAGATGAGTGCCCATGAGCGCTCCTTGGATTTCCTCATTGAACTGCTGCACAAGGATCAG
CTGGATGAGACTGTCAATGTGGAGCCTCTCACCAAGGCCATCAAGTACTATCAGCATCTGTACAGCATCCACCTTGCCGA
ACAGCCTGAGGACTGTACTATGCAGCTGGCTGACCACATTAAGTTCACGCAGAGTGCTCTGGACTGCATGAGTGTGGAGG
TAGGACGGCTGCGTGCCTTCTTGCAGGGTGGGCAGGAGGCTACAGATATTGCCCTCCTGCTCCGGGATCTGGAAACTTC
ATGCAGTGACATCCGCCAGTTCTGCAAGAAGATCCGAAGGCGAATGCCAGGGACAGATGCTCCTGGGATCCCAGCTGCA
CTGGCCTTTGGACCACAGGTATCTGACACGCTCCTAGACTGCAGGAAACACTTGACGTGGGTCGTGGCTGTGCTGCAGG
AGGTGGCAGCTGCTGCTGCCCAGCTCATTGCCCCACTGGCAGAGAATGAGGGGCTACTTGTGGCTGCTCTGGAGGAACT
GGCTTTCAAAGCAAGCGAGCAGATCTATGGGACCCCCTCCAGCAGCCCCTATGAGTGTCTGCGCCAGTCATGCAACATCC
TCATCAGTACCATGAACAAGCTGGCCACAGCCATGCAGGAGGGGGAGTATGATGCAGAGCGGCCCCCCAGCAAGCCTCC
ACCGGTTGAACTGCGGGCTGCTGCCCTTCGTGCAGAGATCACAGATGCTGAAGGCCTGGGTTTGAAGCTCGAAGATCGA
GAGACAGTTATTAAGGAGTTGAAGAAGTCACTCAAGATTAAGGGAGAGGAGCTAAGTGAGGCCAATGTGCGGCTGAGCCT
CCTGGAGAAGAAGTTGGACAGTGCTGCCAAGGATGCAGATGAGCGCATCGAGAAAGTCCAGACTCGGCTGGAGGAGACC
CAGGCACTGCTGCGAAAGAAGGAGAAAGAGTTTGAGGAGACAATGGATGCACTCCAGGCTGACATCGACCAGCTGGAGG
CAGAGAAGGCAGAACTAAAGCAGCGTCTGAACAGCCAGTCCAAACGCACGATTGAGGGACTCCGGGGCCCTCCTCCTTC
AGGCATTGCTACTCTGGTCTCTGGCATTGCTGGTGAAGAACAGCAGCGAGGAGCCATCCCTGGGCAGGCTCCAGGGTCT
GTGCCAGGCCCAGGGCTGGTGAAGGACTCACCACTGCTGCTTCAGCAGATCTCTGCCATGAGGCTGCACATCTCCCAGC
TCCAGCATGAGAACAGCATCCTCAAGGGAGCCCAGATGAAGGCATCCTTGGCATCCCTGCCCCCTCTGCATGTTGCAAAG
CTATCCCATGAGGGCCCTGGCAGTGAGTTACCAGCTGGAGCGCTGTATCGTAAGACCAGCCAGCTGCTGGAGACATTGA
ATCAATTGAGCACACACACGCACGTAGTAGACATCACTCGCACCAGCCCTGCTGCCAAGAGCCCGTCGGCCCAACTTATG
GAGCAAGTGGCTCAGCTTAAGTCCCTGAGTGACACCGTCGAGAAGCTCAAGGATGAGGTCCTCAAGGAGACAGTATCTCA
GCGCCCTGGAGCCACAGTACCCACTGACTTTGCCACCTTCCCTTCATCAGCCTTCCTCAGGGCCAAGGAGGAGCAGCAG
GATGACACAGTCTACATGGGCAAAGTGACCTTCTCATGTGCGGCTGGTTTTGGACAGCGACACCGGCTGGTGCTGACCCA
GGAGCAGCTGCACCAGCTTCACAGTCGCCTCATCTCCTAAGCACTCCTTTCCCCTGCTGTCCCCTTCGACCCTCAGCCCT
CTGGTGCCGCTCTGCCCGATGCACAGCCACCTCAGCCAGCCCCCAGGTAGAAACGTGGGTTAAGCTCTTCCTGCCCCGT
TCAGCTTCACTCCCACCCTTTCAGCGTCCTGCCCCTTCACCTTGACCCGGGTTCCCCCACTCCCATTCCCTGGCCTCTGC
CATAATTTGTTGTTCAACTGCTCCCTCCTTCCTGAGGGGCCTCAGGGCTTGTGGGGGGTAGGCTGAGACCCCACCACCAA
AGGTTAAGTGAGGTCCCCTTGATTGAGGACTTCACCCCTTGATTAAAGCAACTTCTGCTTCAGTGC

Fig. 02: Structure of the dynactin p150 subunit

aa: amino acid
Arp1: Actin related protein 1
bp: base pairs
Cap-Gly: cytoskeleton associated protein, Glycine rich
IC: intermediate chain
Hap1: Huntingtin-associated protein 1
(A) Amino acid sequence of dynactin p150 from human. Dynactin p150 is a 1278 aa long protein and characterized by three central coiled-coil domains, all depicted in grey letters (aa 213-547, aa 943-1049, aa 1182-1211), an N-terminal Cap-Gly domain, depicted in bold and shaded letters (aa 29-95), and a microtubule binding domain, (aa 39-150). The interaction domains include a dynein IC -, (aa 200-811), an Eb5- (aa 410-811), a kinesin II-(aa 600-811), an Arp1-, (aa 1005-1019), and a Hap1 binding site (1023-1223) (B) Dynactin p150 consists of several binding domains, all of which are shown as coloured bars. The coiled coil domains and the Cap-Gly domain are depicted in bars underneath the illustration. (C) Chromosomal organisation of dynactin p150 on human chromosome 2 (2p13). A 19486bp long chromosomal stretch is coding for 32 dynactin p150 exons. The start codon is localized in exon 1, the stop codon is found in exon 32. (D) Nucleotide sequence of dynactin p150 stretching from exon 1-32, which are shown in alternating grey and black letters. The non coding regions before the start codon and after the stop codon are depicted in light green.

The Cap-Gly domain plays a very important role in dynactin function as N-terminal fragments of p150 bind microtubules in vitro [94], as well as in vivo [91]. In addition to this Cap-Gly domain, a segment of basic amino acids, which directly follow the Cap-Gly domain C-terminal, has been described as a second lower affinity microtubule binding site. It has been described to stretch from amino acid 116-145 [92] respectively from amino acid 39-150 by Schroer et al. [81]. This basic domain of dynactin moves progressively along microtubules, a form of one-dimensional diffusion along the microtubules, even in the absence of molecular motors [92]. Dynein processivity is increased fourfold by this process, whereas the Cap-Gly domain rather inhibits dynein motility and remains firmly attached to a single point on microtubules [14]. The ability of binding to microtubules is necessary for enhancing the processivity of the dynein motor [40], which itself binds to the p150 with its intermediate chains presenting as specific and high affinity interaction partners [90]. The enhancement of dynein processivity is needed for the long-range dynein-based movement in neurons; as such humans, who carry a mutant form of dynactin p150, suffer from motor neuron disease [70]. In addition, it was investigated that the Cap-Gly domain may contribute to microtubule minus end anchoring at interphase centrosomes [72, 73] and mitotic spindle poles [23]. Moreover, the Cap-Gly domain of the p150 subunit is capable of binding to other microtubule binding proteins such as end binding 1 (EB1) and cytoplasmic linker protein-170 (CLIP-170) [1, 5, 9, 56, 95].

The binding domains for microtubule-based motors like dynein lie somewhere in the middle portion of the p150 subunit with the binding domain of the dynein intermediate chain stretching out approximately from amino acid 200-811 [91]. Other solution binding studies between the p150 subunit and an N-terminal fragment of the dynein intermediate chain have revealed a strong interaction reaching from amino acid 150-811 [39, 50]. The binding domain for the kinesin family motor Eg5 spreads from amino acid 410-811 [6], whereas the binding domain for kinesin II reaches from amino acid 600-811 [15]. These findings suggest that p150 may provide several overlapping binding sites for various microtubule based motor proteins [81].

But not only does the p150 provide binding sites for motor proteins, it also contains a conserved actin-binding motif that has been proposed to bind the Arp1 filament directly [94].

Furthermore, the C-terminal region, specifically amino acid 1023-1223 of p150, has been detected to interact with the huntingtin-associated protein (HAP-1) [21, 52]. Also, interaction between the C-terminus of p150 and p25 has been reported [66].

The dynactin subunit p150 is encoded by the DCTN1 gene, which is located on chromosome 2p13. It consists of 32 exons and 31 introns and is composed of 19.48 kilo bases (kb) *(Figure 02 C)*.

The dynactin subunit dynamitin (p50) plays an important role in dynactin structure and stability. It connects the two functional structures of dynactin, the p150 subunit and the Arp1 rod [81]. It can interact with p150 and p24/22 [20, 38]. Free excessive dynamitin causes the dynactin complex to be disrupted and to disconnect the p150 and p22/24 subunits from the rest of the complex [10, 20, 38].

p24/22, one of the smallest subunits of the dynactin complex, binds dynamitin directly and may also interact with p150 as both proteins are released from the whole complex by excess of dynamitin [20, 38].

Dynactin is present in the cell at many locations. At centrosomes and spindle pole bodies, dynactin is proposed to contribute to microtubule anchoring [72]. It has also been detected at microtubule plus ends, where it might control microtubule dynamics and the recruitment of other structures. Furthermore, dynactin can be detected on various endomembranes of endocytotic organelles, membranes in the Golgi region [26], or at some time point of the cell cycle also on the nuclear envelope [79]. Although, at all these different locations, dynactin may administrate slightly different functions, it is believed that in all cases dynactin serves in some way in enhancing, recruiting, or targeting dynein. Cytoplasmic dynein is the most important minus end directed microtubule motor protein in the cell. This multi-subunit protein, which is set up of at least six protein subunits, can only accomplish its function as motor protein in the interaction with the dynactin complex. Cytoplasmic dynein is composed of two heavy chains, that bind to microtubules and enable dynein to move in an ATP dependent manner [24], two intermediate chains, that are thought to be able to bind to dynactin p150 and anchor it to its cargo, four light intermediate chains and several light chains, which are defined and named by their molecular mass [3, 69]. The intermediate chains, light intermediate chains, and light chains are believed to maintain the stability of

the complex, modulate its activity, and interact with dynein's cargo proteins [3]. Dynactin increases the average length of cytoplasmic dynein-driven movements without affecting the velocity or microtubule-stimulated ATPase kinetics of cytoplasmic dynein [40]. Since dynein is capable of binding other cellular components by itself or other linker proteins, dynactin may not absolutely be necessary for targeting dynein to binding sites [81]. However, an intact dynactin complex and not just free p150 is required for survival of organisms [81]. Therefore, dynactin probably has a more complex function than just binding dynein and enhancing the motor processivity. It is very likely to provide another docking site in form of the Arp1 rod and therefore stabilise the interaction of the cargo with dynein [81]. Because of these complex tasks of dynein, motor neurons are most vulnerable to defects in dynein function [27].

Cells, in which microtubules are organised centripetal, or in cells with more complex microtubule arrangements like neurons, the movement of organelles or other sub-cellular structures relies on cytoplasmic dynein. This movement is then centripetal or minus- end directed, meaning retrograde in axons [81]. In these processes, dynactin always contributes by enhancing the processivity of the dynein motor and by providing a further docking site as described earlier. These binding and recruiting processes are assisted by a number of factors like beta III spectrin, via which dynactin binds to Golgi membranes [31]. The binding of both dynein and dynactin may furthermore be regulated by Rab6 and bicaudal D (BICD) [59]. Rab6 interacts with p150 [83], whereas BICD contains binding sites for both, dynein and the dynactin subunit dynamitin [32, 33].

Also the movement of mitochondria seems to be dynein/dynactin dependent, as the over-expression of dynamitin, which leads to disruption of the dynactin complex, blocks the sporadic movement of mitochondria [19].

Dynactin is thus required for various functions in the cell such as cytoplasmic organization like ER-to Golgi trafficking and sub-cellular motility at all stages of the cell cycle, including endosome and lysosome motility, spindle assembly, and retrograde axonal transport in post mitotic neurons. There it provides the link between the specific cargo, the microtubule, and cytoplasmic dynein. This provides an idea of how important the functional intact dynactin complex is to survival of any cell and how even a slight dysfunction may wreak havoc to the cell.

1.3. Dynactin as a risk factor or disease causing gene

Mutations in different motors, which are required in axonal transport, like dynein, kinesin or dynactin, are clearly sufficient to cause motor neuron degeneration [11]. But it is still unclear, whether defects in axonal transport are causative or rather contributory factors to ALS. As neurons, especially motor neurons, being cells with tremendous long extended processes compared to other cells, they are particularly vulnerable to defects in active transport. This leads to the assumption that mutations in motor proteins, especially in the motor protein enhancer dynactin, may cause or contribute to the development of ALS. This assumption derives from several described mutations in patients, which were found in the p150 subunit of dynactin.

The G59S mutation lowers the affinity of p150 to microtubules and cells from affected patients show features of disruption of dynein/dynactin function [51], which also results in the formation of large scale aggregates in patient motor neurons [71]. The structure of the Cap-Gly domain, in which the G59S mutation is located, suggests that the introduction of the mutation induces a conformational change leading to an enhanced tendency for the polypeptide to misfold and aggregate [12].

Other heterozygous missense mutations (T1249I, M571T, R785W) in patients with both sporadic and familial ALS were found [62]. Furthermore, a heterozygous mutation in the dynactin gene (R1101K) was identified in a family with both ALS and frontotemporal dementia (FTD) with an autosomal dominant pattern of inheritance [61]. Five disease-segregating mutations affecting the Cap-Gly domain of dynactin were also found in eight families suffering from Perry syndrome, a disease previously known as a TDP-43 proteinopathy [22]. All of these mutations encoding G71R, G71E, G71A, T72P, and Q74P in exon 2 of DCTN1 were very closely located to the G59S mutation, that had been described to cause a slowly progressive autosomal dominant form of lower motor neuron disease leading to vocal fold paralysis, progressive facial weakness as well as weakness and muscle atrophy in the hands [70].

Based on the finding of the missense mutation (G59S) in the dynactin p150 subunit [70], a large screening effort of the 32 exons and 31 introns of the dynactin p150 gene was performed. Between the years of 2002 and 2007, from 1708 ALS/MND patients, 778 healthy controls and 318 neurological controls, such as

multiple sclerosis, parkinsonism, especially multiple system atrophy (MSA) and progressive supranuclear palsy (PSP) patients, and Chorea Huntington patients, blood was taken and examined for mutations in the DCTN1 gene. 23 exonic base pair exchanges were identified. These exchanges were single nucleotide polymorphisms (SNP) leading to an amino acid exchange. All amino acid exchanges were in highly conserved areas *(Table 01)*.

I will further refer to the SNPs as mutations, assuming that these SNPs are disease causing or risk factors for MND. Mutations are permanent sequence changes in the genetic constitution of a subject. Mutations refer to a single base pair exchange, which either lead to an amino acid exchange or remain silent. Furthermore, mutations are also defined as chromosomal changes or variations of the whole genome. Mutations can either occur in germ cells and therefore manifest in all body cells, or take place in an early stage of the embryonic development, leading to a manifestation in all somatic cells that develop from the originally mutated cell. If base pair changes occur with a statistical probability of more than 1 % in a population, one refers to the changes to polymorphisms. The exchange may either affect exonic or intronic sequences. A mutation, base pair exchange, or polymorphism does not necessarily lead to a disease or malfunction.

The ALS/MND patients were a collective of typical as well as atypical sporadic and familial ALS patients (Ludolph et al., unpublished). However, a number of sequence changes could also be detected in healthy controls (n=38) but for none of the mutations a clear co-segregation could be shown. But a number of sequence changes also were found only in ALS/MND patients (n=13) and the overall amount of sequence changes in ALS/MND patients exceeded the amount of sequence changes found in controls The difference between the occurrence of the mutations in patients and controls was statistically significant ($p < 0.01$).

Table 01: All 23 sequence changes found in MND patients

aa: amino acid
MND: motor neuron disease
AUS: Austria; D: Germany; ITL: Italy; PL: Poland; S: Sweden
The table shows 23 exonic sequence changes in the DCTN1 gene coding for the dynactin subunit p150, that have been discovered in MND patients, neurological controls, and healthy controls. Those sequence changes, which were focused on in this thesis, are depicted in red. Altogether, a collective of 1708 MND patients, 778 healthy and 318 neurological controls have been included in investigation. The percentages of mutations found relatively to all MND patients, all neurological or healthy controls are given next to the absolute number detected. The mutations, which have only been found in MND patients, are highlighted in blue.

Exon	aa-position and exchange	MND (n110 out of 1708) 6.44%	Neurological controls (n19 out of 318) 5.97%	Healthy controls (n38 out of 778) 4.88%	Affected domain	Origin
2	**Gly 34 Gln**	**1 (0.06%)**	**-**	**1 (0.13%)**	**Cap-Gly**	**D**
2	**Asp 63 Tyr**	**1 (0.06%)**	**-**	**-**	**Cap-Gly, microtub. binding**	**D**
7	Arg 148 Trp	1 (0.06%)	-	-	microtub. binding	S
7	Arg 149 Gln	1 (0.06%)	-	-	microtub.binding	S
8	Ser 157 Ile	1 (0.06%)	-	1 (0. 31%)	-	D
8	Ser 174 Ile	-	-	1 (0.13%)	-	D
8	**Ile 196 Val**	**18 (1.05%)**	**6 (1.89%)**	**5 (0.64%)**	**-**	**S,D,PL,AUS**
8	Arg 238 Trp	-	1 (0.31%)	-	coiled coil I, dynein IC	D
10	Asp 333 Gly	3 (0.18%)	-	3 (0.39%)	dynein IC	S,D
14	Arg 495 Gln	51 (2.99%)	4 (1.26%)	15 (1.93%)	dynein IC, Eg5	S,D,PL,AUS
15	Arg 532 Leu	-	1(0.31%)	-	dynein IC, Eg5	D
16	Met 571 Thr	2 (0.12%)	-	-	dynein IC, Eg5	D
19	Gly 737 Gln	-	-	1 (0.13%)	dynein IC, Eg5, kinesin2	D
20	Met 760 Val	1 (0.06%)	-	-	dynein IC, Eg5, kinesin2	D
21	Ile 780 Leu	2 (0.12%)	-	-	dynein IC, Eg5, kinesin2	S
21	Arp 785 Trp	2 (0.12%)	-	-	dynein IC, Eg5, kinesin2	D
21	Pro 811 Arg	-	1 (0.31%)	-	dynein IC, Eg5, kinesin2	D
23	Tyr 878 Cys	1 (0.06%)	-	-	-	D
26	Lys 1008 Gly	1 (0.06%)	-	-	coiled coil II, Arp1	D
26	**Arg 1049 Gln**	**5 (0.29%)**	**1 (0.31%)**	**6 (0.77%)**	**coiled coil II, Hap1**	**S,D**
28	Arg 1101 Lys	3 (0.18%)	2 (0.62%)	-	Hap1	D
29	Pro 1144 Thr	1 (0.06%)	-	-	Hap1	D, ITLY
32	Thr 1249 Ile	14 (0.82%)	3 (0.94%)	5 (0.64%)	-	S,D

1.4. Clinical phenotypes of patients carrying chosen p150 mutations

Four mutations out of the 23 found were then selected, based on preliminary transfection studies in Cos-7 cells and frequency of occurrence *(Figure 03)*.

A

AGAGGCTAGCACGGTTCCTGACAAGTCTAGAGCAGCACTAGCGCAGAGTGAGACTCATCAGCTGGCAAGCAGGATTCTGT
GTCTCTGGGTTCAGGAATCCTCAGGCAGCAGAGGGGACTTGCTCCTCAGCCCCCATCACTGCCCCCACCCCTACCCGTGT
AGGCCACCGAGTGAGGCCCATGGACTGGGGAGGGCTGTGCCTGACGACTCCTGTGTCCCTCTATGAGGGCCCAGCGCCC
TGACCCTCCTGCCTAGGTTTCTACCTTTTCTCTCTGTCTTTGGCCAGCTGGGGGAGGGGGTAGAGGCCGGGTGAGCAACAT
GGCACAGAGCAAGAGGCACGTGTACAGCCGGACGCCCAGCGGCAGCAGGATGAGTGCGGAGGCAAGCGCCCGGCCTCT
GCGGGTGGGCTCCCGTGTAGAGGTGATTGGAAAAGGCCACCGAGGCACTGTGGCCTATGTTGGAGCCACACTGTTTGCCA
CTGGCAAATGGGTAGGCGTGATTCTGGATGAAGCAAAGGGCAAAAATGATGGAACTGTTCAAGGCAGGAAGTACTTCACTT
GTGATGAAGGGCATGGCATCTTTGTGCGCCAGTCCCAGATCCAGGTATTTGAAGATGGAGCAGATACTACTTCCCCAGAGA
CACCTGATTCTTCTGCTTCAAAAGTCCTCAAAAGAGAGGGAACTGATACAACTGCAAAGACTAGCAAACTGCGGGGACTGAA
GCCTAAGAAGGCACCGACAGCCCGAAAGACCACAACTCGGCGACCCAAGCCCACGCGCCCAGCCAGTACTGGGGTGGCT
GGGGCCAGTAGCTCCCTGGGCCCCTCTGGCTCAGCGTCAGCAGGTGAGCTGAGCAGCAGTGAGCCCAGCACCCCGGCTC
AGACTCCGCTGGCAGCACCCATCATCCCCACGCCGGTCCTCACCTCTCCTGGAGCAGTCCCCCCGCTTCCTTCCCCATCC
AAGGAGGAGGAGGGACTAAGGGCTCAGGTGCGGGACCTGGAGGAGAAACTAGAGACCCTGAGACTGAAACGGGCAGAAG
ACAAAGCAAAGCTAAAAGAGCTGGAGAAACACAAAATCCAGCTGGAGCAGGTGCAGGAATGGAAGAGCAAAATGCAGGAG
CAGCAGGCCGACCTGCAGCGGCGCCTCAAGGAGGCGAGAAAGGAAGCCAAGGAGGCGCTGGAGGCAAAGGAAGAACGCTATA
TGGAGGAGATGGCTGATACTGCTGATGCCATTGAGATGGCCACTTTGGACAAGGAGATGGCTGAAGAGCGGGCTGAGTCC
CTGCAGCAGGAGGTGGAGGCACTGAAGGAGCGGGTGGACGAGCTCACTACTGACTTAGAGATCCTCAAGGCTGAGATTGA
AGAGAAGGGCTCAGATGGCGCTGCATCCAGTTATCAGCTCAAGCAGCTTGAGGAGCAGAATGCCCGCCTGAAGGATGCCC
TGGTGAGGATGCGGGATCTTTCTTCCTCAGAGAAGCAGGAGCATGTGAAGCTCCAGAAGCTCATGGAAAAGAAGAACCAAG
AGCTGGAAGTTGTGAGGCAACAGCGGGAGCGTCTGCAGGAGGAGCTAAGCCAGGCAGAGAGCACCATTGATGAGCTCAA
GGAGCAGGTGGATGCTGCTCTGGGTGCTGAGGAGATGGTGGAGATGCTGACAGATCGGAACCTGAATCTGGAAGAGAAAG
TGCGCGAGTTGAGGGAGACTGTGGGAGACTTGGAAGCGATGAATGAGATGAACGATGAGCTGCAGGAGAATGCACGTGAG
ACAGAACTGGAGCTGCGGGAGCAGCTGGACATGGCAGGCGCGCGGGTTCGTGAGGCCCAGAAGCGTGTGGAGGCAGCC
CAGGAGACGGTTGCAGACTACCAGCAGACCATCAAGAAGTACCGCCAGCTGACCGCCCATCTACAGGATGTGAATCGGGA
ACTGACAAACCAGCAGGAAGCATCTGTGGAGAGGCAACAGCAGCCACCTCCAGAGACCTTTGACTTCAAAATCAAGTTTGC
TGAGACTAAGGCCCATGCCAAGGCAATTGAGATGGAATTGAGGCAGATGGAGGTGGCCCAGGCCAATCGACACATGTCCC
TGCTGACAGCCTTCATGCCTGACAGCTTCCTTCGGCCAGGTGGGGACCATGACTGCGTTCTGGTGCTGTTGCTCATGCCTC
GTCTCATTTGCAAGGCAGAGCTGATCCGGAAGCAGGCCCAGGAGAAGTTTGAACTAAGTGAGAACTGTTCAGAGCGGCCT
GGGCTGCGAGGAGCTGCTGGGGAGCAACTCAGCTTTGCTGCTGGACTGGTGTACTCGCTGAGCCTGCTGCAGGCCACGC
TACACCGCTATGAGCATGCCCTCTCTCAGTGCAGTGTGGATGTGTATAAGAAAGTGGGCAGCCTGTACCCTGAGATGAGTG
CCCATGAGCGCTCCTTGGATTTCCTCATTGAACTGCTGCACAAGGATCAGCTGGATGAGACTGTCAATGTGGAGCCTCTCA
CCAAGGCCATCAAGTACTATCAGCATCTGTACAGCATCCACCTTGCCGAACAGCCTGAGGACTGTACTATGCAGCTGGCTG
ACCACATTAAGTTCACGCAGAGTGCTCTGGACTGCATGAGTGTGGAGGTAGGACGGCTGCGTGCCTTCTTGCAGGGTGGG
CAGGAGGCTACAGATATTGCCCTCCTGCTCCGGGATCTGGAAACTTCATGCAGTGACATCCGCCAGTTCTGCAAGAAGATC
CGAAGGCGAATGCCAGGGACAGATGCTCCTGGGATCCCAGCTGCACTGGCCTTTGGACCACAGGTATCTGACACGCTCCT
AGACTGCAGGAAACACTTGACGTGGGTCGTGGCTGTGCTGCAGGAGGTGGCAGCTGCTGCTGCCCAGCTCATTGCCCCAC
TGGCAGAGAATGAGGGGCTACTTGTGGCTGCTCTGGAGGAACTGGCTTTCAAAGCAAGCGAGCAGATCTATGGGACCCCC
TCCAGCAGCCCCTATGAGTGTCTGCGCCAGTCATGCAACATCCTCATCAGTACCATGAACAAGCTGGCCACAGCCATGCAG
GAGGGGGAGTATGATGCAGAGCGGCCCCCCAGCAAGCCTCCACCGGTTGAACTGCGGGCTGCTGCCCTTCGTGCAGAGA
TCACAGATGCTGAAGGCCTGGGTTTGAAGCTCGAAGATCGAGAGACAGTTATTAAGGAGTTGAAGAAGTCACTCAAGATTAA
GGGAGAGGAGCTAAGTGAGGCCAATGTGCGGCTGAGCCTCCTGGAGAAGAAGTTGGACAGTGCTGCCAAGGATGCAGAT
GAGCGCATCGAGAAAGTCCAGACTCGGCTGGAGGAGACCCAGGCACTGCTGCGAAAGAAGGAGAAAGAGTTTGAGGAGA
CAATGGATGCACTCCAGGCTGACATCGACCAGCTGGAGGCAGAGAAGGCAGAACTAAAGCAGCGTCTGAACAGCCAGTCC
AAACGCACGATTGAGGGACTCCGGGGCCCTCCTCCTTCAGGCATTGCTACTCTGGTCTCTGGCATTGCTGGTGAAGAACAG
CAGCGAGGAGCCATCCCTGGGCAGGCTCCAGGGTCTGTGCCAGGCCCAGGGCTGGTGAAGGACTCACCACTGCTGCTTC
AGCAGATCTCTGCCATGAGGCTGCACATCTCCCAGCTCCAGCATGAGAACAGCATCCTCAAGGGAGCCCAGATGAAGGCA
TCCTTGGCATCCCTGCCCCCTCTGCATGTTGCAAAGCTATCCCATGAGGGCCCTGGCAGTGAGTTACCAGCTGGAGCGCT
GTATCGTAAGACCAGCCAGCTGCTGGAGACATTGAATCAATTGAGCACACACACGCACGTAGTAGACATCACTCGCACCAG
CCCTGCTGCCAAGAGCCCGTCGGCCCAACTTATGGAGCAAGTGGCTCAGCTTAAGTCCCTGAGTGACACCGTCGAGAAGC
TCAAGGATGAGGTCCTCAAGGAGACAGTATCTCAGCGCCCTGGAGCCACAGTACCCACTGACTTTGCCACCTTCCCTTCAT
CAGCCTTCCTCAGGGCCAAGGAGGAGCAGCAGGATGACACAGTCTACATGGGCAAAGTGACCTTCTCATGTGCGGCTGGT
TTTGGACAGCGACACCGGCTGGTGCTGACCCAGGAGCAGCTGCACCAGCTTCACAGTCGCCTCATCTCCTAAGCACTCCTT
TCCCCTGCTGTCCCCTTCGACCCTCAGCCCTCTGGTGCCGCTCTGCCCGATGCACAGCCACCTCAGCCAGCCCCCAGGTA
GAAACGTGGGTTAAGCTCTTCCTGCCCCGTTCAGCTTCACTCCCACCCTTTCAGCGTCCTGCCCCTTCACCTTGACCCGGG
TTCCCCCACTCCCATTCCCTGGCCTCTGCCATAATTTGTTGTTCAACTGCTCCCTCCTTCCTGAGGGGCCTCAGGGCTTGTG
GGGGGTAGGCTGAGACCCCACCACCAAAGGTTAAGTGAGGTCCCCTTGATTGAGGACTTCACCCCTTGATTAAAGCAACTT
CTGCTTCAGTGC

B

```
   1 MAQSKRHVYSRTPSGSRMSAEASARPLRVGSRVEVIGKGHRGTVAYVGATLFATGKWVGV
  61 ILDEAKGKNDGTVQGRKYFTCDEGHGIFVRQSQIQVFEDGADTTSPETPDSSASKVLKRE
 121 GTDTTAKTSKLRGLKPKKAPTARKTTTRRPKPTRPASTGVGASSSLGPSGSASAGELSS
 181 SEPSTPAQTPLAAPIIPTPVLTSPGAVPPLPSPSKEEEGLRAQVRDLEEKLETLRLKRAE
 241 DKAKLKELEKHKIQLEQVQEWKSKMQEQQADLQRRLKEARKEAKEALEAKERYMEEMADT
 301 ADAIEMATLDKEMAEERAESLQQEVEALKERVDELTTDLEILKAEIEEKGSDGAASSYQL
 361 KQLEEQNARLKDALVRMRDLSSSEKQEHVKLQKLMEKKNQELEVVRQQRERLQEELSQAE
 421 STIDELKEQVDAALGAEEMVEMLTDRNLNLEEKVRELRETVGDLEAMNEMNDELQENARE
 481 TELELREQLDMAGARVREAQKRVEAAQETVADYQQTIKKYRQLTAHLQDVNRELTNQQEA
 541 SVERQQQPPPETFDFKIKFAETKAHAKAIEMELRQMEVAQANRHMSLLTAFMPDSFLRPG
 601 GDHDCVLVLLLMPRLICKAELIRKQAQEKFELSENCSERPGLRGAAGEQLSFAAGLVYSL
 661 SLLQATLHRYEHALSQCSVDVYKKVGSLYPEMSAHERSLDFLIELLHKDQLDETVNVEPL
 721 TKAIKYYQHLYSIHLAEQPEDCTMQLADHIKFTQSALDCMSVEVGRLRAFLQGGGQEATDI
 781 ALLLRDLETSCSDIRQFCKKIRRRMPGTDAPGIPAALAFGPQVSDTLLDCRKHLTWVVAV
 841 LQEVAAAAAQLIAPLAENEGLLVAALEELAFKASEQIYGTPSSSPYECLRQSCNILISTM
 901 NKLATAMQEGEYDAERPPSKPPPVELRAAALRAEITDAEGLGLKLEDRETVIKELKKSLK
 961 IKGEELSEANVRLSLLEKKLDSAAKDADERIEKVQTRLEETQALRKKEKEEEETMDALQ
1021 ADIDQLEAEKAELKQRLNSQSKRTIEGLRGPPPSGIATLVSGIAGEEQQRGAIPGQAPGS
1081 VPGPGLVKDSPLLLQQISAMRLHISQLQHENSILKGAQMKASLASLPPLHVAKLSHEGPG
1141 SELPAGALYRKTSQLLETLNQLSTHTHVVDITRTSPAAKSPSAQLMEQVAQLKSLSDTVE
1201 KLKDEVLKETVSQRPGATVPTDFATFPSSAFLRAKEEQQDDTVYMGKVTFSCAAGFGQRH
1261 RLVLTQEQLHQLHSRLIS
```

C

```
5'  ·····GCCACTGGCAAATGGGTAGGCGTGATTCTGGATGAAGCA····· 3'
    ·····GCCACTGGCAAATGGGTAAGCGTGATTCTGGATGAAGCA·····
WT      G  T  V  A  Y  V  G  A  T  L  F  A  T
G59S    G  T  V  A  Y  V  S  A  T  L  F  A  T
```

```
5'  ·····TGGGTAGGCGTGATTCTGGATGAAGCAAAGGGCAAAAAT····· 3'
    ·····TGGGTAGGCGTGATTCTGTATGAAGCAAAGGGCAAAAAT·····
WT      W  V  G  V  I  L  D  E  A  K  G  K  N
D63Y    W  V  G  V  I  L  Y  E  A  K  G  K  NA
```

```
5'  ·····CGGGTGGGCTCCCGTGTAGAGGTGATTGGAAAAGGCCAC····· 3'
    ·····CGGGTGGGCTCCCGTGTACAGGTGATTGGAAAAGGCCAC·····
WT      R  V  G  S  R  V  E  V  I  G  K  G  H
E34Q    R  V  G  S  R  V  Q  V  I  G  K  G  H
```

```
5'  ·····CCGCTGGCAGCACCCATCATCCCCACGCCGGTCCTCACC····· 3'
    ·····CCGCTGGCAGCACCCATCATCCCCACGCCGGTCCTCACC·····
WT      P  L  A  A  P  I  I  P  T  P  V  L  T
I196V   P  L  A  A  P  I  V  P  T  P  V  L  T
```

```
5'  ·····CGCACGATTGAGGGACTCCGGGGCCCTCCTCCTTCAGGC····· 3'
    ·····CGCACGATTGAGGGACTCCAGGGCCCTCCTCCTTCAGGC·····
WT      R  T  I  E  G  L  R  G  P  P  P  S  G
R1049Q  R  T  I  E  G  L  Q  G  P  P  P  S  G
```

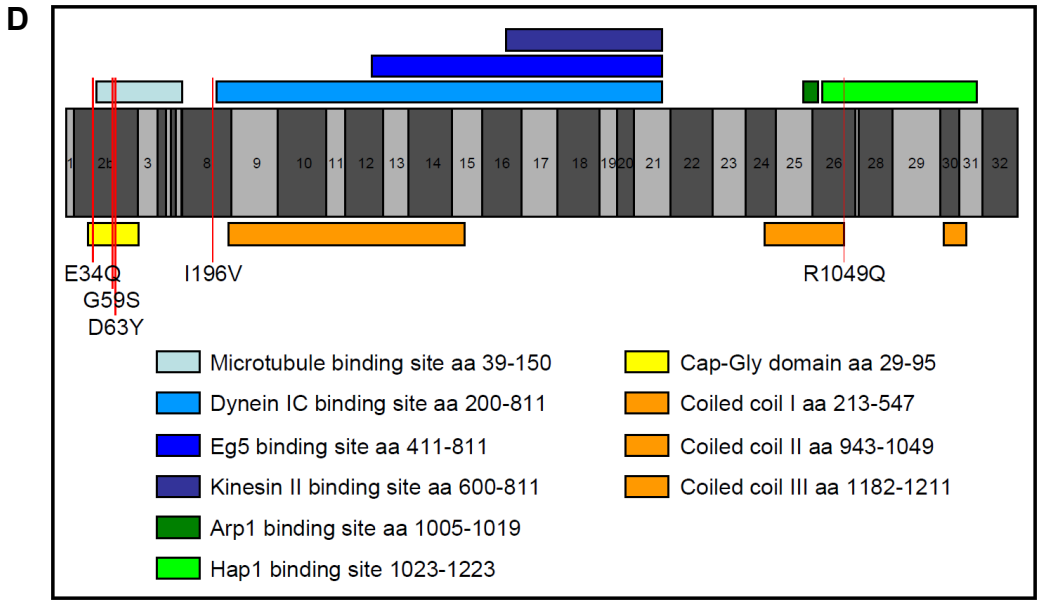

Fig. 03: Location of the mutations in the nucleotide and the amino acid sequence

Cap-Gly: cytoskeleton associated protein, Glycine rich
Hap1: Huntingtin-associated protein1
aa: amino acid
IC: intermediate chain
nt: nucleotide
(A) The nt sequence of dynactin p150 stretches from exon 1-32, which are shown in alternating grey and black letters. The non coding regions are depicted in light green. The triplets, which are affected from the mutations, are illustrated in red. (B) The selected mutations (E34Q, G59S, D63Y, I196V, and R1049Q) are displayed in red in the aa sequence. (C) For each mutation, the according nt sequence is illustrated with six triplets before and after the affected one. The exchanged nt is depicted in red. Underneath the nt sequence the corresponding aa sequence is displayed with the particular exchange of the aa in bold letters. (D) The sequence changes are illustrated as red dashes and show, which domains and binding sites are affected.

The D63Y mutation was chosen because of its very close location to the previously described G59S in exon 2, although no co-segregation could be detected for it. It was only found in one ALS patient but in no healthy or neurological controls. It lies within the Cap Gly domain and also in the microtubule binding site. Later it gained even more importance in regards to the mutations found in the Perry syndrome, which are also very closely located to the D63Y mutation [22]. The patient presented with progressive muscle atrophy (PMA), with an onset at the age of 62. The primary symptoms were distal asymmetric muscle atrophy in the lower limbs with the dominating degeneration of the second motor neuron [29].

Another mutation that was chosen to work with, the E34Q was also found in one ALS patient, presenting with classical ALS with the participation of both lower and upper motor neurons and in one healthy control. It is located in the Cap Gly domain, which is very important for the microtubule binding ability.

The third chosen mutation, I196V, is located in exon 8, shortly before the dynein intermediate chain binding site. It was found significantly more often in ALS patients but could also be detected in healthy and neurological controls. The ALS patients carrying this mutation developed their first symptoms between the ages of 54 and 66. The main primary symptoms were asymmetric flaccid paresis of the upper extremities and the degeneration of the spinal anterior horn was dominant in these patients. One patient suffered from classical symptoms of parkinsonism and another one showed signs of a cerebellar syndrome. Striking was the appearance of extra motoric symptoms in five patients, which suffered from diffuse paraesthesia. In the collective of neurological controls, three patients suffered from PSP, one from MSA and two patients presented with isolated FTD [29].
The R1049Q mutation was chosen because of its striking phenotype after preliminary transfections. Interestingly, it was found to lie in the second coiled coil domain, which is very important for inter-subunit interaction, as well as in the Hap1 binding site. This mutation was not only found in ALS patients but in neurological and healthy controls alike. The age of onset of patients presenting with ALS and primary lateral sclerosis (PLS) was between 62 and 73, the life span after detection of the first symptoms amounted between 29 and 65 months. The phenotypes were very heterogeneous concerning the type of manifestation (bulbar paralysis, para spastic, asymmetrical paresis of the lower extremity), as well as the dominantly affected motor neuron [29].

Given that all of these mutations affect regions, which are highly conserved among the p150 protein, they are therefore potential candidates as causal or risk factors for the development of ALS.
Therefore, the current interpretations of the clinical findings remain unclear and functional studies in vitro and in vivo are required to delineate the functional impact of each of the mutations.

1.5. Aim of the thesis

The aim of the doctoral thesis was to study four of the mutations in the dynactin p150 subunit found in a patient collective as well as in healthy and neurological controls. Then, the foundation was to be laid for the generation of transgenic mice models on the basis of in vitro morphological studies. These four sequence changes were chosen out of the collective of all 23 mutations, as they initially appeared to be more relevant than others based on preliminary transfection studies and their location in the p150 subunit.

Therefore, motor neuron cultures from rat embryos needed to be established in order to study consequences of human dynactin mutations in these primary motor neurons.

The distribution and localization pattern of the mutated dynactin p150 subunit was to be investigated in motor neurons and cell lines to infer to loss or gain of function in case of abnormal distributed protein, or if the mutations altered the structural integrity of the dynactin complex.

Furthermore, known interaction partners were to be depicted to further investigate the question if the mutated protein would have an impact on the localization and therefore the function of its binding partners.

2. Material and Methods

2.1. Materials

2.1.1. Laboratory animals

For the preparation of primary motor neurons (2.2.1), pregnant rats were killed by an overdose of CO_2.

2.1.2. Chemicals and biochemical reagents

The used chemicals of the following companies were of analytical purity. The origin of products of other companies is named in the methods part.

AppliChem (Darmstadt)
Merck (Darmstadt)
Sigma-Aldrich (Taufkirchen)
Serva (Heidelberg)
Roth (Karlsruhe)
Usb (Cleveland, USA)
PAA (Pasching, Austria)
VWR/Electran (Darmstadt)
Perbio (Bonn)

2.1.3. Consumable material

Cell-culture flasks, 25 cm^2 (Nunc, Wiesbaden)
Cell-culture 24-well plates (Nunc, Wiesbaden)
Cell scrapers (Becton Dickinson, Franklin Lakes, USA)
Centrifuge-falcons 15 ml, 50 ml (Nunc, Wiesbaden)
Cover glasses, 13 mm (Glaswarenfabrik Kark Hecht KG, Sondheim)
Electroporation cuvette (BioRad, Munich)
Freezer tubes 1.8 ml (Nunc, Wiesbaden)
Gloves (Sempermed, Wien)
µdishes (Ibidi, Martinsried/ Munich)
Neubauer counting chambers (Brand, Wertheim)
Object slides (Menzel GmbH, Braunschweig)
Pasteur pipettes (Brand, Wertheim)
Petri dishes 94 mm (Nunc, Wiesbaden)

Pipette tips 10 µl, 200 µl, 1000 µl (Eppendorf, Hamburg)
Pipettes for pipette boy 10 ml, 25 ml (Becton Dickinson, Franklin Lakes, USA)
Reaction tubes 0.1 ml, 0.5 ml, 2 ml (Eppendorf, Hamburg)
Sterile filters 0.22 µm, 0.45 µm (Whatman GmbH, Dassel)
Syringes 5 ml (Braun, Melsungen)
3 MM Whatman paper (Schleicher & Schuell, Dassel)

2.1.4. Hardware/ Equipment

Aspirator (Vacusafe, Integra Biosciences, Zizers, Switzerland)
Beaker glasses 50, 100, 500, 1000 ml (Schott, Mainz)
Beckmann centrifuge J25 (Beckmann coulter, Krefeld)
Blotting Clip (BioRad, Munich)
Centrifuge Multifuge (Heraeus Holding, Hanau)
Dissecting set of instruments (VWR international, Darmstadt)
Eppendorf centrifuge 5804R (Eppendorf, Hamburg)
Freezer -70° C (Forma Scientific, San Bruno, USA)
Freezer -20° C (Liebherr, Ochsenhausen)
Gel chambers (BioRad, Munich)
Gel carriers (BioRad, Munich)
Glass slides 0.75 mm (BioRad, Munich)
Ice machine Scotsman AF 10 (Scotsman Ice Systems, Vernon Hills, USA)
Image developer CURIX 60 (AGFA Health Care GmbH, Berlin)
Incubator Heraeus BBD 6220 Thermo scientific (Heraeus Holding, Hanau)
Microscope (Zeiss, Oberkochen)
PCR-machine mastercycler gradient (Eppendorf, Hamburg)
Pipette boy (Hirschmann, Eberstadt)
Pipettes P10, P20, P100, P200, P1000 (Eppendorf, Hamburg)
Shaker Ika Vibrax VXR-basic (IKA, Staufen)
Spectral photometer (Beckmann Coulter, Krefeld)
Sterile bench (Nunc, Wiesbaden)
Table top centrifuge Biofuge pico (Heraeus-Kendro, Hanau)
Tank-Blot-Chamber (BioRad, Munich)
Test Tube rotator (Snijders scientific, Tilburg, The Netherlands)
Thermomixer (Eppendorf, Hamburg)

Thermoshaker for culture flasks (Biotech International, Brussels, Belgium)
Voltage-generator (BioRad, Munich)
Vortexer (VWR international, Darmstadt)

2.1.5. Electronic data processing programs

Axio Vision Rel. 4.7 (Zeiss, Oberkochen)

2.2. Cell culture

Cell culturing was performed under sterile conditions under a sterile bench and the incubation took place in an incubator at 37° C in a water saturated atmosphere of 5 % CO_2 and 95 % air.

2.2.1. Primary motor neurons

All animal experiments were performed in compliance with the guidelines for the welfare of experimental animals issued by the Federal Government of Germany, the National Institutes of Health and the Max Planck Society. The primary motor neurons were obtained from rat embryos at embryonic day fourteen (E14.5) from pregnant CD rats (Charles River Laboratories International, Wilmington, USA).

2.2.1.1. Preparation and culturing of motor neurons

We set up our protocol based on the paper of Martinou et al. [58].
The pregnant rat was killed with an overdose of CO_2. The uterus was taken out and the embryos were freed from the egg integuments and laid into pre cooled dissection solution. Under a microscope, cooled in dissection solution, the embryos were decapitated. Then the embryos were positioned with the back facing up and several layers of embryonic tissues were removed to expose the spinal cord and the spinal cords were dissected. Then the meninges and dorsal root ganglia were stripped off. The spinal cords were cut in pieces and again put in dissection solution in a 15 ml falcon. Afterwards, the falcons containing the spinal cords were centrifuged for 2 min at 1500 rpm at RT. The dissection solution was decanted. The pellet, consistent of spinal cord pieces, was then digested with 1ml of TrypLE™ Express (Gibco, Karlsruhe) for 15 min at RT. To stop the digestion, the falcon was filled up with PBS-- (PAA, Pasching, Austria) and again centrifuged for 2 min at 1500 rpm at RT. The supernatant was decanted and the spinal cords

were treated with 400 µl of Deoxyribonuclease I for 10 min at 37° C. Again the reaction was stopped by filling the falcon up with PBS-- and centrifuged at 1500 rpm at RT and the supernatant was then decanted. Then, 3 ml of the plate medium without serum replacement was added and the tissue was dissociated with a Pasteur pipette. The single cell suspension was then layered onto a 3.5 % BSA solution and then centrifuged for 20 min at 80 g at RT. Subsequently, the supernatant was decanted and the pellet was resuspended in PBS-- and then layered onto the discontinuous Nycodenz-gradient. The gradient was centrifuged for 20 min at 700 g and 4° C. Following, the upper 3 ml of the gradient were collected and 9 ml of plate medium without serum replacement were added. The cell suspension was centrifuged again at 1000 x g for 10 min at 4° C. After centrifugation, the supernatant was discarded and the pellet was resuspended in plate medium with 1 % serum replacement. The cells were counted in a Neubauer counting chamber, then diluted up to 17.5 x 10^4 per well. The cells were then plated on 24-well-plates, which had been filled with a 13 mm cover slip in every well and had been coated with Poly-l-Ornithine solution (Sigma-Aldrich, Taufkirchen) and PBS-- 3:17 for half an hour at 37° C. The 24-well-plate had then been washed 3 times with PBS-- and afterwards coated with Natural Mouse Laminin (Invitrogen, Carlsbad, USA) and PBS-- 5:1000 for 1 hour at 37° C.
The cells were incubated in a water-saturated atmosphere of 5 % CO_2 and 95 % air at 37º C.
After three hours, when the cells were sedimented, the medium was changed to plate medium without serum replacement. On day in vitro 6 (DIV), the medium was changed again to plate medium with serum (FBS), (Hyclone, Logan, USA).

Dissection solution:

- 1 % Antibiotic Antimycotic 100 x liquid (Invitrogen, Carlsbad, USA)
- 1 % D-Glucose (Invitrogen, Carlsbad, USA)
- ad 100 % HBSS-- (Gibco, Karlsruhe)

BSA:

- 96.5 % PBS--
- 3.5 % Albumin from bovine serum (RIA Grade) (Sigma-Aldrich,Taufkirchen)

Deoxyribonuclease:

- 1 ml HBSS--
- 1 µl DNAse (Deoxyribonuclease I), (Invitrogen, Carlsbad, USA)

Plate Medium:

- 33 % D-MEM (Invitrogen, Carlsbad USA)
- 2 % B-27 Supplement (50x) without vitamin A (Gibco, Karlsruhe)
- 1 % GlutaMax™ I-(100x), liquid (Invitrogen, Carlsbad USA)
- 1 % Antibiotic Antimycotic 100 x liquid
- 1 % NEAA (Invitrogen, Carlsbad, USA)
- ad 100 % knockout DMEM –F12, Lomix (Gibco, Karlsruhe)

with serum replacement:

- plate medium prepared as above
- 1 % Knockout™ SR, Serum Replacement for Embryonic Stem Cells (Gibco, Karlsruhe)

with serum:

- plate medium prepared as above
- 1 % Serum: FBS

Nycodenz Gradient:

- PBS--
- Nycodenz 60 % (w/v) Solution in water (SERVA, Heidelberg)

A 30 % solution of Nycodenz was prepared by mixing 1.5 ml Nycodenz 60 % with 1.5 ml PBS--. Then 3 different solutions of increasing density were prepared:

1) 750 µl Nycodenz 30 % + 2250 µl PBS--
2) 1000 µl Nycodenz 30 % + 2000 µl PBS--
3) 1250 µl Nycodenz 30 % + 1750 µl PBS--

The solution 1 was then given in a 15 ml falcon. Afterwards, solution 2 was given beneath solution 1 with a 5 ml syringe. And finally, solution 3 was added beneath solution 1 and 2 with the syringe.

2.2.1.2. Transfections

Transfections of primary motor neurons were conducted with *Optifect™ Reagent* (Invitrogen, Carlsbad, USA). For each well of a 24 well plate, the following mixture of 3 µl *Optifect™ Reagent* and 50 µl Lomix was set up and incubated for 5 min at RT. Meanwhile, 1 µg DNA per 24 well plate well was mixed with 50 µl of Lomix and then 53 µl of the Optifect-Lomix-mixture was added, mixed well, and incubated for 25 min at RT. Afterwards, 500 µl of plate medium with serum per 24 well plate well was added to the Lomix-Optifect™-DNA-mixture. The old medium was aspirated from the cells and 603 µl of the transfection solution was added to each well. The cells were then incubated o.n. in a water saturated atmosphere of 5 % CO_2 and 95 % air at 37º C.

For double transfections, 1 µg DNA of each plasmid and 6 µl *Optifect™ Reagent* was used respectively.

2.2.2. Cell lines

2.2.2.1. Cos-7cells

Cos-7 cells were bought from the Deutsche Sammlung für Mikroorganismen und Zellkutur (DSMZ). Cos-7 is a cell line derived from green monkey kidney and the cells grow as monolayer. They were cultured in 10ml flasks in a water-saturated atmosphere of 5 % CO_2 and 95 % air at 37º C. Every 3 days, when cells were microscopically determined confluent at about 70 %, the cells were split 1 in 5.

Therefore, the old medium was poured off and the cells were washed with 1 ml PBS--. Then 1 ml Trypsin 0.125 % Versen was added and the cells were incubated for 10 min at 37° C. Subsequently, the flasks were tapped so the cells would detach from the ground and 1 ml of culture medium was added. The cell suspension was centrifuged for 2 min at 1500 rpm at RT in a 15 ml falcon and the supernatant was then discarded. The pellet was resuspended in 5 ml culture medium and 1 ml of the suspension was given in a new flask with 9 ml culture medium.

culture medium:

- 90 % D-MEM
- 10 % FBS

Trypsin 0.125% Versen

- 5 % Trypsin 0.25 % (Biochrom AG,Berlin)
- 45 % PBS--
- 50 % Versen

Versen

- 8 g NaCl
- 0.2 g KCl
- 1.382 g Na_2HPO_4
- 0.29 g KH_2PO_4
- 0.5 g EDTA
- ad 1 l H_2O bidest, autoclave

2.2.2.2. HeLa-cells

HeLa-cells were bought from the DSMZ. HeLa is a HPV-positive cell line derived from a human cervix carcinoma of a 31-year-old index patient, whose initials serve as eponym. The cells were cultured in 10 ml flasks in a water-saturated atmosphere of 5 % CO_2 and 95 % air at 37º C. Every 3 days, when cells were microscopically determined confluent at about 70 %, the cells were split 1 in 5. The procedure was the same as described above with Cos-7 cells.

culture medium:

- 89 % MEM (Invitrogen, Carlsbad, USA)
- 10 % FBS
- 1 % NEAA

2.2.2.3. Plating of cell lines

When 24-well plates were used, 13 mm cover slips were added to each well. Then the cover slips were coated with Poly-L-Lysine (0.05 mg/ml, Sigma-Aldrich, Taufkirchen) 1:10 in PBS-- for 1 h in the incubator. The 24-well plates were then washed 3 times with PBS--.

The HeLa or Cos-7 cells were trypsinated as described in 2.2.2.1. For 24-well plates, the cells were split 1:15. For 94 mm Petri dishes, the cells were split 1:12. The plated cells were incubated in the incubator in a water-saturated atmosphere of 5 % CO_2 and 95 % air at 37º C o.n.

2.2.2.4. Transfections of cells lines

Polyfect^R Transfection Reagent (Quiagen, Hilden) was used for transfection of cell lines according to the information given by the manufacturer. The cells were transfected o.n. or several hours, depending on what they were used for, and then used for immunostainings (2.4), or for the preparation of cell lysates (2.3.1.2)

respectively. For double transfections, 0.5 µg DNA of each plasmid and the double amount of *Polyfect^R Transfection Reagent* was used respectively. For transfection of mitochondria the *pTurboRFP-mito vector, 4.7 kb* (Evrogen, Moscow, Russia) was used.

2.2.2.5. Deep freezing of cell lines

Trypsinated cells (content of one 75 mm culture flask at about 70 % confluence) were given into a 15 ml falcon and centrifuged at 1000 g at RT for 5 min.The supernatant was discarded and the pellet was resuspended in culture medium and 10 % DMSO (Merck, Darmstadt) to 10^6 cells/ml. 1 ml aliquots were pipetted in freezer tubes and stepwise cooled to -70° C in a cryo container (Nalgene, Neerijse, B) and then stored in fluid nitrogen at -196° C.

2.2.2.6. Thawing of cell lines

Aliquots of frozen cell-suspensions were thawed at RT and given in 15 ml falcons with 10 ml of culture medium. After centrifugation (1000 rpm, 5 min, at RT), the supernatant was discarded and the pellet was resuspended in 10 ml culture medium and then cultured in 10 ml flasks. The freshly thawed cells were incubated for 24 h in the incubator and then the medium was changed to fresh culture medium. The cells were then cultured as described above.

2.3. Protein Biochemistry

2.3.1. Protein preparation

2.3.1.1. Rat brain and spinal cord lysates

For rat brain and spinal cord lysates, a pregnant rat was killed with an overdose of CO_2. With a guillotine, the rat was decapitated and the skull was opened. The brain was taken out and applied into a falcon with solution A after weighing it (2 ml solution A/100 mg brain/spinal cord). Furthermore, the spinal cord from the adult rat was taken out and also applied to a falcon with solution A. The embryos (E17) were dissected in ice cold dissection solution (2.2.1.1) and the spinal cords, free of meninges and dorsal root ganglia, were taken out and placed in a falcon with solution A as well.

The brain respectively the spinal cords were homogenized in a potter on ice with 12 strokes at 900 rpm with a teflon douncer. The homogenate was then

transferred to a centrifugation tube and centrifuged at 4° C and 1000 g for 10 min. The supernatant was transferred to a beaker (supernatant 1). The pellet was transferred back into the potter glass and filled up with the same volume of solution A as before and the homogenization procedure was repeated. The homogenate was then transferred into a centrifugation tube and centrifuged at 4° C and 1000 g for 10 min. The supernatant (supernatant 2) was combined with supernatant 1. This mixture was then centrifuged at 4° C and 12000 g for 20 min. The resulting supernatant was discarded and the remaining pellet was resuspended in 5 ml RIPA buffer. To extract the proteins, the lysate was shaken for 1 h in an overhead shaker at 4° C. Afterwards, the lysate was centrifuged again at 4° C and 12000g for 20 min and the supernatant carefully was transferred into a fresh tube and the appropriate volume of gel loading Western blot buffer was added.
Aliquots were frozen at -70° C or processed further for SDS-PAGE.

Solution A:

- 16 ml 2.0 M sucrose
- 1 ml HEPES pH 7.4
- 2 tablets complete EDTA-free protease inhibitor (Roche, Grenzach Wyhlen)
- ad 100 ml H_2O bidest

RIPA-buffer:

- 50 mM Tris-HCl pH 8.0
- 150 mM NaCl
- 0.1 % SDS
- 0.5 % Sodiumdesochycholate
- 1.0 % Nonidet NP-40

2.3.1.2. Cell lysates of cultured cells

Cos-7 cells, respectively HeLa cells, plated on 94 mm Petri dishes were washed 2 times with ice cold PBS. The remaining PBS was pipetted off and the lysis was performed according to the instructions of the *µMACS Micro Bead Kits* (Miltenyi Biotech, Germany). 2 % of protease-inhibitor cocktail tablets complete EDTA free (Roche, Mannheim) was added to the lysis buffer.
The lysate was either used directly for SDS-PAGE analysis or was continued processing for immunoprecipitations.

PBS 10x:

- 90.0 g NaCl
- 1.22 g KH_2PO_4
- 8.15 g Na_2HPO_4
- ad 1 l H_20 bidest

PBS 1x:

- 10 ml PBS 10x
- ad 1 l H_2O bidest

2.3.1.3. Immunoprecipitations

For immunoprecipitations, the cell lysate of cultured cells (2.3.2.1) were used. The *µMACS Micro Bead Kits* (Miltenyi Biotech, Germany) was used, but the instructions were modified.

When the antibody needed to be coupled to the magnetic protein coupled beads, 50 µl of the magnetic protein A/ protein G-coupled beads were mixed with 2 µg of the antibody and incubated on ice for 30 min. Then, 300 µl of the cell lysates were added and incubated for 2 h at 4° C in an overhead shaker. When anti-GFP beads (Miltenyi Biotech, Bergisch Gladbach) were used, the cell lysates were added directly to 50 µl of anti-GFP beads and incubated as directed above. The *µMACS* microcolumns were attached to the magnetic stand and calibrated by adding 200 µl of the lysis buffer with 2 % of protease-inhibitor cocktail tablets complete EDTA free. The antibody-lysate-bead mixture was then applied onto the microcolumns and the flow through was discarded. Afterwards, the microcolumns were washed 8 times with 200 µl of wash buffer 1 from the *µMACS Micro Bead Kits* (Miltenyi Biotech, Germany) and then two times with wash buffer 2 from the *µMACS Micro Bead Kits*. Afterwards, 20 µl of preheated (95° C) elution buffer was applied to the microcolumns and incubated for 5min. Subsequently, 50µl of elution buffer was added and the flow through was collected in 1.5 µl eppendorf tubes. Then, DL-Dithiothreitol (DTT) 1:10 was added and the eluted protein was then further processed in SDS-Page (2.3.2) or frozen at -70° C.

elution buffer

- 50 mM Tris HCl (pH 6.8)
- 1 % SDS
- 1 mM EDTA
- 10 % glycerol
- 0.005 % bromphenol blue

2.3.2. SDS-Polyacrylamide gel electrophoresis (SDS-PAGE)

The protocol was obtained from Liebau et al. [54, 55] and slightly varied.

The SDS-PAGE divides proteins, according to their molecular weight as described by Laemmli et al. [44] in a denaturising Polyacrylamide gel. After complete polymerisation of running- and stacking-gel between two 0.75 mm glass plates (BioRad, Munich), the gel was clamped in a running chamber (BioRad, Munich). The gel comb was then removed and the chamber filled with 1 times running buffer. The lysed probes (2.2.1.2) respectively (2.2.1.1.) were denaturised by heating them up for 3 min at 95° C. Afterwards, the probes were centrifuged for 5 min at 7000 rpm at RT. Then 3x SDS buffer was added to each probe and 10 µl of the probes were given into each well respectively 5 µl of the *PageRuler™ Prestained Protein Ladder* (Fermentas, St. Leon-Rot) were applied to the first well. A constant voltage of 85 V was applied for 15 min, until the proteins had reached the running gel. Then the voltage was raised to 100 V, until the running front had reached the lower end of the gel.

3x SDS-buffer:

- 2.27 g Tris-HCl 62.5 mM, pH 6.8
- 6 g 2 % SDS
- 30 g 10 % sucrose
- 100 ml H_2O bidest
- bromphenol blue

5x running buffer:

- 15.1 g Tris ultrapure
- 47.0 g Glycine
- ad 900 ml H_2O bidest
- 50 ml SDS 10 %
- ad 1 l H_2O bidest

1.0 M Tris-HCl, pH 6.8:

- 121.14 g Tris ultrapure
- ad 800 ml H_2O bidest
- adjust pH with HCl
- ad 1 l H_2O bidest

1.5 M Tris-HCl, pH 8.8:

- 181.5 g Tris ultrapure
- ad 900 ml Aqua bidest
- adjust pH with HCl
- ad 1 l H_2O bidest

10 % running gel:

- 4.9 ml H_2O bidest
- 2.5 ml 30 % Acr.-Bis Sol. (29:1)
- 2.5 ml 1.5 M Tris, pH 8.8
- 100 µl SDS 10%
- 200 µl APS 10 %

10 % stacking gel:

- 3.6 ml H_2O bidest
- 630 µl 30 % Acr.-Bis Sol. (29:1)
- 630 µl 1.5 M Tris pH 6.8
- 50 µl SDS 10 %
- 80 µl APS 10 %

- 20 µl TEMED
- 2 µl TEMED

10 % SDS:

- 10 g SDS
- ad 100 ml H_2O bidest

2.3.3. Western Blot

The proteins that were divided up in the SDS-PAGE were transferred to a Polyvenyldifluorid- (PVDF-) membrane (Hybond, Amersham Biosciences, Freiburg) by means of a tank blot and then detected via a peroxidise-coupled second antibody. The PVDF-membrane was activated in methanol for 30 s and then like the gel, the filter-sponges and the Whatman-papers drained in 1 times blotting-buffer. Then the components were applied to the blotting-clip (BioRad, Munich) in the following order:

filter-sponge
2 Whatman-papers
SDS-gel
PVDF membrane
2 Whatman-papers
filter-sponge.

The blotting clip was then inserted in the blotting tank (BioRad, Munich). Additionally, for chilling the whole application, an ice-tank was inserted as well. Afterwards, the tank was filled with 1 times blotting buffer and a magnetic stir bar was added (150 rpm), so that the buffer would be mixed well at all time. Finally, a voltage of 90V was applied for 90 min. Thereafter, the membrane was taken out and was blocked with PBS + 0.1 % Tween 20 (Roth Karlsruhe) + 5 % skimmed milk powder (Roth, Karlsruhe) for 2 hours by shaking it lightly at RT. The 1st antibody was, according to its dilution, applied in PBS + 0.1 %Tween 20 + 5 % of the 5 % skimmed milk powder solution and incubated o.n. at 4° C by shaking it slightly.

Then, the membrane was washed 3 times for 10 min with PBS + Tween 20. The peroxidise-coupled 2nd antibody was diluted 1:1500 in PBS + Tween 20 0.1 % + 5 % of the 5 % skimmed milk solution. It was incubated for 1 h at RT. Afterwards, the membrane was washed again 3 times for 10 min in PBS + 0.1 % Tween 20.

primary antibodies:

- β-Actin, ms monoclonal 1:10000
- Dynactin p150, ms (BD Transduction Laboratories™, San Jose) 1:1000
- Dynein IC 74.1 MAB1618, ms monoclonal (Millipore, Schwalbach) 1:2500
- FUS/TLS, ms monoclonal (Santa Cruz, Heidelberg) 1:250
- GFP, ms monoclonal (BD Biosciences Clontech, Palo Alto, USA) 1:4000
- Tubulin-α, ms monoclonal (Sigma, Saint Louis, USA) 1:5000
- Tubulin-β neuronal Class III, ms/rb monoclonal (Covance, Berkeley, USA) 1:1000/1:5000

secondary, peroxidase-coupled antibodies:

- anti ms Immunoglobulin/HRP (Dako Cytomation, Glostrup, DK) 1:1500
- anti rb Immunoglobulin/HRP (Dako Cytomation, Glostrup, DK) 1:1500

10x blotting-buffer:

- 151.5 g (250 mM) Tris
- 720 g (1.9 M) glycine
- ad 4 l H_2O bidest

1x blotting-buffer:

- 80 ml10x blotting buffer
- 200 ml methanol
- ad 1 l H_2O bidest

2.3.4. Detection

The membrane was drained and incubated for 5 min with a mixture of solution A and B (according to the manufacturer's instructions) of *Super Signal®West Pico Chemiluminescent Substrate* (Pierce, Bonn). In the dark chamber, a radiographic film (Hyperfilm, Amersham Biosciences, Freiburg) was applied (2 s - 5 min, depending of the strength of the signal) that was then developed.

2.3.5. Overlay assay

After blocking the membrane with PBS (2.3.1.2) + 5 % skimmed milk powder for 2 hours by shaking it lightly at RT, cell lysates of cultured cells (2.3.1.2) or of rat spinal cord or brain (2.3.1.1) was layered onto the membrane and heat sealed in a plastic foil. It was slightly shaken at 4° C o.n. On the next day, the membrane was washed 3 times with PBS for 1.5 min and then treated like a normal western blot with the difference that the antibodies were prepared in PBS + 5 % skimmed milk powder and the washing was performed with PBS.

2.4. Immunecytochemistry

2.4.1. Fixation and poration of cells

The protocol was obtained from Liebau et al. [53].

The medium on the cells (24 well plates) was poured off and the wells were fixed with 500 µl PFA per well for 20 min. Then the PFA was poured off and the cells were washed 2 times with 500 µl per well PBS++ (PAA, Pasching, Austria). Subsequently, 500 µl Triton X 0.2 % was added to each well for 3 min to porate the cells. The Triton X was poured off and the blocker was added (500 µl/well for 30 min).

Triton X 0.2 %

- 50 ml PBS++
- 100 µl Triton X 100 (Roche, Grenzach-Wyhlen)

PFA:

- 10 g paraformaldehyde
- 200 ml H_2O bidest

blocker:

- 750 µl Goat Serum (Chemicon Billerica, USA)
- 14.25 ml PBS++
- adjust pH to 7.4
- 25 ml 10x PBS--
- 12.5 ml 2 M sucrose

2.4.2. Staining

The primary antibodies were diluted in 100 µl blocker per well and were incubated for 1 h in a light proof staining chamber at RT. The cover slips were then washed in PBS++ and meanwhile the second antibody was prepared and diluted in PBS++ 100 µl per well. The second antibody dilution was then added to each well and incubated again for 1 h in a light proof staining chamber at RT. The cover slips

were then washed with PBS++ for 5 min, following 5 min in PBS-- and subsequently 5 min in H_2O bidest. The cover slips were then dripped off on a tissue paper and then laid on an object slide on which a droplet of *Prolong antifade reagent with Dapi* (Invitrogen, Carlsbad, USA) had been applied before.

primary antibodies:

The appliance of some of the antibodies was obtained from Hermann et al. [30]

- ARP-1, gtt polyclonal (Santa Cruz, Heidelberg) 1:100
- Bassoon, ms monoclonal (Stressgen Bioreagents Corp, Canada) 1:150
- Dynactin (H-300), rb polyclonal (Santa Cruz, Heidelberg) 1:250
- Dynactin p50, ms (BD Transduction Laboratories™, San Jose, USA) 1:500
- Dynactin p62, gt polyclonal (Santa Cruz, Heidelberg) 1:100
- Dynactin p150, ms (BD Transduction Laboratories™, San Jose, USA) 1:250
- Dynein HC (R-325), rb polyclonal (Santa Cruz, Heidelberg) 1:50
- FUS/TLS, ms monoclonal (Santa Cruz, Heidelberg) 1:250
- Gephyrin, ms monoclonal (Synaptic Systems, Göttingen) 1:100
- Glial fibrillary acidic protein (GFAP), rb polyclonal (Chemicon, USA) 1:1000
- Golgin-97, ms monoclonal (Invitrogen, Carlsbad USA) 1:500
- SMI 32 (NF- H), ms monoclonal (Covance, Emeryville, USA) 1:1000
- Synaptophysin, rb polyclonal (Abcam, Cambridge, UK) 1:300
- TARDP, rb polyclonal (Abcam, Cambridge, UK) 1:500
- Tubulin-α, ms monoclonal (Sigma, Saint Louis, USA) 1:1000
- Tubulin-α, rb (Cell signalling Technology, Danvers, USA) 1:50
- Tubulin-β neuronal class III, ch polyclonal (Covance, Berkely, USA) 1:1000
- Vimentin VIM 3B4, ms monoclonal (Millipore, Billerica, USA) 1:250

secondary antibodies:

- Alexa Fluor 488 anti-gt (Molecular Probes, Eugene, USA) 1:500
- Alexa Fluor 488 anti-ms (Molecular Probes, Eugene, USA) 1:500
- Alexa Fluor 488 anti-rb (Molecular Probes, Eugene, USA) 1:500
- Alexa Fluor 568 anti-gt (Molecular Probes, Eugene, USA) 1:500
- Alexa Fluor 568 anti-ms (Molecular Probes, Eugene, USA) 1:500
- Alexa Fluor 568 anti-rb (Molecular Probes, Eugene, USA) 1:500

- Alexa Fluor 647 anti-ch (Molecular Probes, Eugene, USA) 1:500
- Alexa Fluor 647 anti-gt (Molecular Probes, Eugene, USA) 1:500
- Alexa Fluor 647 anti-ms (Molecular Probes, Eugene, USA) 1:500
- Alexa Fluor 647 anti-rb (Molecular Probes, Eugene, USA) 1:500

2.4.3. Microscopy

Images were captured using an upright fluorescence microscope (Axioskop 2, Zeiss, Oberkochen, Germany) equipped with a Zeiss CCD camera (16 bits; 1280X 1024 pixels per Image), and analysed using Axiovision software (Zeiss).

2.4.4. Counting of stained cells

To determine the purity of the motor neuron cultures, the number of SMI 32 positive cells was counted after immunecytochemistry with SMI 32 and tubulin-βIII. SMI 32 reacts with a non-phosphorylated epitope in neurofilament heavy and can be used as a motor neuron marker [89]. Therefore cells from three different preparation days were used and 300 cells were counted. The percentage of SMI 32 positive cells was then determined.

2.5. Microbiological methods

2.5.1. Culturing of E.coli

The multiplication of electro-competent E.coli of the DH5B-strain was performed in sterile LB-medium at 37° C and 200 rpm on a round shaker. Depending on the resistance of the particular plasmid, ampicillin (75 µg/ml) or kanamycin (50 mg/ml) was added to select those bacteria that contain the wanted plasmid.

For the generation of LB-agar-plates, the agar was added to distilled water, dissolved, autoclaved, and after cooling to 60° C the antibiotic was added and the agar was poured into Petri-dishes. The LB medium was also autoclaved before the antibiotic was added.

Glycerine-cultures were generated from 500 µl of the bacteria culture (OD_{600}: 0.9) and 500 µl 100 % glycerine and then stored at -70° C.

LB medium:

- 20 g LB broth base (Invitrogen, Carlsbad USA)
- ad 1 l H_2O bidest

LB agar:

- 32 LB-agar (Invitrogen, Carlsbad USA)
- ad 1 l H_2O bidest

2.5.2. Generation of electrical competent bacteria

100 ml of sterile 2YT-medium were inoculated with 150 µl E.coli DH5B from a o.n.-culture and multiplyed on a round shaker at 37° C and 200 rpm until the culture reached a OD_{600} of 0.5. After 30 min incubation on ice, the bacteria were centrifuged at 2000 g and 4° C for 10 min. The pellet was resuspended in 50 ml ice cold H_2O bidest. The suspension was then washed 2 times in H_2O bidest and centrifuged as described above. Finally, the pellet was resuspended in an equivalent volume of 10 % glycerine. 50 µl aliquots were set up and the bacteria were frozen at -70° C.

2YT- medium:

- 16.0 g peptone
- 10.0 g yeast extract
- 5.0 g NaCl
- ad 1 l H_2O bidest

2.5.3. Transformation of electrical competent bacteria

50 µl aliquots of electrical competent bacteria (2.5.2) were thawed on ice, mixed with 1-2 µl ligation mixture (2.6.7) and transferred into a cooled electroporation cuvette. The cuvette was set into the electroporator and a voltage of 1.8 kV was applied. The bacterial suspension was then aspirated in 1 ml of pre warmed SOB medium and incubated in a 2 ml reaction tube in an overhead shaker at 37° C for 45 min. The bacterial suspension was then centrifuged at 3500 g for 3 min at RT. The pellet was resuspended in 100 µl of the supernatant and plated on a selection agar dish with antibiotic containing agar. The Petri dish was incubated at 37° C in an incubator.

SOB medium:

- 20.0 g peptone
- 5.0 g yeast extract
- 0.5 g NaCl
- 20 mM $MgCl_2$
- ad 1l H_2O bidest

2.6. Molecular biological methods

2.6.1. Isolation of plasmid DNA from E.coli by means of alkaline lysis

1.5 ml of an o.n. culture was given in a 1.5 ml tube and centrifuged at 13000 rpm for 1 min at RT. The supernatant was decanted and the procedure was repeated in the same 1.5 ml tube. The remaining pellet was resuspended in solution 1. Then, 200 µl of solution 2 (alkaline lysis buffer) was added, carefully mixed, and incubated for 5 min at RT. Subsequently, 100 µl of ice cold solution 3 (neutralising buffer) was added, carefully mixed, and incubated on ice for 5 min. The suspension was then centrifuged at 13000 rpm for10 min at RT. The supernatant was pipetted into another 1.5 ml tube and 800 µl of 98 % ethanol was added. The mixture was frozen at -70° C for 2 h. After those 2 hours the mixture was centrifuged at RT and 13000 rpm for 8 min. The supernatant was discarded and the pellet was washed with 500 µl of 75 % ethanol and then centrifuged again at 13000 rpm at RT for 10 min. The supernatant was discarded again and the pellet was dried in the air and afterwards resuspended in 50 µl of H_2O bidest. The DNA was stored at -20° C.

Solution 1 (lysis buffer)

- 50 mM glucose
- 25 mM Tris/HCl (pH 8.0)
- 10 mM EDTA

Solution 2 (alkaliner lysis buffer)

- 200 mM NaOH
- 1 % SDS (m/v)

Solution 3 (neutralising buffer):

- 3 M potassiumacetat
- 11.5 % acetic acid (m/v)

2.6.2. Isolation of plasmid DNA from E.coli by means of anion exchange columns

For sequencing purposes, plasmid DNA was isolated from 3 ml bacterial culture with the *Jetquick Plasmid Mini Prep Spin* Kit (Genomed, Löhne) according to the directions of the manufacturer. Bigger amounts of DNA were isolated endotoxin free with the *Nucleo-Bond_ PC 500 EF- Kit* (Machery-Nagel, Duren) according to the directions of the manufacturer. The so attained DNA was stored at -20° C and was used for transfections of eukaryotic cells.

2.6.3. Determination of the concentration of nucleic acids

The measuring of nucleic acid concentrations was performed spectrophotometric with H_2O bidest as reference (wave length: 260 nm) in a spectral photometer.

2.6.4. Restriction analysis

The following restriction endonucleases were used for the generation of DNA fragments for ligation purposes. They were used according to the instructions of the respective manufacturer in respect of reaction temperature and -duration:
EcoRI, XbaI (Invitrogen, Carlsbad, USA)

analytical preparation:

- 17 µl DNA
- 2µl 10x restriction buffer
- 1 U restriction endonuclease
- ad 20 µl H_2O bidest

preparative preparation

- 10 µg DNA or 50 µl PCR product
- 8 µl 10x restriction buffer
- 3-4 U restriction endonuclease
- ad 80 µl H_2O bidest

6X loading dye solution (Fermentas, Leon-Rot) was added to the probes after incubation, according to the directions of the manufacturer. The probes were then divided by gel electrophoresis on a 1 % agarose gel (2.6.5). The fragments were detected via uv illumination and documented. The fragment size was estimated with the help of the *MassRuler^{TM} Express Forard DNA Ladder Mix, ready-to-use* (Fermantas, Leon-Rot).

2.6.5. DNA-agarose-gel-electrophoresis

1 % agarose was heated up in 1x TAE buffer, ethidiumbromide stock solution (Roth, Karlsruhe) (diluted 1:1000) was added and poured into a gel chamber (BioRad, Munich). The gel electrophoresis was performed and a constant voltage of 85 V was applied. The result was interpreted via uv illumination using a video documenting machine (Pharmica Biotech, Freiburg).

50x TAE- buffer pH 8.3:

- 100.0 ml EDTA pH 8.0
- 42.0 g Tris
- 57.0 ml glacial acidic acid
- ad 1 l H_2O bidest

2.6.6. Purification of DNA from agarose gels

DNA fragments were identified on the basis of the *MassRuler^{TM} Express Forard DNA Ladder Mix, ready-to-use* (Fermantas, Leon-Rot). They were then cut out with a disposable scalpel and purified with the *Jetquick Gel Extraction Spin* Kits (Genomed, Löhne), according to the instructions of the manufacturer.

2.6.7. Ligation

A T4 DNA ligase (Invitrogen, Carlsbad, USA) was used to enzymatically link different DNA fragments. The molar proportion vector: insert amounted 1:3.

Ligation

- 50-100 ng linearised plasmid-DNA +DNA-insert
- 1 µl ligase-buffer 5x
- 1 U T4 DNA ligase
- ad 10 µl H_2O bidest

The ligation was incubated either way at 4° C o.n. or at RT for 3 h. Following, it was used for transformation of electrical competent bacteria (2.5.3)

2.6.8. Selection of oligonucleotides

The primer for the polymerase chain reaction (PCR) were selected in a manner that they were 27-33 bases long with a content of about 50 % GC. The following primers were acquired from MWG-Biotech (Ebersberg):

Table 02: Oligonucleotides used for primers

Primer for PCR	5'-sequence-3'
DCTN1-pEGFP-C1 f	*GAATTC*CG**ATG**GCACAGAGCAAGAGGCACG
DCTN1-pEGFP-C1 r	*TCTAG*GC**TTA**GGAGATGAGGCGACTGTGAA

2.6.9. Polymerase chain reaction (PCR)

DNA fragments were selectively amplified, utilizing the polymerase chain reaction (PCR). Primer (2.6.8) bind at the 5' respectively the 3' end of the DNA template. Thereupon, the thermo stable Taq-polymerase elongates the short double strands. For PCR the *High fidelity PCR Supermix* (Invitrogen, Carlsbad USA) was used. Besides the Taq-polymerase it also contains a Pfu-polymerase with proofreading activity, a dNTP mix and the required buffer.

PCR-mixture:

- 1 µl DNA-template (1 ng/µl)
- 1 µl 5'-primer (50 ng/µl)
- 1 µl 3'-primer (50 ng/µl)
- 47 µl *High fidelity PCR Supermix*

The PCR was set up in a thermocycler (Eppendorf, Hamburg) with the following programme:

Table 03: PCR-protocol

Step	**Temperature**	**Duration**	**Cycles**
Denaturation	95°C	3min	1
Denaturation	95°C	30s	35
Primer attachment	60°C	30s	35
Elongation	72°C	1min/kb	35
Elongation	72°C	10min	1

3. Results

3.1. Establishment of primary motor neuron cultures

To study the mutations in an in vitro cell system that is better comparable to neurons in the nervous system than cell lines, we established the culturing of primary motor neurons from embryonic rats. Therefore we used rat embryos at the age of embryonic day E14. The exact procedure of the preparation is described in *2.2.1.1. preparation and culturing of motor neurons* and shown in figure 04.

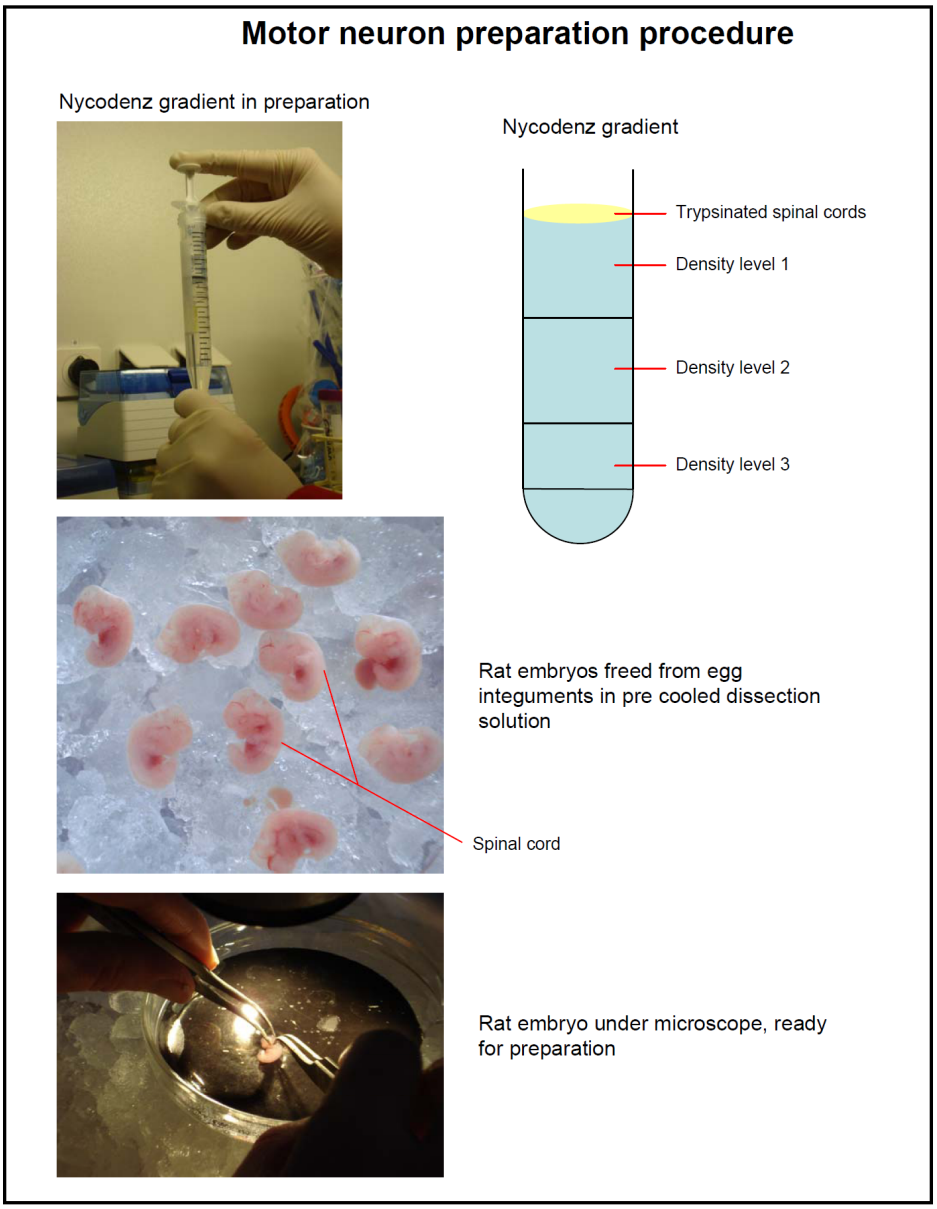

Fig. 04: Motor neuron preparation procedure

The figure shows the preparation procedure for primary motor neurons from rats. Therefore, a Nycodenz gradient with three density layers is prepared with a syringe in a 15 ml falcon, which is later used to separate the motor neurons from other cells in the spinal cord. The embryos freed from egg integuments are depicted in a Petri dish and under the microscope where the spinal cords are extracted from the embryos.

Our aim was to establish a culture of motor neurons with a very high purity, so we could use the cells for transfection studies in a comparable fashion to cell lines. To achieve the highest concentration of motor neurons we at first varied the centrifugation steps and finally reached a purity of motor neurons of up to 70 %, determined by counting of SMI32 positive cells as described in *2.4.3 Counting of stained cells*. Moreover, we wanted to work with a culture that not only contained a high amount of motor neurons, but also was viable for a long period so we could study mature neurons. We found that our cultures were viable for up to seven weeks. That is when most of the neurons detached from the ground and went into apoptosis.

In order to study the development of the cultured motor neurons, immunecytochemistry was performed every day up to age of eighteen days in vitro when the morphology of the neurons did not seem to change anymore, whereas the neurites still grew longer. At day in vitro three (DIV), the cells became already SMI32 positive, but had only very short primary neurites. Most of them showed a polarization into two directions. In many cases we could detect many secondary neurites branching out from the primary neurites, forming into a ramified bundle *(Figure 05)*.

On DIV 5 the bundle of branching out neurites had already developed into several larger primary neurites, suggesting an organization into dendrites and the axon. The pre-synaptic vesicle membrane glycoprotein synaptophysin could also be seen already this early, but could be more abundantly detected with each day that the cells grew. At first, synaptophysin could only be detected in a very indistinct pattern giving the impression of a rather blurred distribution, but from DIV 5 on the staining became more conspicuous and precisely located at synaptic sites. Soon, the neurites grow out and could not be displayed in one visual field anymore. On DIV 18 the amount of synapses had ascended to a very high level as illustrated by the synaptic marker synaptophysin.

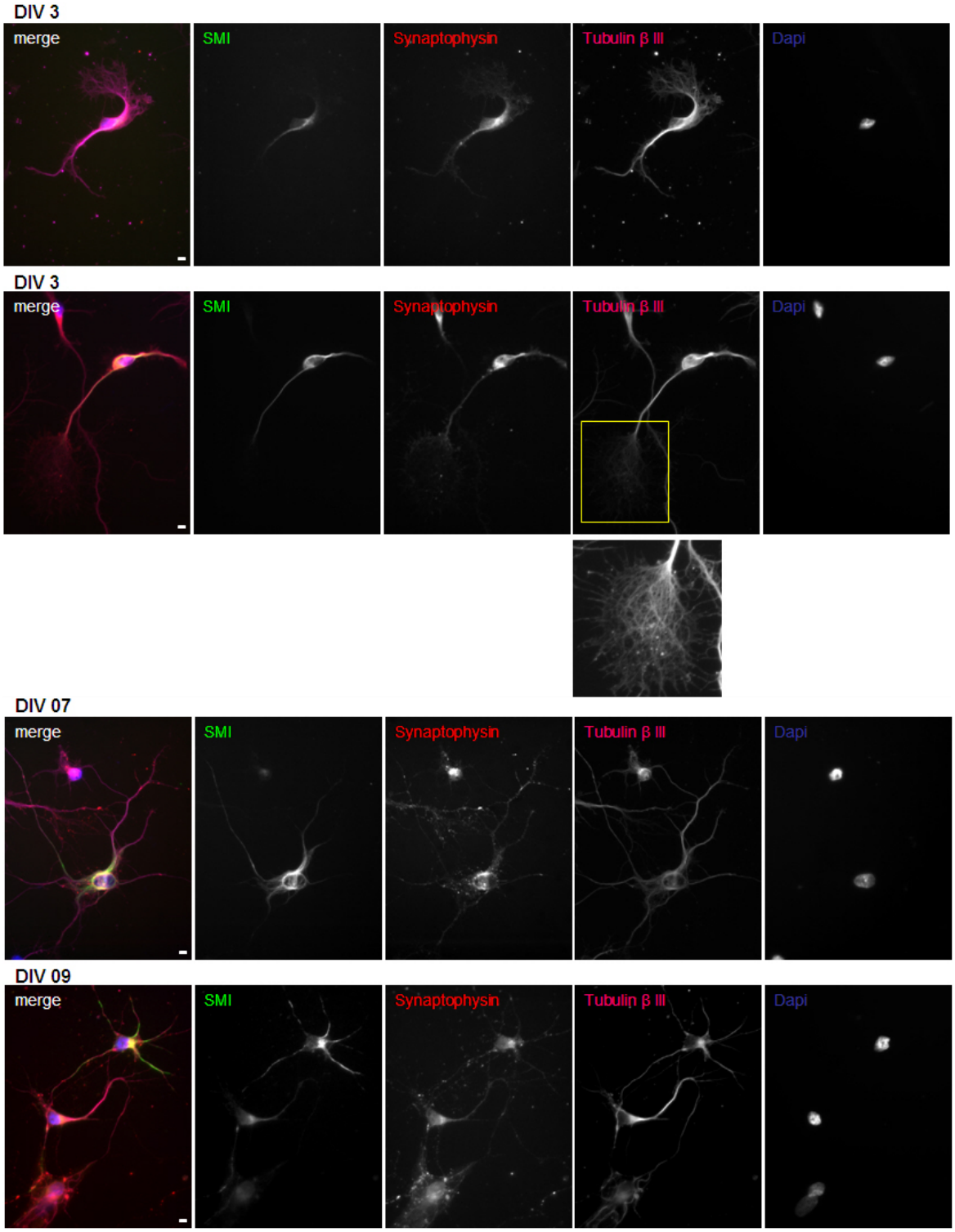
DIV 3
merge
SMI
Synaptophysin
Tubulin β III
Dapi
DIV 3
merge
SMI
Synaptophysin
Tubulin β III
Dapi
DIV 07
merge
SMI
Synaptophysin
Tubulin β III
Dapi
DIV 09
merge
SMI
Synaptophysin
Tubulin β III
Dapi

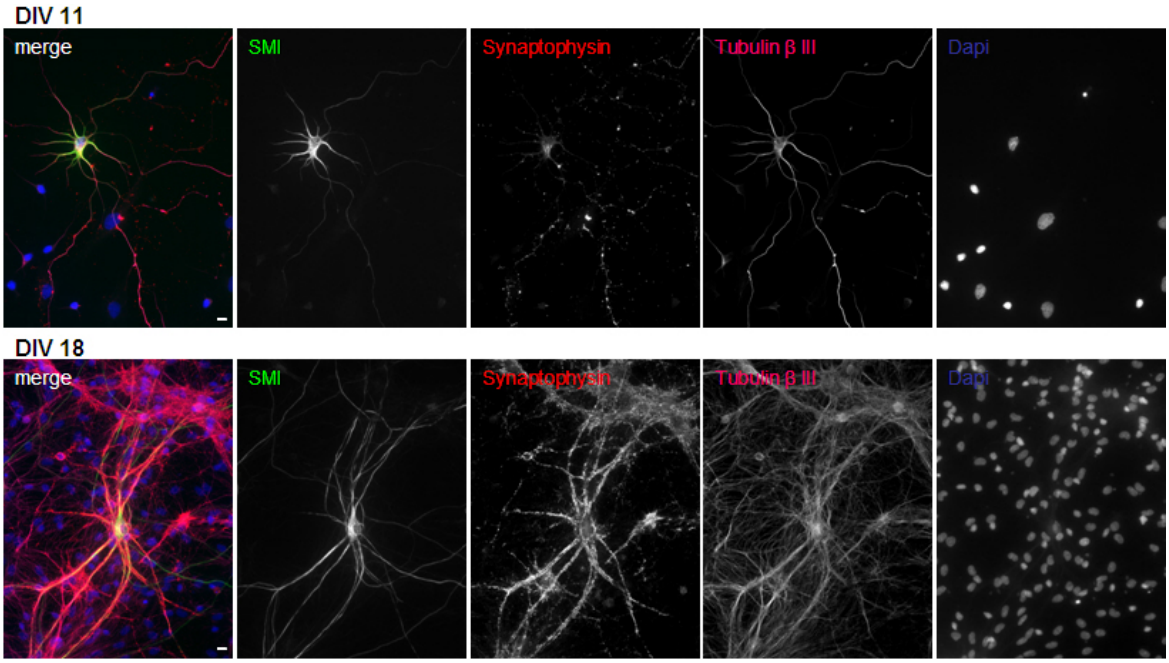

Fig. 05: Motor neuron development

scale bar: 10 µm *Dapi: 4',6-diamidino-2-phenylindole*
DIV: day in vitro
SMI: motor neuron marker
Development of primary motor neurons is shown from DIV 3 to DIV 18. The cells are stained with SMI (green), to show that motor neurons are used and tubulin-β III (magenta), a neuron specific marker of the microtubule cytoskeleton. To show the enrichment with synapses, synaptophysin (red) is used as a synaptic marker. The cell nuclei are stained with Dapi (blue).

For the purpose of characterizing the synapses a little further, we performed different synaptic immunecytochemical stainings. On that account we used pre- and postsynaptic markers including synaptophysin and proline rich synapse associated protein (ProSAP2) *(Figure 06)*.

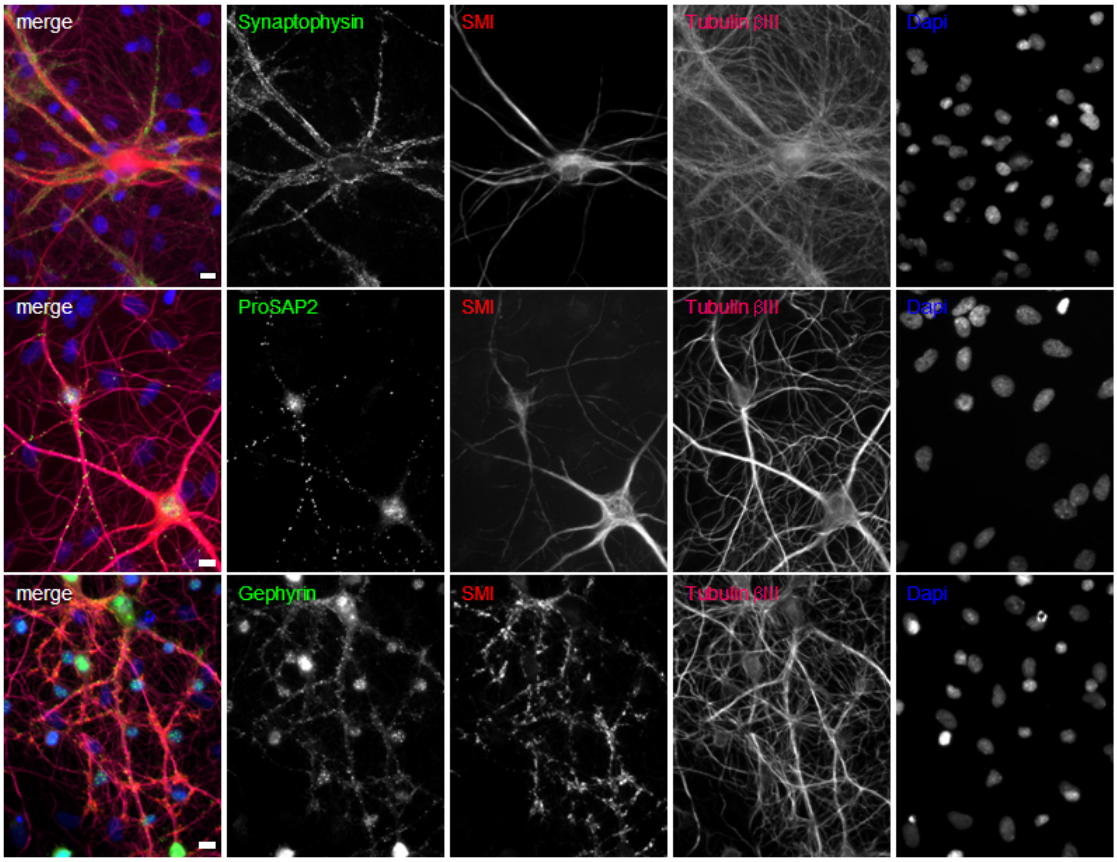

Fig. 06: Synapses in primary motor neuron cultures

scale bar: 10 µm, *Dapi: 4',6-diamidino-2-phenylindole*
ProSAP2: proline rich synapse associated protein 2
SMI: motor neuron marker
Primary motor neuron cultures were analysed for their synaptic contacts distribution. Synaptophysin, a pre-synaptic vesicle protein, ProSAP, a postsynaptic scaffolding molecule, and gephyrin, an inhibitory synapse marker, are depicted in green. SMI specifically stains motor neurons (red). Tubulin-β III (magenta) is a neuron specific marker of the microtubule cytoskeleton. Cell nuclei are stained with Dapi (blue).

Furthermore, we looked at inhibitory markers like gephyrin. We used motor neurons on DIV 18, as the neuritic network is best pronounced from DIV 18 on. Synaptophysin, a general pre-synaptic marker and a vesicle membrane glycoprotein, showed a very widespread distribution along the motor neuronal neurites, indicating that the cultures undergo the normal development of forming synaptic contacts. ProSAP2, a postsynaptic density protein, which functions as a scaffolding molecule, especially in excitatory synapses, could also be very abundantly detected along the neurites of the motor neurons. A very high amount of the synaptic contacts appears to be of inhibitory nature, as is indicated by the marker of inhibitory synapses gephyrin.

In order to decide which markers would be helpful for further studies with the mutations, we stained the untransfected motor neuron cultures for the cytoskeletal marker tubulin to visualize the microtubules in the cells *(Figure 07)*.

We used both tubulin-α and tubulin-β to see if the structures overlap completely. Tubulin-α detects any tubulins in the culture, whereas for the tubulin-β we used a neuronal specific subspecies, tubulin-β III, which only reacts with neuronal tubulins. Hence, we later used only the neuronal specific tubulin-β III, as it would not show the glial cells. Also, we stained for glial fibrillary acidic protein (GFAP) to visualize the remaining glial cells in our cultures. Regarding these cytoskeletal stainings, we found that the motor neurons had formed a very intensely branched network, interacting with each other via synaptic contacts. This observation was very important for us as only a functionally intact neuronal network would be of avail for further transfection studies.

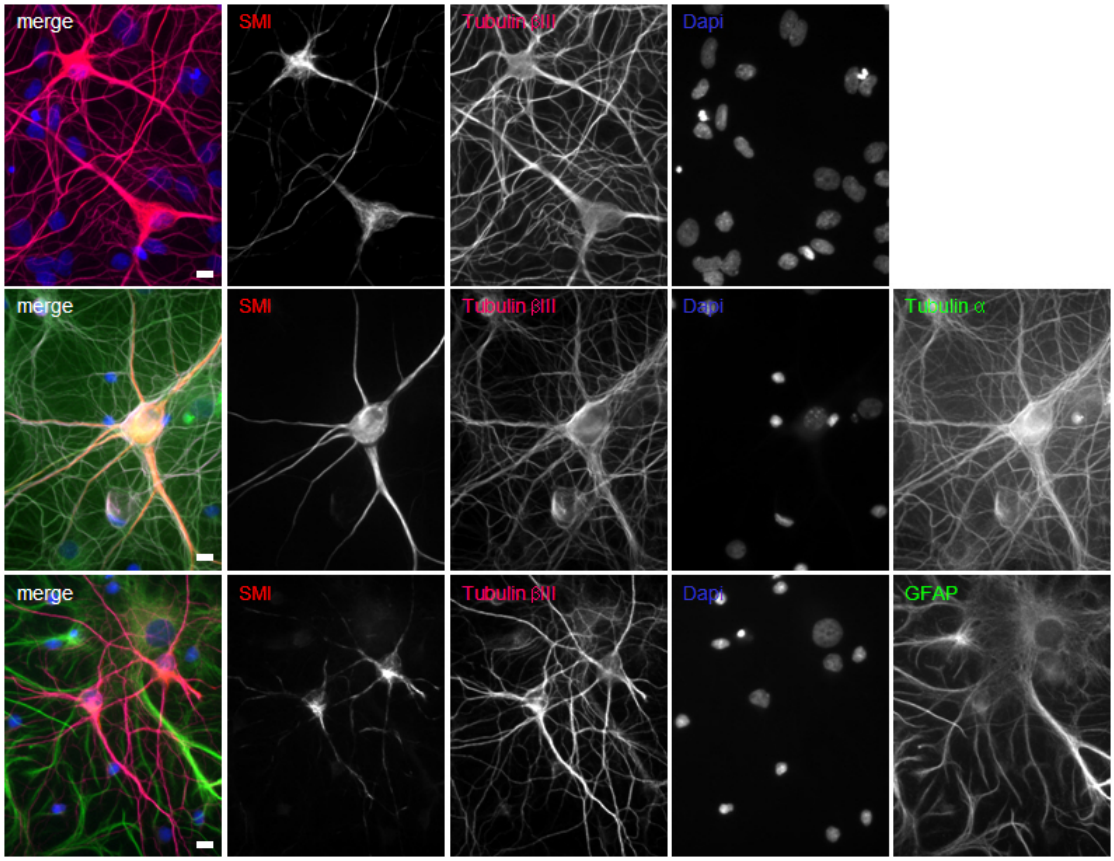

Fig. 07: Tubulins in motor neurons

scale bar: 10 µm *Dapi: 4',6-diamidino-2-phenylindole*
GFAP: glial fibrillary associated protein
SMI: motor neuron marker
The cytoskeleton of motor neurons is depicted, using different microtubule markers. Tubulin-β III (magenta) is a neuron specific microtubule marker, whereas tubulin-α (green) is not specific and stains microtubules in all cell types. Both tubulins co-localize completely in motor neurons. GFAP (green) is used to display the glial cells in the cultures; it stains glial cell specific intermediate filaments. SMI (red) is used as a motor neuron marker. Nuclei are stained with Dapi (blue).

Given that we wanted to use the motor neuron culture for transfection studies with different GFP-constructs of p150, we needed to allow for best transfection rates. We found out that the best time for transfection is between DIV5 and DIV10.

To visualize the expression of endogenous p150, the dynein intermediate chain as the direct interaction partner of p150, and tubulin-α, we performed a western blot using rat brain lysates and lysates of spinal cords of rat embryos from E14. We found that each of the three proteins was expressed highly in rat brains as well as spinal cords *(Figure 08)*.

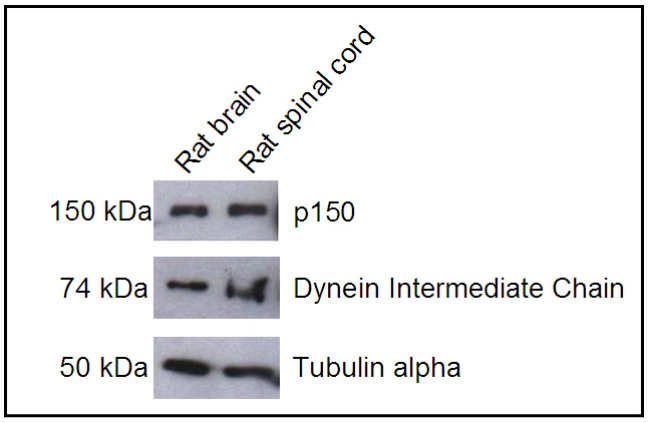

Fig. 08: Western blots of p150, tubulin and dynein IC in rat brain and spinal cord

IC: Intermediate chain
kDa: kilo Dalton
E14: embryonic day 14
To provide evidence that p150, tubulin-α, and the dynein intermediate chain are expressed in rat brain and spinal cords of rat embryos, a western blot detecting these proteins was performed using lysates. The brain was taken from an adult rat and the spinal cords were taken from rat embryos on E14, the same day motor neurons are prepared from embryo spinal cords.

3.2. Morphological studies of the p150 mutations in cell lines

In addition to the primary motor neurons, we chose to work with a cellular system that is not as sensitive as the primary motor neurons. We decided to use Cos-7 cells, because they are a cell line from kidney fibroblasts of the African green monkey, which is easily transfectable and endogenously expresses all the different proteins that we wanted to study. Additionally, Cos-7 cells have a very flat cell body and cytoskeletal elements can better be examined after immunecytochemistry than in a spherical cell body. At first we had a closer look at the normal appearance of Cos-7 cells and stained the untransfected cells for different cytoskeletal elements and proteins that are parts of the dynein/dynactin complex *(figure 09)*.

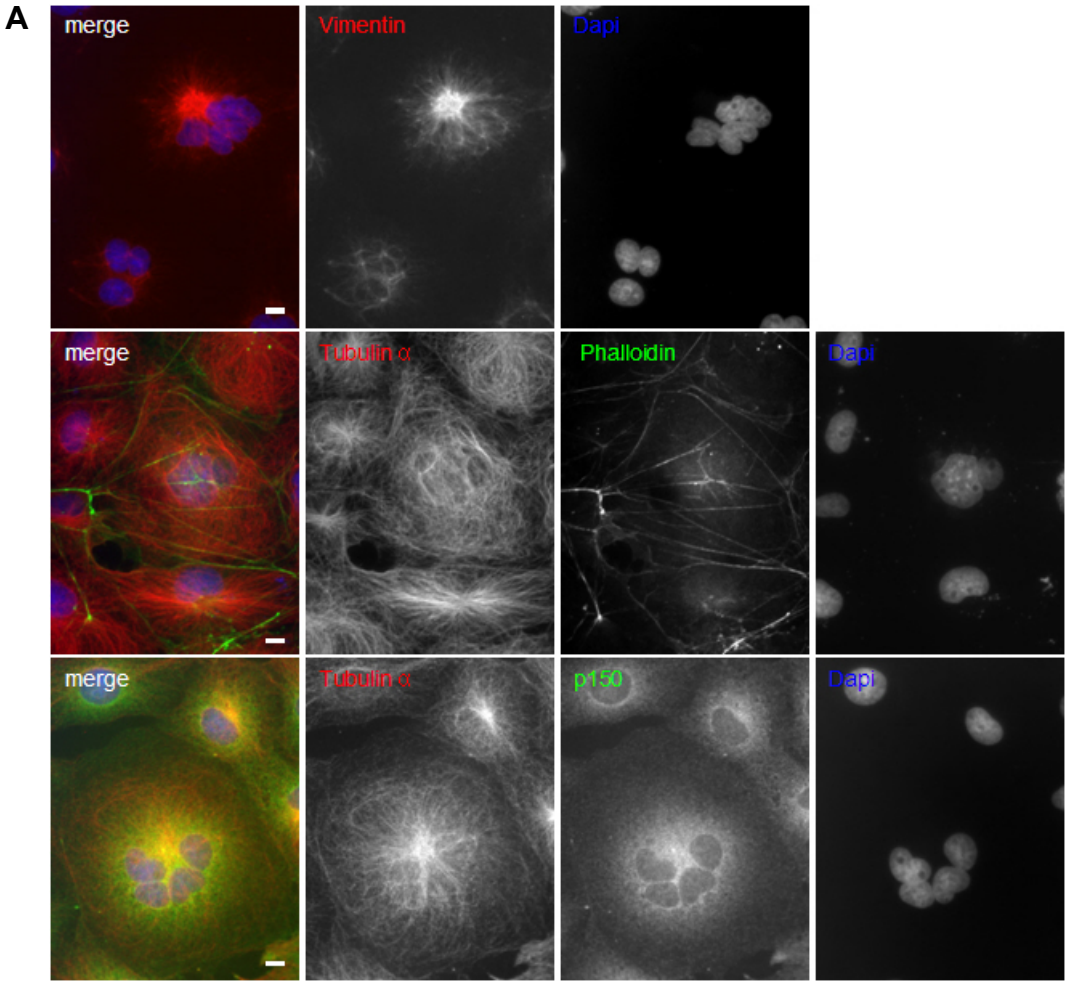
A
merge
Vimentin
Dapi
merge
Tubulin α
Phalloidin
Dapi
merge
Tubulin α
p150
Dapi

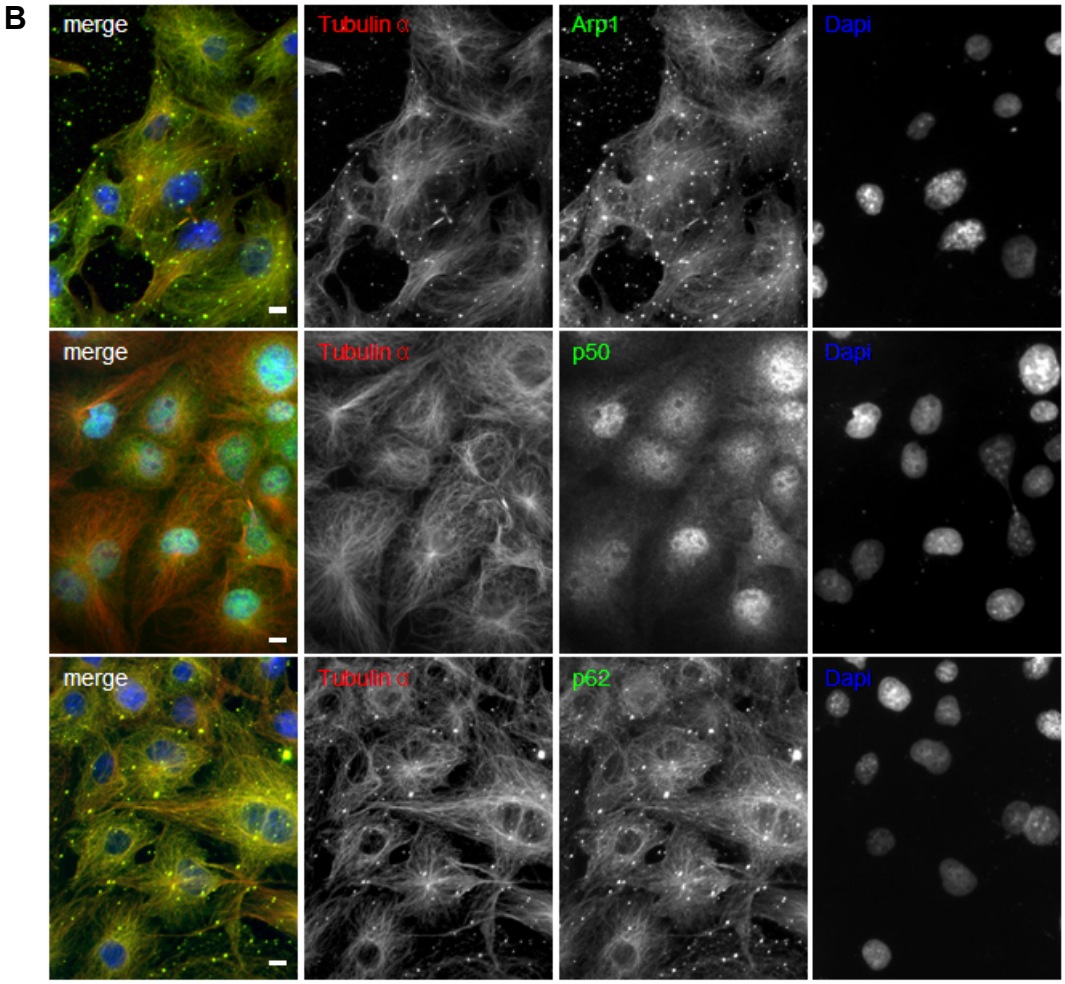

Fig. 09: Characterization of the cytoskeleton and the dynactin complex in Cos-7 cells

scale bar: 10 µm *Dapi: 4',6-diamidino-2-phenylindole*
Arp1: actin related protein 1
To characterize the cytoskeletal set of the different components, we stained Cos-7 cells for tubulin-α (red), representing the microtubules, vimentin (red), representing the intermediate filaments, and phalloidin (green), representing the actin fibres. The dynactin complex is composed of several subunits. We displayed p150, the microtubule and dynein intermediate chain binding subunit, dynamitin (p50) in (A), the connecting subunit between the Arp1 rod and p150, and p62 in (B), all of which are depicted in green. Cell nuclei are stained with Dapi (blue).

At the cytoskeleton we focused on the microtubules, which were stained against tubulin-α. Here we discovered that the microtubule skeleton was spread out through the entire cytoplasm and that in some cells the microtubules seemed to be organised from one central focus point spreading out in different directions towards the cell membrane. However, this arrangement could not be described in every cell. Another cytoskeletal element, which we inspected, was the actin filaments. It was detected with phalloidin. Many of the detected filaments were located along the cell membrane, probably representing the cortical actin net and membrane skeleton, which is composed of stabilised actin filaments and interacting proteins. Other filaments seemed to span through the entire cell, also

crossing through the cell centre. In the cell, actin filaments are often bundled into networks. The third component of the cytoskeleton is the intermediate filaments. We stained against vimentin, a marker of type III intermediate filaments, which are found in mesenchymal cells, to display the distribution of intermediate filaments in Cos-7 cells. In most of the cells the intermediate filaments seemed to be organised from one focal point close to the nucleus directing in a star like manner to the periphery of the cell. In other cells, the intermediate filaments appeared to be organised more widely in the cytoplasm with several densifications, probably demonstrating the points, where they fix organelles in the cytoplasm.

Since we wanted to study the impact of the mutations on the whole dynactin complex, we had a look at the endogenous dynactin in Cos-7 cells. Therefore we stained against several different subunits of the dynactin complex. At first we looked at the p150 subunit itself, which was evenly distributed in the entire cell, sparing only the nucleus with a finely punctated pattern. Around the nucleus, a little densification of p150 could be observed. On the contrary, the Actin related protein (Arp1) showed a filamentous pattern and co-localized with tubulin-α, suggesting an interaction between the microtubules and the Arp1 rod, either directly or through other subunits of the dynactin complex. Dynamitin or p50, the connecting subunit between p150 and the Arp1 rod, again showed a punctate pattern, but very slightly there was a fine co-localization also with the microtubules, represented by the tubulin-α staining. The ostensible nuclear distribution was due to the antibody not to an actual nuclear distribution. The p62 subunit then showed a pattern that was very similar to Arp1 distribution. A complete co-localization with tubulin-α could be detected for p62 as well.

3.2.1. Morphology of different p150 mutations in Cos-7 cells

After we had an idea of how the normal cytoskeleton on Cos-7 cells is organised and what the distribution of the dynactin complex is like, we transfected the Cos-7 cells with the different constructs of mutated p150 *(Figure 10).* We used the wild type GFP-tagged construct as control. Additional to the wild type control, we used a construct with a G59S mutated p150 as gold standard, since this mutation had been previously described as a disease causing mutation. At first we looked at the transfected empty GFP-vector to get an impression of how GFP itself arranges in

the cell. The GFP-transfected cells looked evenly transfected with a relatively equal dispersion among the cytoplasm. Around the nucleus there was a little enrichment detectable and throughout the cell, several vacuoles without any GFP could be detected. There was no co-localization with tubulin-α observable. The wild type construct showed an arrangement that completely co-localized with the filamentous structures of tubulin-α. Very fine filaments could be obtained that were arranged nearly circular around the nucleus.

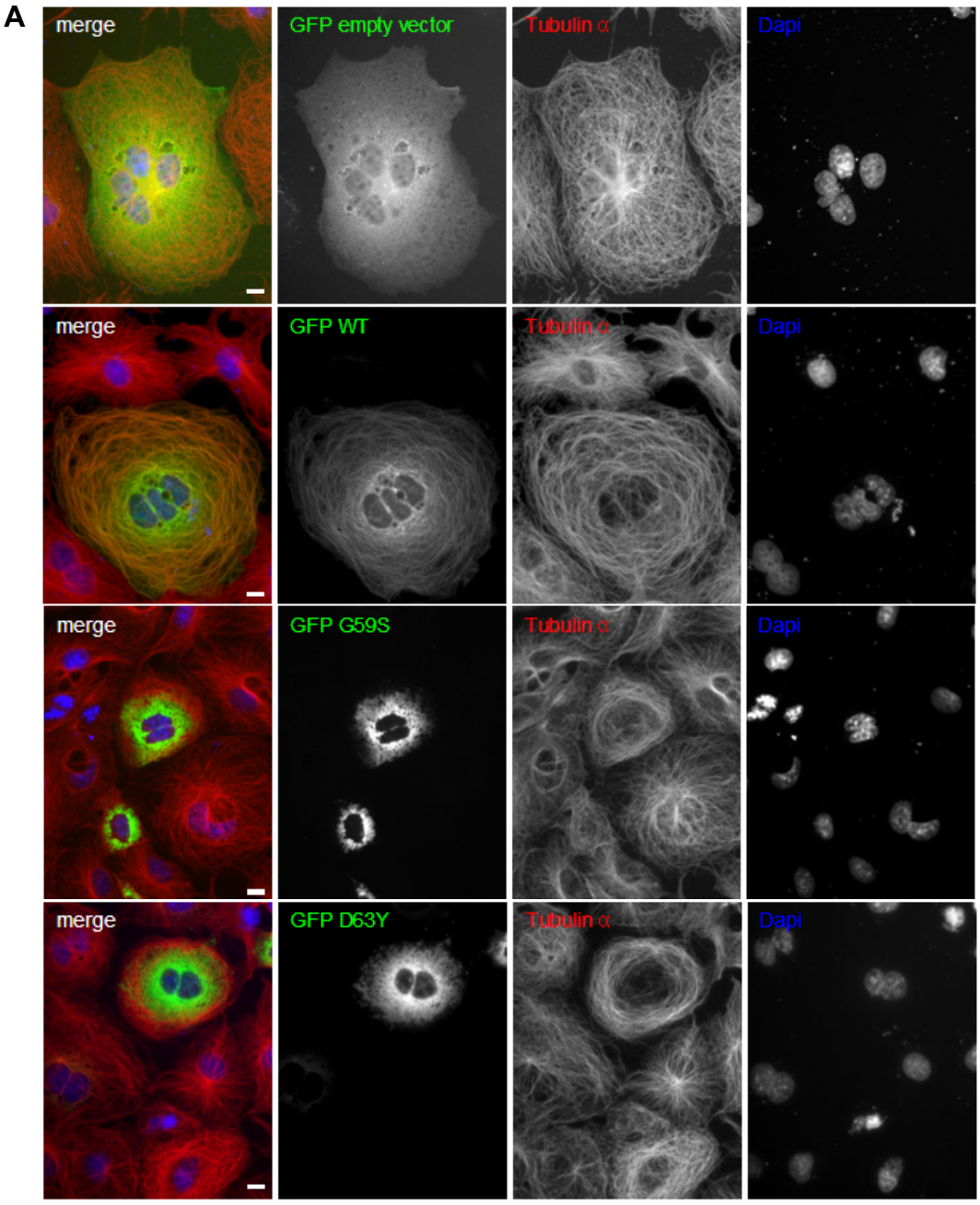

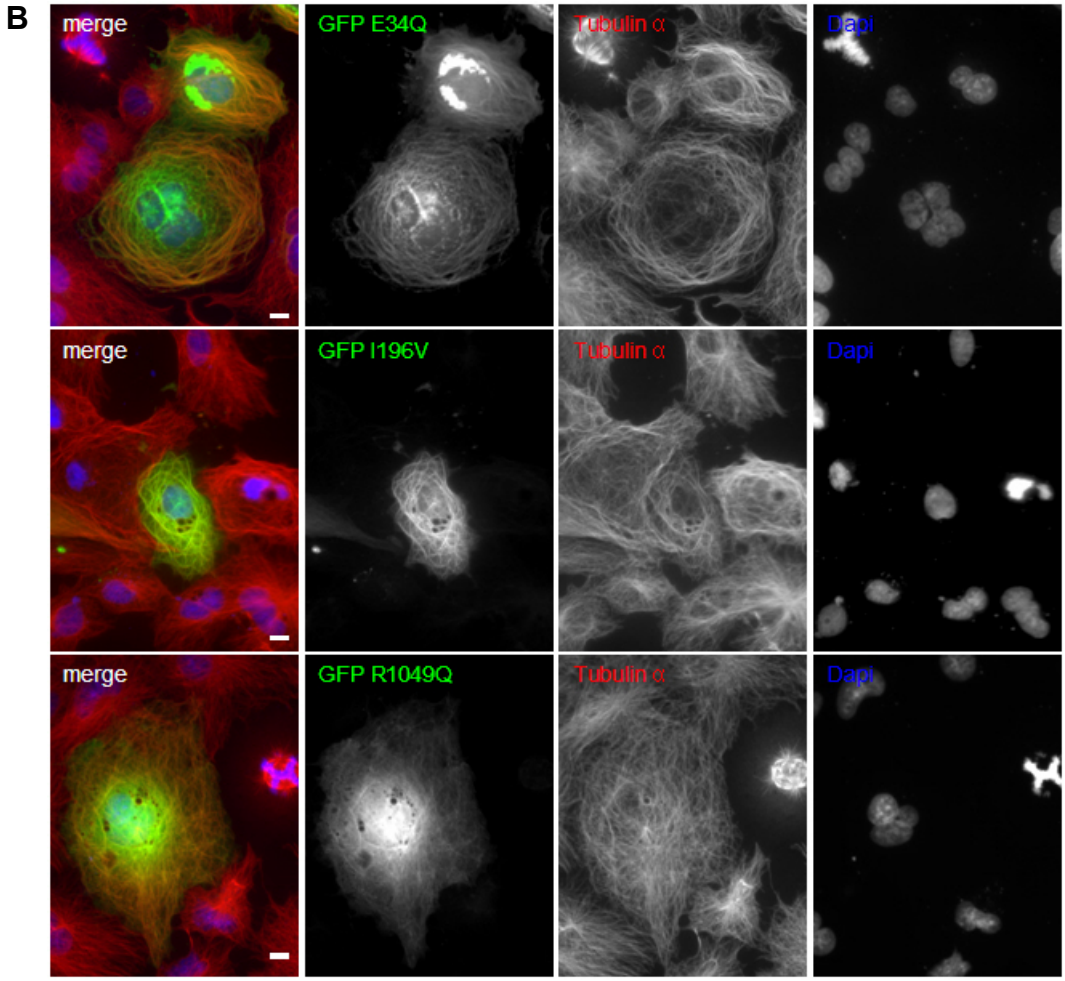

Fig. 10: Expression and distribution of mutated p150 in Cos-7 cells

scale bar: 10 µm *Dapi: 4',6-diamidino-2-phenylindole*
GFP: green fluorescent protein
Cos-7 cells are transfected with p150 in a GFP-vector (green) and stained against tubulin-α (red). Cell nuclei are stained with Dapi (blue). (A)The over expressed wild type dynactin p150 shows a fibre like distribution in the cell that is consistent with the immunecytochemical staining of tubulin-α. Cos-7 cells, over expressing mutant G59S and D63Y p150, show large scale cytoplasmic inclusions of aggregated p150. (B) E34Q p150 over expressed cells show inclusions and p150 that co-localizes with tubulin at the same time. The distribution of I196V p150 is filamentous with co-localization with tubulin, which appears thickened compared to the wild type. The R1049Q p150 displays an amorphous pattern of p150 additional to few very fine fibres, which co-localize with tubulin-α.

All characterized mutated DCTN1 constructs displayed variations in distribution, localization and formation of intracellular clusters.The feature which distinguishes the wild type from our gold standard, the G59S, was the formation of aggregates. Cells transfected with this mutated construct showed aggregates of p150 that were spread out through the entire cell with a concentration around the nucleus. The aggregates varied in size. Sometimes they presented as one continuous big aggregate *(Figure 10*) and occupied a significant portion of the cytoplasm, but they could also present as smaller aggregates that were disseminated throughout the

entire cell *(Figure 19).* The aggregates of p150 showed no co-localization whatsoever with tubulin-α, but were independently located in the cell.

Very similar to the gold standard G59S presented the mutation D63Y, which is also located in exon 2. Also in cells transfected with the D63Y mutated construct we observed the formation of granular, non fibrillary inclusions that looked very much alike the aggregates found in cells transfected with the G59S construct. Very comparable to the gold standard, we found a massive accumulation of intracellular inclusions in D63Y transfected cells. Likewise, we could distinguish between cells that presented with one continuous perinuclear cluster and cells that showed smaller aggregates spread out throughout the cytoplasm. The second mutation that is also located in exon 2, the E34Q, has to be grouped somewhat between the wild type and the gold standard. In this mutation the filamentous structure of p150 was not completely abolished as clusters and filaments could be detected at the same time. Those filaments, that could be seen, co-localized perfectly with tubulin-α, whereas the clusters were located very closely to the nucleus. The aggregates in this mutation also did not co-localize with tubulin. The I196V showed a very different phenotype from all the other mutations. No aggregates of p150 could be detected. Instead we observed a filamentous structure that also co-localized with tubulin-α. But the striking difference was that these filaments appeared to be thickened compared to wild type transfected cells and also the surrounding non transfected cells. The last mutation, the R1049Q also presented with a very peculiar phenotype. At first sight the pattern of p150 resembled the empty GFP-vector transfected cells with an amorphous distribution among the entire cell. But after a closer look there was also a very fine filamentous pattern observable additionally to the diffuse dispersal of p150. These filaments co-localized with tubulin-α.

To asses, whether the inclusions found in the cytoplasm were really comprised of p150 aggregates, we used a p150 antibody to detect p150 itself. We found a complete co-localization of p150 stainings and GFP-labelled inclusions *(Figure 11).*

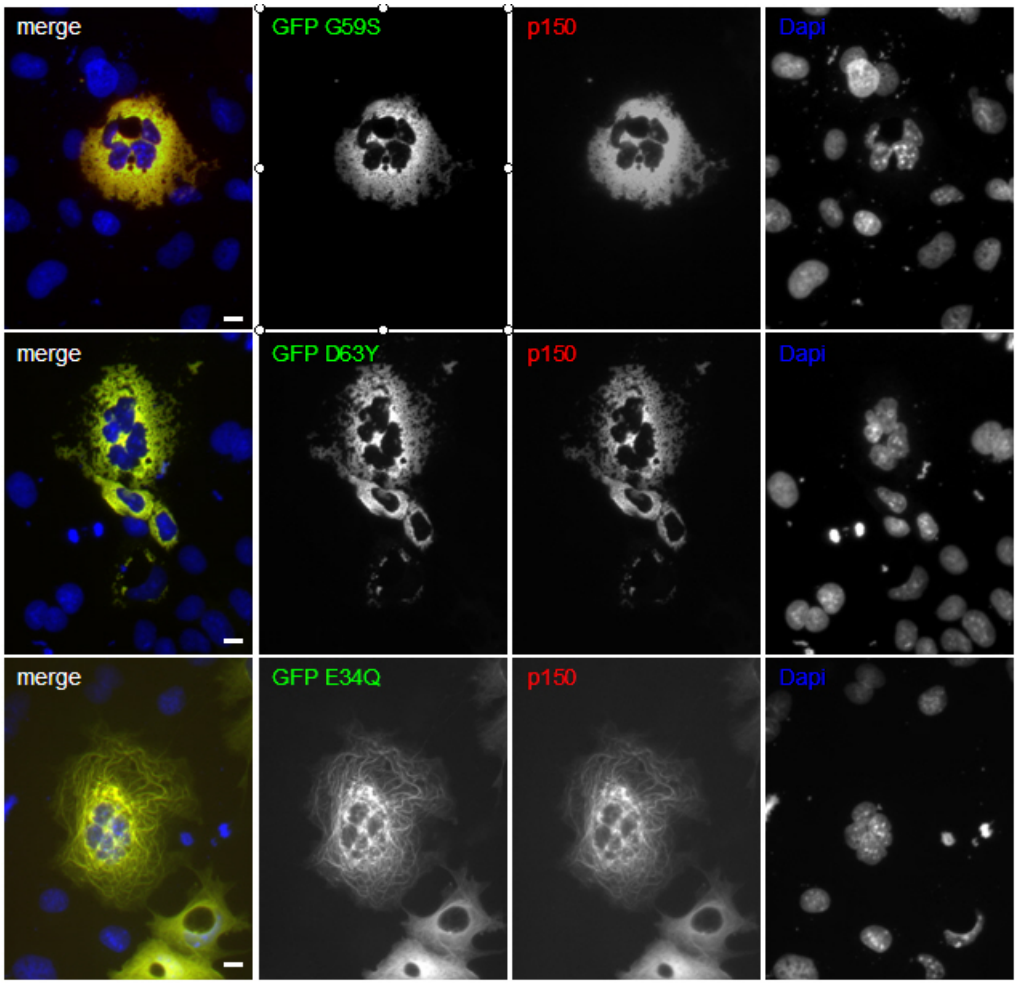

Fig. 11: Proof of p150 detection

scale bar: 10 µm *Dapi: 4',6-diamidino-2-phenylindole*
GFP: green fluorescent protein
To proof that the inclusions really consist of aggregated p150, we stained these inclusion for p150 (red) and found a complete co-localization of p150 staining and over expressed GFP-tagged p150 (green). Cell nuclei are stained with Dapi (blue).

3.2.2. Time dependency of the formation of aggregates

Because of the distinctive feature of the formation of p150 subunit aggregates, we decided to further investigate this feature. Since the aggregates could also be detected in wild type transfected cells after a certain duration of transfection, we decided to check the time dependency of clustering in transfected cells *(Figure 12)*. Accordingly, we checked two different time points of transfection. We determined the percentage of cells showing aggregates of p150 after six hours and after sixteen hours of transfection. For the wild type we found a percentage of three percent after six hours in comparison to 22 percent after six hours. So even after a very short period of transfection we could find cells that were showing some form

of aggregates. But never could we find cells that resembled the gold standard as even after a longer period of transfection the cells still showed a filamentous dispersion of p150 with the addition of some aggregates. The gold standard G59S showed only aggregates, even after just six hours of transfection 100 percent of all transfected cells displayed aggregates. Nearly the same applied to the D63Y mutation in which we observed a percentage of 94 percent after six hours and a percentage of 98 percent after sixteen hours of transfection. The remaining six, respectively two percent did not show any clustering but instead an amorphous distribution of p150. Another peculiarity was that the aggregates appeared to become gradually larger in size with a longer transfection period. So after sixteen hours more of the continuous dense large inclusions could be detected. The E34Q mutation presented with a rather big percental difference between the two time points. After six hours of transfection only thirteen percent of transfected cells could be detected, whereas the percentage increased to 61 percent after sixteen hours. Even then in all transfected cells a filamentous structure of the remaining non aggregated protein was found. The percentage of cells with protein aggregates of the I196V mutation resembled very much the wild type. After six hours eight percent could be determined and after sixteen hours the amount ascended to 26 percent. The R1049Q mutation also presented with quite a disparity between the two time points with four percent after six hours and 42 percent after sixteen hours. In contrast to the protein aggregates in the gold standard and the D63Y mutation, they were mainly located around the nucleus and not scattered in the whole cell.

A

	6 h transfection	16 h transfection
Wild type	3 %	22 %
G59S	100 %	100 %
D63Y	94 %	98 %
E34Q	13 %	61 %
I196V	8 %	26 %
R1049Q	4 %	42 %

B

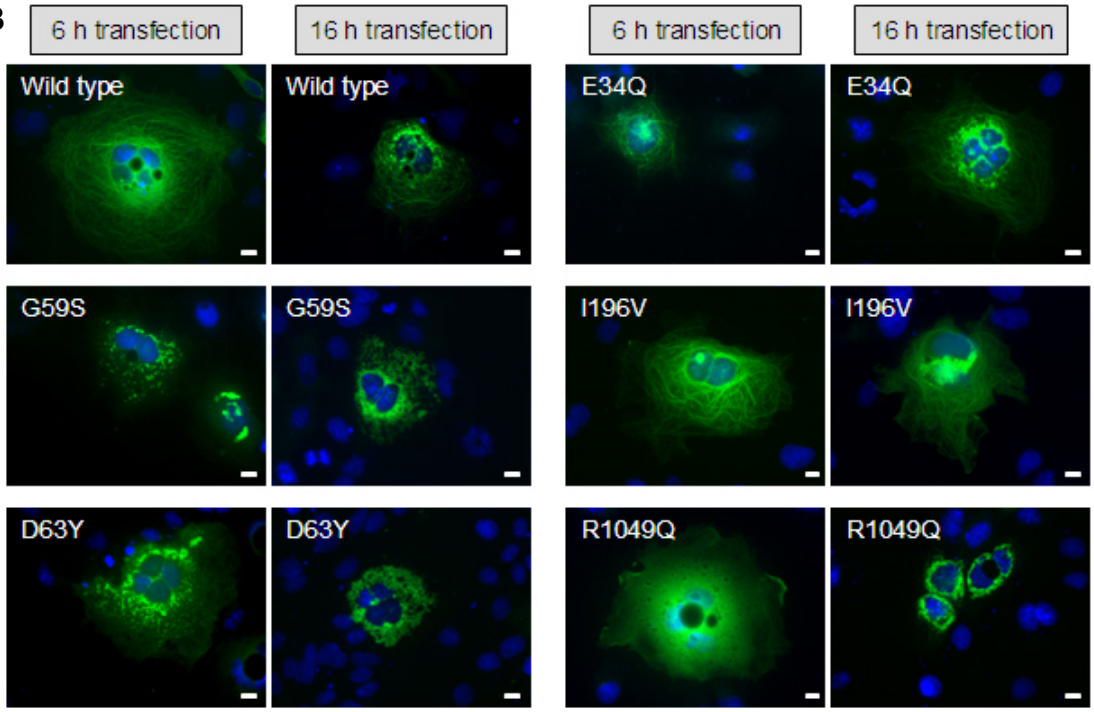

Fig 12: Clustering ratio of p150-transfected Cos-7 cells

scale bar: 10 µm *Dapi: 4',6-diamidino-2-phenylindole*
GFP: green fluorescent protein
Cos-7 cells are transfected with p150 in a GFP-vector (green) and the cell nuclei are stained with Dapi (blue). (A) The chart shows the percentage of cells with obvious clusters of over expressed protein in the cells. The counting was done after six hours and after sixteen hours of transfection. 200 cells were counted for each sequence change. (B) Exemplarily, each sequence change and the wild type are shown after six hours and sixteen hours transfection.

3.3. Over expression of mutated p150 in motor neurons

After we had over expressed the dynactin p150 subunit in Cos-7 cells, we also wanted to see the effect of transfections in our primary motor neuron system. First of all we compared the wild type p150 in Cos-7 cells to wild type p150 in motor

neurons. To be sure that both cell types express dynactin p150 also endogenously, we performed a Western blot analysis looking for p150 and as a loading control for β-actin *(Figure 13)*. In both Cos-7 cells and motor neurons endogenous p150 could easily be detected.

To assure that the transfected GFP construct can be detected with the same antibody that was used for endogenous dynactin p150, we also stained in transfected Cos-7 cells for p150 and found a complete congruence between the transfected GFP-p150 construct and the staining for p150.

Since we had worked with different tubulin subunits for both cell types, we wanted to show, that the tubulin-βIII subunit is a neuron specific subspecies, whereas tubulin-α is ubiquitously found in any cell type. In a Western blot analysis we could show that tubulin-βIII could not be detected in Cos-7 cells, whereas tubulin-α could be found in Cos-7 cells and motor neurons alike.

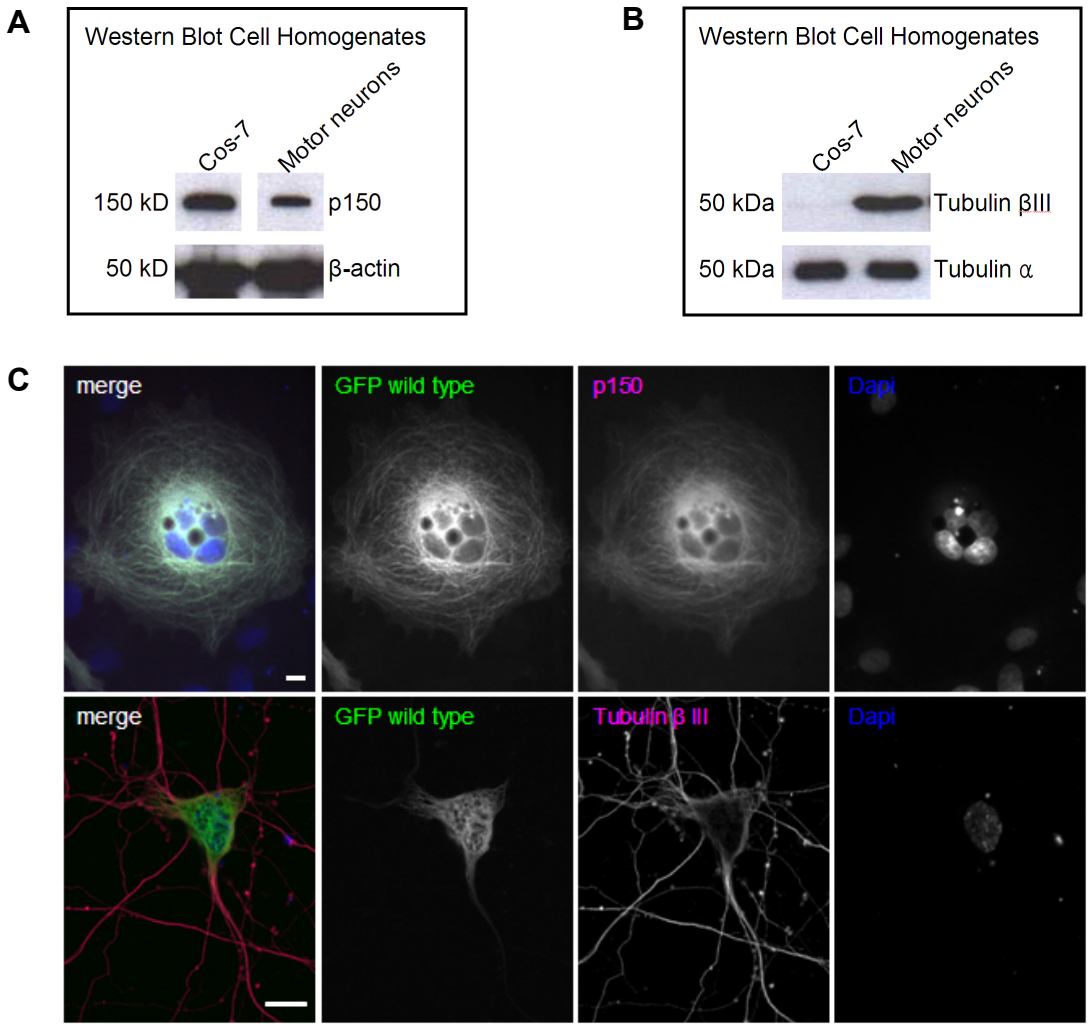

Fig. 13: Expression and distribution of p150 and microtubules in motor neurons and Cos-7 cells

scale bar: 10 µm *Dapi: 4',6-diamidino-2-phenylindole*
GFP: green fluorescent protein
(A) Western blot anti dynactin p150 shows the expression of endogenous p150 in primary rat motor neurons and Cos-7 cells. The staining against β-actin is used as a loading control. (B) Cos-7 cells and primary rat motor neurons are transfected with wild type p150 in a GFP-vector (green) and then stained against p150 in Cos-7 cells respectively tubulin-βIII in primary rat motor neurons (magenta). Cell nuclei are stained with Dapi (blue). The expression of over expressed wild type dynactin p150 in Cos-7 cells and motor neurons shows a fibre like distribution in the cell that is consistent with the immunecytochemical staining of p150 and tubulin-βIII. (C) Western blot anti tubulin-βIII and tubulin-α shows that tubulin-α is ubiquitously expressed in neurons and Cos-7 cells, whereas tubulin-βIII is a neuron specific tubulin subspecies.

We then compared the transfected motor neurons to Cos-7 cells. The principal of the morphological features, which were delineated before in Cos-7 cells, applied to motor neurons in a comparable fashion. The wild type transfected motor neurons showed a filamentous distribution in the cell body and neurites alike. These filaments co-localized with tubulin-βIII, a neuron specific microtubule marker, which is analogous to tubulin-α in Cos-7 cells. The morphological features of the gold standard G59S in motor neurons were very much the same as in Cos-7 cells

(Figure 14). Very obvious aggregates could be detected in the cytoplasm but also in the neurites in the axon and dendrites alike. Furthermore, the aggregates were also clearly separate from the tubular structures of the microtubules and showed no co-localization with tubulin. All this is to a somewhat lesser degree also true for the D63Y mutation. Aggregates of over-expressed p150 could also be detected in cells transfected with the D63Y mutation. These aggregates were located in neurites and the cell body and no co-localization with tubulin could be seen. Somewhat different did the E34Q transfected cells present. Similarly to the gold standard and the D63Y could we find aggregates of p150 in the cytoplasm and the neurites but to some extend also filamentous structures, which co-localized with tubulin, could be detected. That also reflects the morphology in Cos-7 cells. In sharp contrast to these two mutations, we could not observe aggregates in the I196V but instead also found thickened filaments here similar to the thickened filaments in Cos-7 cells. The co-localization of the filaments with tubulin could be confirmed in this mutation as well. The R1049Q mutation also showed a very similar characteristic in motor neurons compared to Cos-7 cells. p150 followed a very amorphous pattern, but additionally showed some very fine filaments though, that co-localized with tubulin. In summary, the morphological characteristics of the various mutations in motor neurons are very much comparable to those seen in Cos-7 cells.

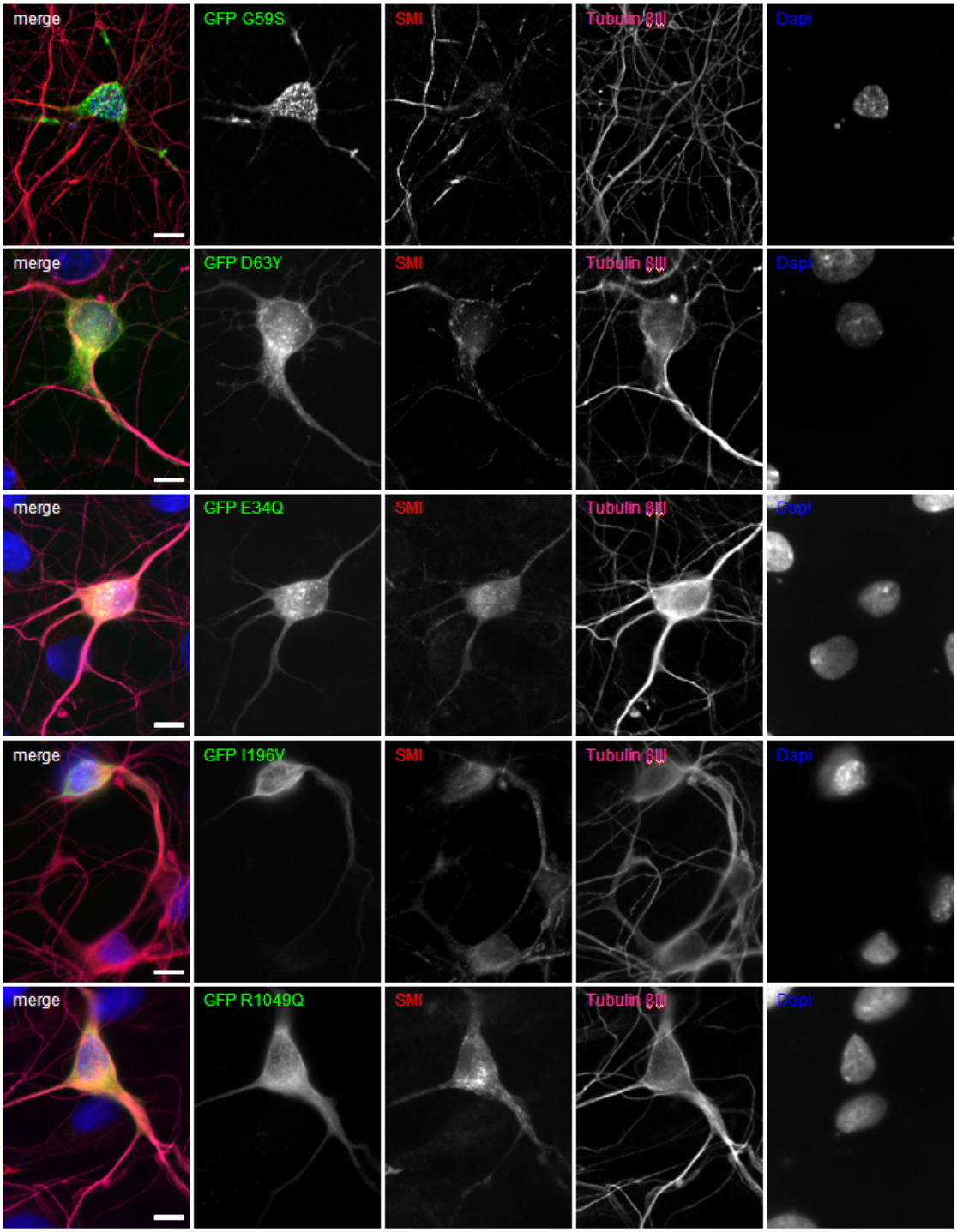

Fig. 14: Expression and distribution of mutated p150 in primary motor neurons.

scale bar: 10 µm *Dapi: 4',6-diamidino-2-phenylindole*
GFP: green fluorescent protein
SMI32: motor neuron marker
The motor neurons are transfected with GFP-tagged mutated p150 constructs (green). Motor neurons are stained with SMI 32 (red) and tubulin-βIII (magenta), a neuron specific microtubule marker. Very similar features of distribution of p150 compared to the Cos-7 cells can be observed. The G59S and D63Y p150 both show striking aggregates in the whole cell soma including axons and dendrites. The E34Q also shows formation of aggregates to a lesser extent, but still some tubular structures can be observed. In cells, transfected with I196V p150, the tubular structures appear thickened in comparison to the wild type. The distribution of the R1049Q looks amorphous and homogenous in the cell.

3.4. Impact of p150 mutations on other subcellular components in Cos-7 cells

To fully characterize the impact the p150 mutations might have on the cytoskeletal set up and on the whole dynactin/dynein complex, we went back to the Cos-7 cell system and over expressed the different GFP-tagged p150 constructs. Then we immunecytochemically determined different proteins of the cytoskeleton and the dynein/dynactin complex

3.4.1. The impact of p150 mutations on cytoskeletal elements

To continue the morphological studies in terms of where the mutated protein is located in the cell and what other parts of the cell might be affected, we investigated other structures of the cytoskeleton. Another very important part of the cytoskeleton, besides the microtubules, is the actin net. Accordingly, we used phalloidin to illustrate the arrangement of actin fibres in transfected cells *(Figure 15)*.

As described earlier with untransfected cells, many detected actin filaments could be located along the cell membrane but also spanning through the cell. The same arrangement of actin fibres could be revealed in transfected cells. The set-up was neither changed by transfections with wild type p150 nor by any of the mutations. Furthermore, no co-localization of any protein-aggregates and the actin-filaments could be detected.

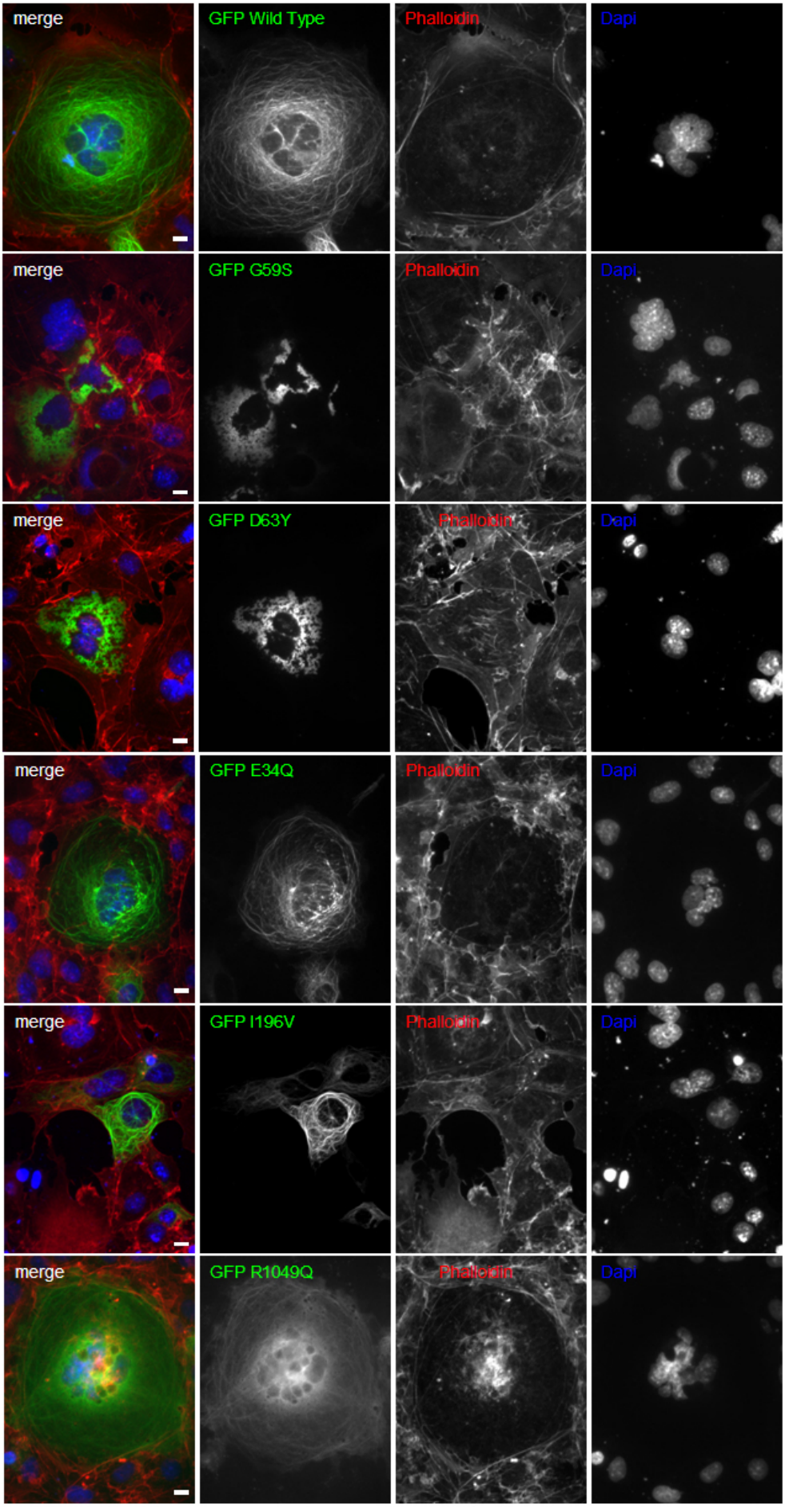
merge
GFP Wild Type
Phalloidin
Dapi
merge
GFP G59S
Phalloidin
Dapi
merge
GFP D63Y
Phalloidin
Dapi
merge
GFP E34Q
Phalloidin
Dapi
merge
GFP I196V
Phalloidin
Dapi
merge
GFP R1049Q
Phalloidin
Dapi

Fig. 15: Distribution of endogenous actin in p150 transfected Cos-7 cells

scale bar: 10 µm *Dapi: 4',6-diamidino-2-phenylindole*
GFP: green fluorescent protein
Cos-7 cells are transfected with a GFP-tagged p150 construct (green) and then stained against actin with phalloidin (red). Cell nuclei are stained with Dapi (blue). The actin cytoskeleton is organised near the inner face of the peripheral membrane and in the area around the nuclear membrane. This distribution is not affected by over expression of any of the modified proteins. The aggregates that are seen in G59S, D63Y, and E34Q, do not affect the localization of the actin cytoskeleton.

Intermediate filaments are the third component of the cytoskeleton. To display the intermediate filaments in Cos-7 cells, we stained against vimentin, the intermediate filaments found in mesenchymal cell types *(Figure 16)*.

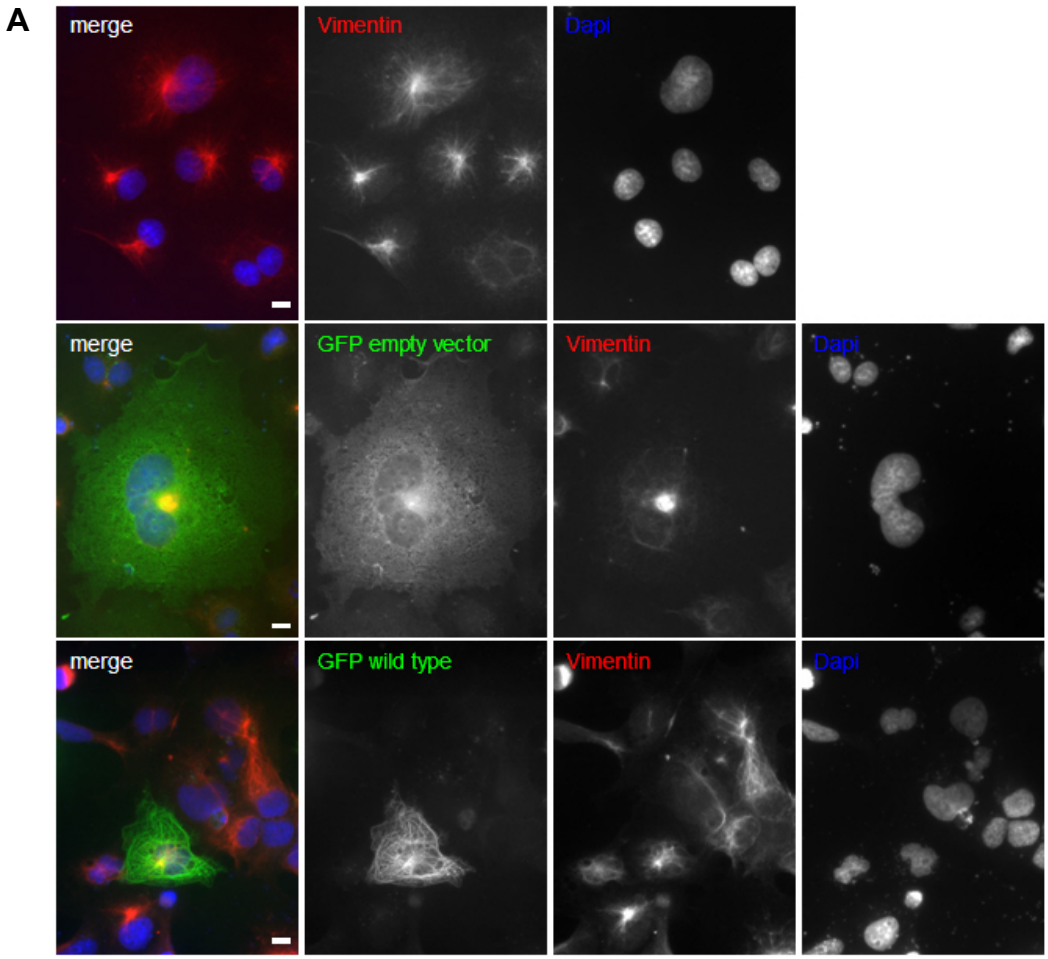

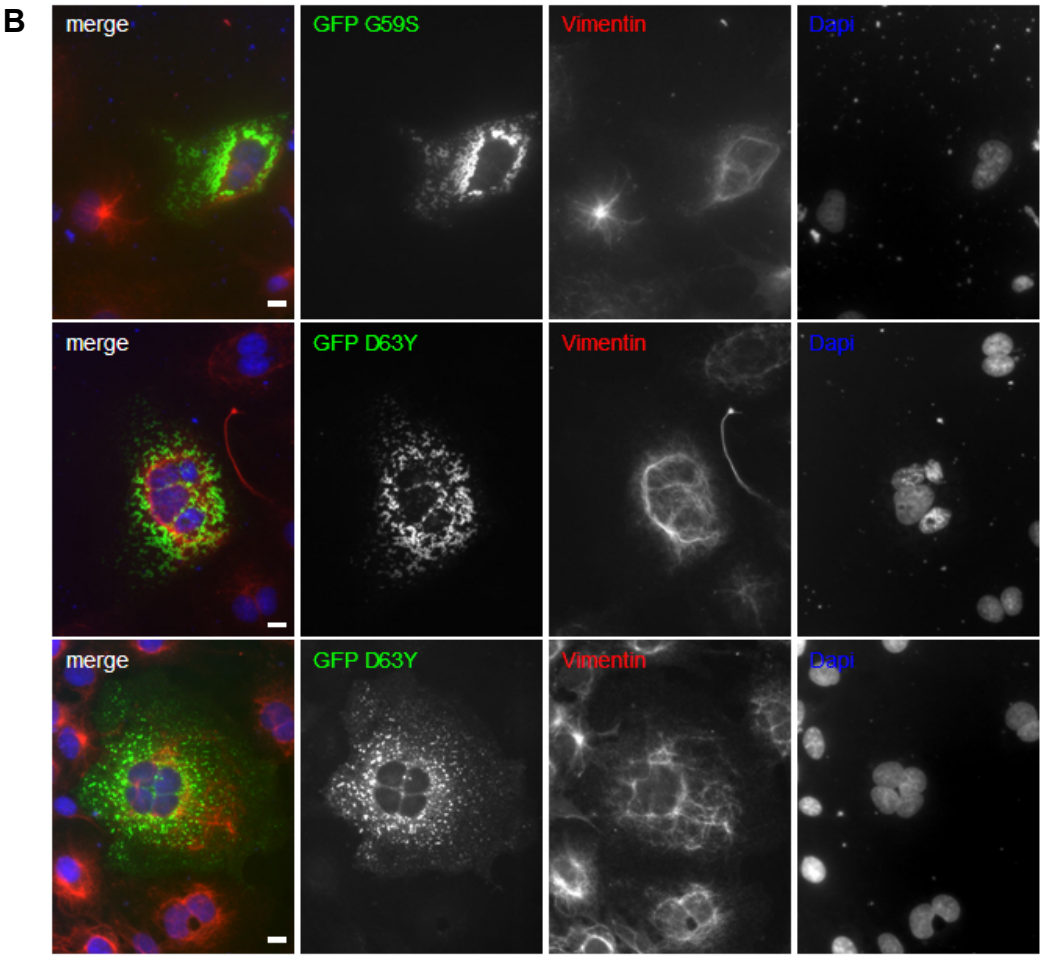
B
merge
GFP G59S
Vimentin
Dapi
merge
GFP D63Y
Vimentin
Dapi
merge
GFP D63Y
Vimentin
Dapi

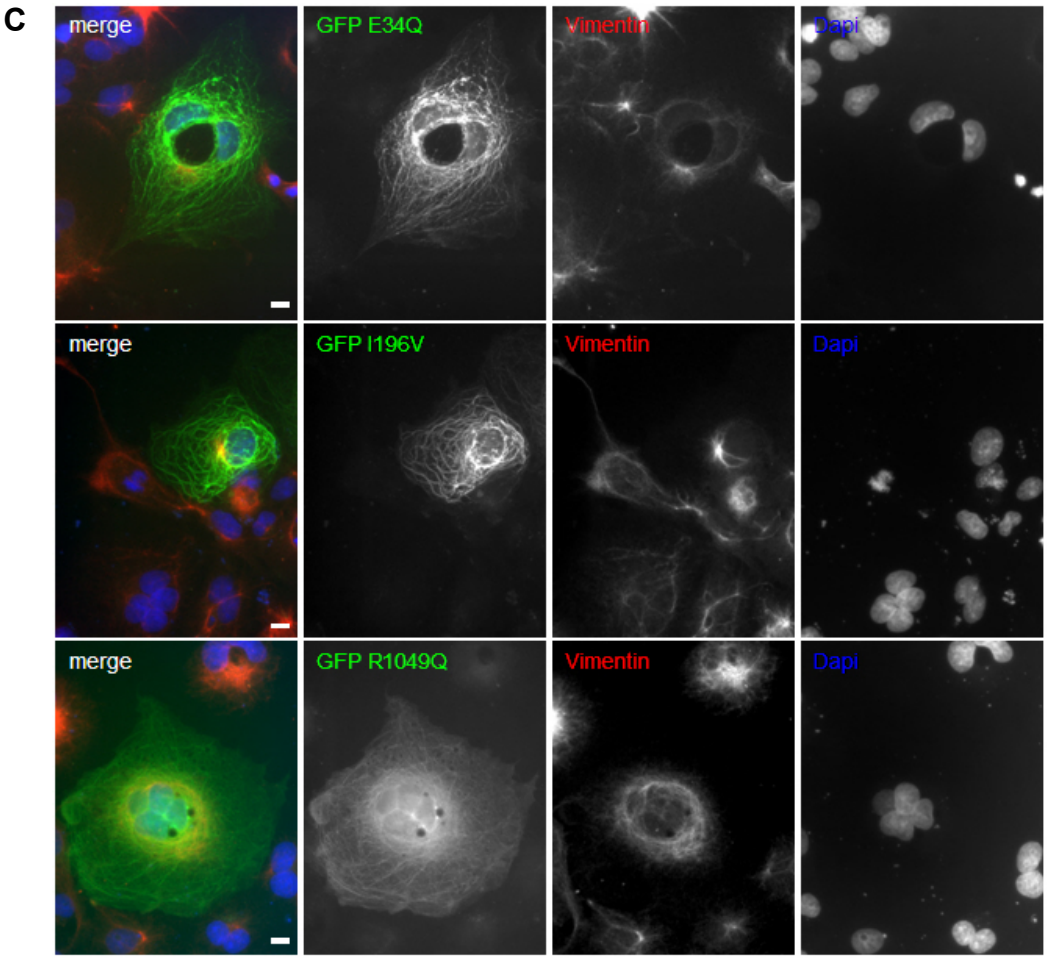

Fig. 16: Distribution of endogenous intermediate filaments in p150 transfected Cos-7 cells

scale bar: 10 µm *Dapi: 4',6-diamidino-2-phenylindole*
GFP: green fluorescent protein
Cos-7 cells are transfected with a GFP-tagged p150 construct (green) and stained against vimentin, mesenchymal cell specific intermediate filaments (red). Cell nuclei are stained with Dapi (blue). (A) The arrangement of intermediate filaments is shown in untransfected cells and cells transfected with an enmpty GFP vector as well as a wild type GFP vector. (B) The arrangement of intermediate filaments seems to be disturbed and reorganised in G59S p150 and D63Y p150 transfected cells, forming a circular cage around the nucleus and partly the inclusions. (C) In cells transfected with the remaining mutations no changes of the arrangement of intermediate filaments was observed.

We over expressed wild type p150, all mutated p150 constructs, and the empty GFP vector in Cos-7 cells. We found that neither in the wild type or empty GFP vector transfected cells the mutations induced any change of the arrangement of intermediate filaments. In the G59S and D63Y p150 transfected cells we saw a slight rearrangement of intermediate filaments. It appeared that in most of the transfected cells, the intermediate filaments seemed to form an oval rim around a central portion of the cytoplasm including the nucleus and enclosing some of the p150 inclusions but far not all of them. Especially those that were located more in the periphery were excluded. We also found that in very few D63Y p150

transfected cells, the arrangement of intermediate filaments seemed to be undisturbed when rather small inclusions showed a very scattered distribution all over the cytoplasm with no remarkable perinuclear accumulation. In cells transfected with other mutated p150 constructs, the intermediate filament set up was maintained in a way very similar to untransfected cells, most of them showing a star like arrangement close to the nucleus. Also, the E34Q p150 transfected cells showed no change in the intermediate filament arrangement. In the R1049Q p150 transfected cells, we saw very few cells as well, which suggested a slight difference to untransfected cells, with a rather round arrangement, but this observation was not consistent, as most of the cells presented with an unremarkable distribution.

3.4.2. Impact of p150 mutations on mitochondrial dispersion and morphology

Since the dynactin complex also plays an important role in cellular transport mechanisms like moving around subcellular compartments, amongst others, mitochondria, we focused on mitochondria, them being the most important energy supply of the cell. We started with transfection of a mitochondrial marker and later on co-transfected with the respective mutated p150 GFP-construct *(Figure 17)*.

We observed different morphological characteristics of mitochondria arrangement in the cells when we single-transfected with the mitochondrial marker. In some cells we discovered a very scattered pattern throughout the entire cell with a focus point around the nucleus, respectively nuclei. In these cells the mitochondria appeared very long and tubular. In other cells we found rather small mitochondria that were all arranged centrally around the nucleus, very closely packed.

A

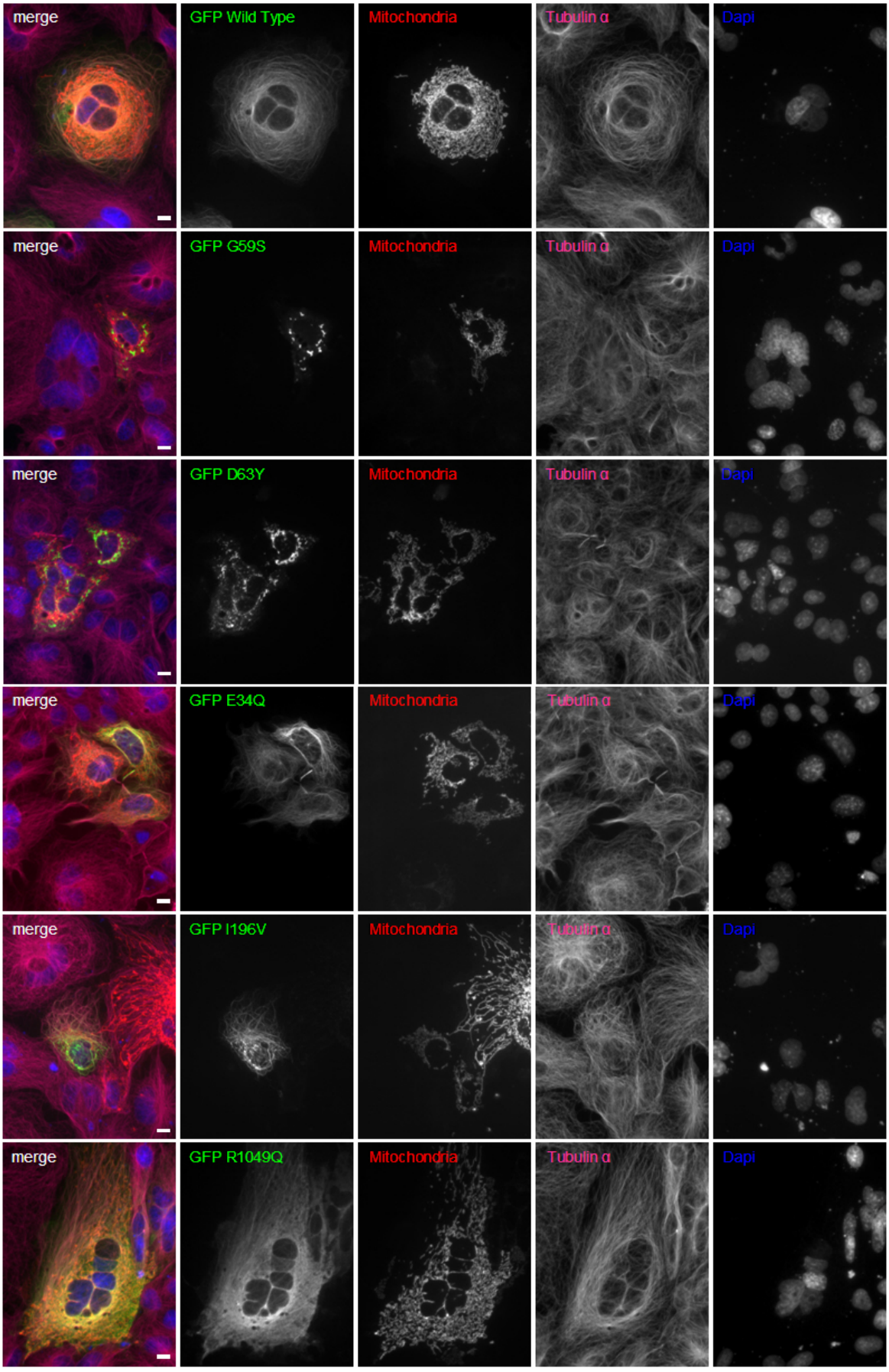
merge
GFP Wild Type
Mitochondria
Tubulin α
Dapi
merge
GFP G59S
Mitochondria
Tubulin α
Dapi
merge
GFP D63Y
Mitochondria
Tubulin α
Dapi
merge
GFP E34Q
Mitochondria
Tubulin α
Dapi
merge
GFP I196V
Mitochondria
Tubulin α
Dapi
merge
GFP R1049Q
Mitochondria
Tubulin α
Dapi

B

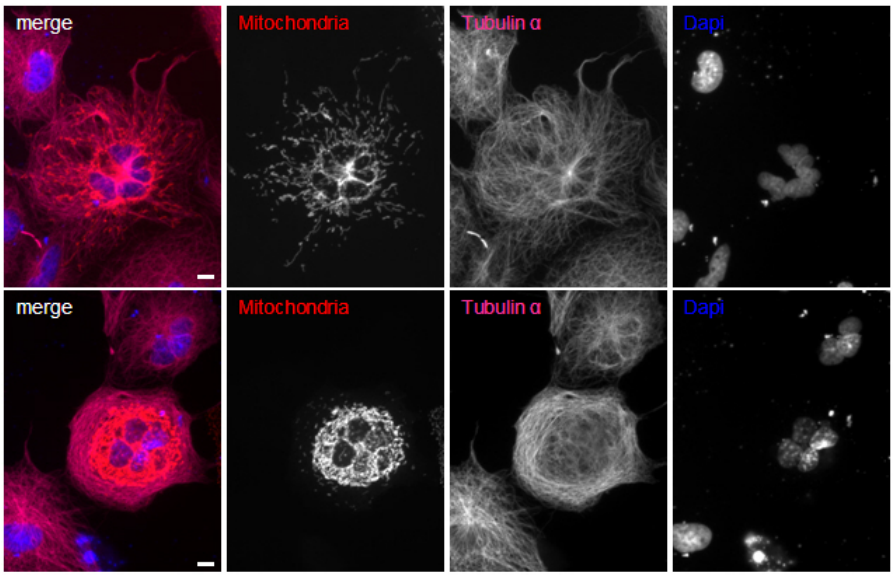

Fig. 17: Arrangement of mitochondria in p150 transfected Cos-7 cells

scale bar: 10 µm *Dapi: 4',6-diamidino-2-phenylindole*
GFP: green fluorescent protein
RFP: red fluorescent protein
Cos-7 cells are transfected with a GFP tagged p150 construct (green), co-transfected with a pTurboRFP-mito vector (red), and stained against tubulin-α (magenta). Cell nuclei are stained with Dapi (blue). (A) Cos-7 cells are co-transfected with the GFP construct (green) and the pTurboRFP-mito vector (red). (B) Cos-7 cells are single transfected with the pTurboRFP-mito vector (red). In some cells the mitochondria are distributed centrally around the nucleus, in other cells the mitochondria are spread out throughout the entire cytoplasm.

After studying the co-transfected cells, we found that the mutated protein has no impact on mitochondria morphology. We still could observe different types of mitochondria distribution, but never did we see any co-localizations of mitochondria and aggregates of mutated p150 protein. In cells transfected with mitochondrial marker and the G59S or the D63Y, which both form typical p150 aggregates, the aggregates seemed to be located next to the mitochondria and did not incorporate them.

3.4.3. Dynactin complex

Because of the structure of the whole dynactin complex, we decided to further investigate not only the p150 subunit of the complex but also other important subunits. To study the arrangement of the whole complex, we stained different subunits of the endogenous dynactin complex in the Cos-7 cells to see, whether dislocation of the p150 subunits also results in dislocation of the other subunits if the dynactin complex. We concentrated on the actin related protein, Arp1, which functions as the rod of the whole complex, dynamitin, p50, as the connecting

subunit between Arp1 and p150, and finally on p62 which participates in binding to different subunits of dynactin and other subcellular structures.

The endogenously stained Arp1 showed a filamentous distribution *(Figure 18)*.

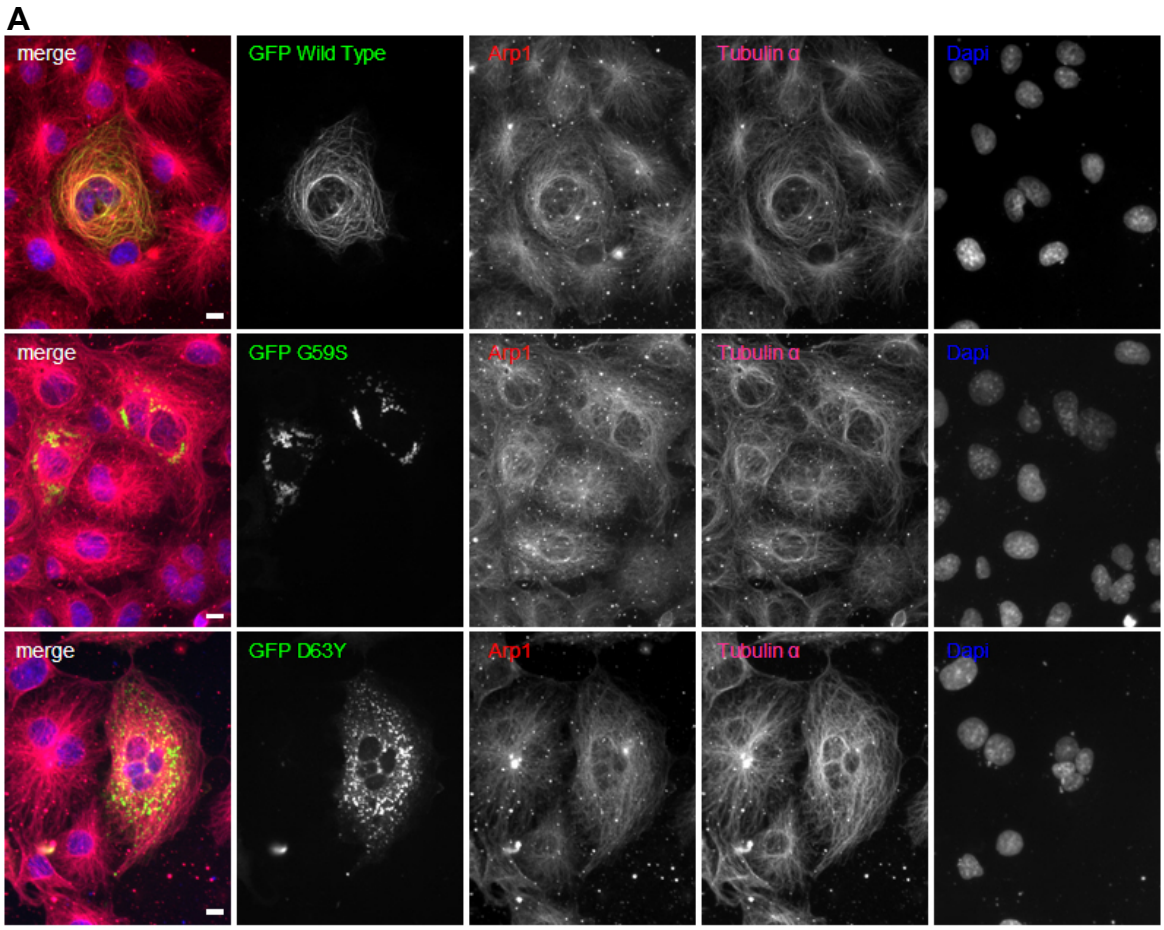

B

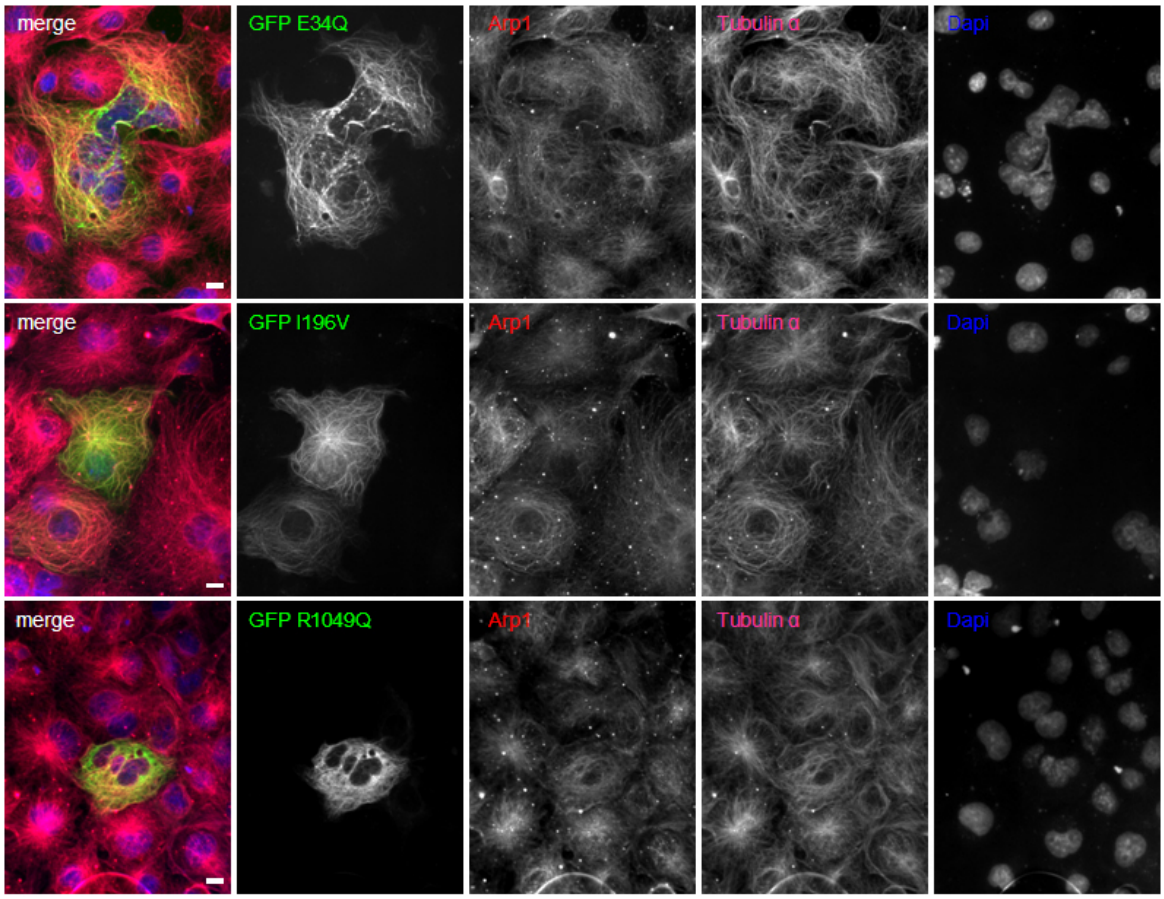

Fig. 18: Distribution of endogenous Actin related protein 1 in p150 transfected Cos-7 cells

scale bar: 10 µm *Dapi: 4',6-diamidino-2-phenylindole*
Arp1: Actin related protein 1
GFP: green fluorescent protein
Cos-7 cells are transfected with a GFP-tagged p150 construct (green) and then stained against Arp1 (red) and tubulin-α (magenta). Cell nuclei are stained with Dapi (blue). The distribution of endogenous Arp1 shows a pattern, co-localizing with filamentous structures of the tubulin-α cytoskeleton. This distribution is not affected by over expression of any of the modified proteins. (A) aggregates that are seen in G59S, D63Y do not affect the localization of Arp1. (B) Also aggregates in E34Q have no affect on ARrp1.

These detected filaments co-localized completely with tubulin-α. When the cells were transfected with the different mutated p150 constructs, there was no change detectable in the distribution of Arp1. In Wild-type transfected cells, the filaments of p150, Arp1 and tubulin-α co-localized completely. In cells transfected with the gold standard, or the D63Y mutation in which aggregates of p150 were observable, we could not detect any co-localization of p150 and Arp1. Instead the clusters were discontiguous from the Arp1 filaments. In cells transfected with the E34Q mutation we saw a co-localization of Arp1 and p150 in those parts where p150 remained filamentous, whereas the aggregated parts showed no co-localization

with Arp1. In I196V transfected cells we observed the same morphology as in wild type transfected cells. A complete co-localization of Arp1, p150, and tubulin-α could be detected with the difference of seeing much thicker filaments than in the wild type. In R1049Q transfected cells the morphology of the Arp1 did not change either. Those few fine filaments of p150 that could be observed in the R1049Q mutation co-localized with Arp1 and tubulin-α.

Dynamitin showed a very similar distribution pattern in Cos-7 cells compared to Arp1 *(Figure 19)*.

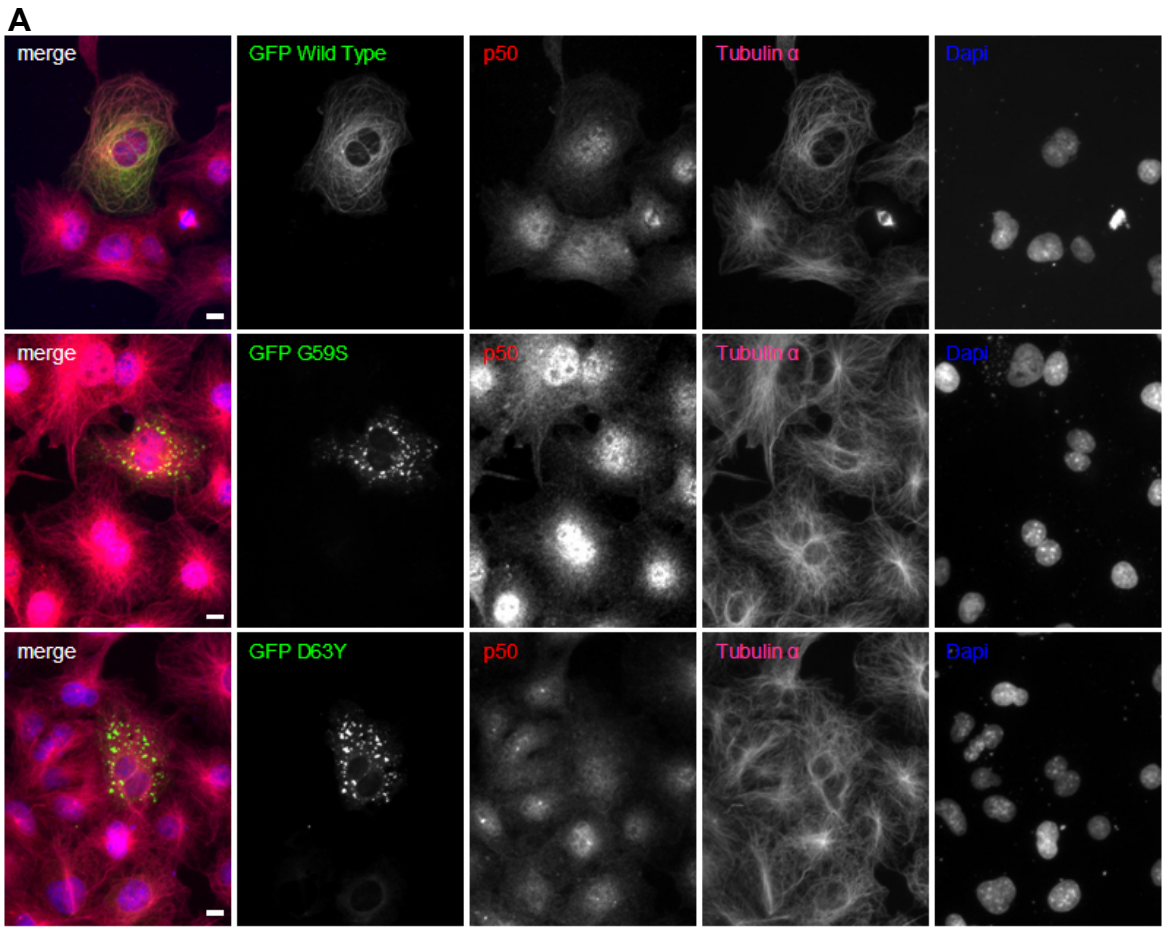

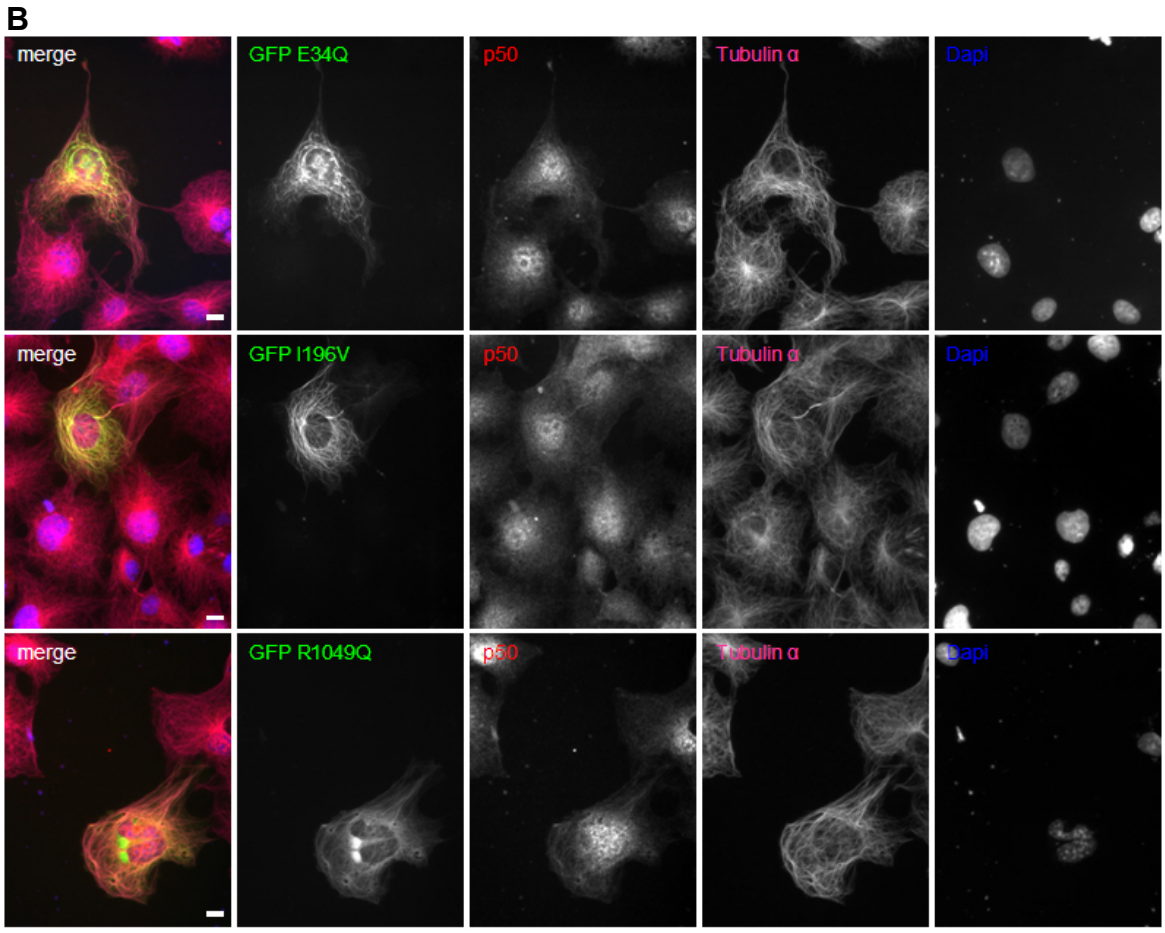

Fig. 19: Distribution of endogenous dynamitin (p50) in p150 transfected Cos-7 cells

scale bar: 10 µm *Dapi: 4',6-diamidino-2-phenylindole*
GFP: green fluorescent protein
Cos-7 cells are transfected with a GFP-tagged p150 construct (green) and then stained against p50 (red) and tubulin-α (magenta). Cell nuclei are stained with Dapi (blue). The distribution of endogenous p50 shows a pattern, co-localizing with filamentous structures of the tubulin-α cytoskeleton. This distribution is not affected by over expression of any of the modified proteins. (A) Wild type, G59S and D63Y transfected cells are shown. (B) E34Q, !96V and R1049Q tranfescted cells show no alterations of the p50 distribution.

Although the antibody bound a little bit non specific, a filamentous structure of p50 could be observed. These filaments co-localized with tubulin-α and in wild type transfected cells also with p150. Any other mutation of p150 that showed a filamentous structure co-localized also with p50. This applied to the E34Q, the I196V, and to the R1049Q to that extend to which it showed filaments. The aggregates that were observed in Cos-7 cells transfected with the G59S, the D63Y and the E34Q mutation did not co-localize with any stained protein.

The same morphological characteristics that were described for Arp1 and p50 applied also to p62 *(Figure 20)*. The staining revealed a filamentous pattern of the endogenous p62 that co-localized with tubulin-α and wild type as well as any

filament showing p150 mutation. Any aggregates of mutated over-expressed p150 were detached from any filamentous structure and showed no co-localization with p62.

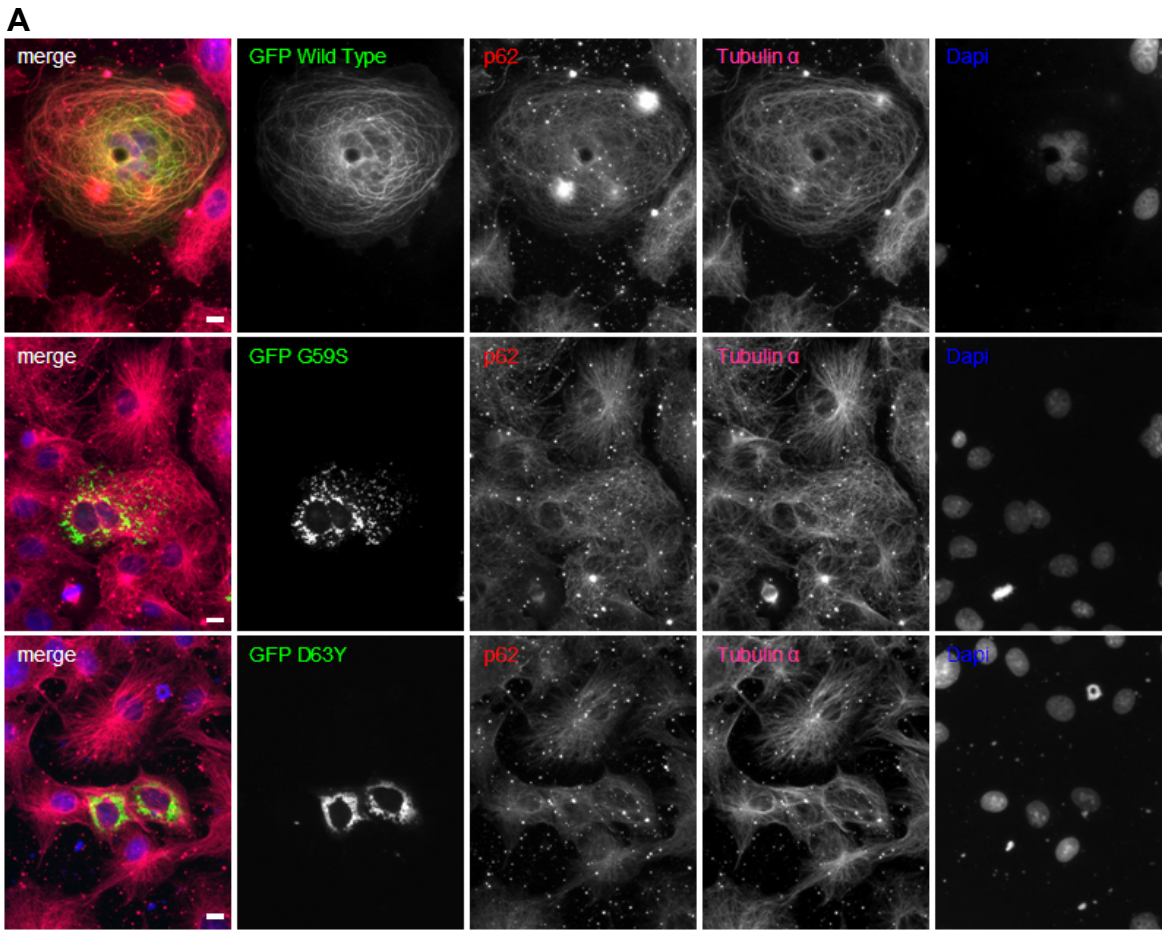

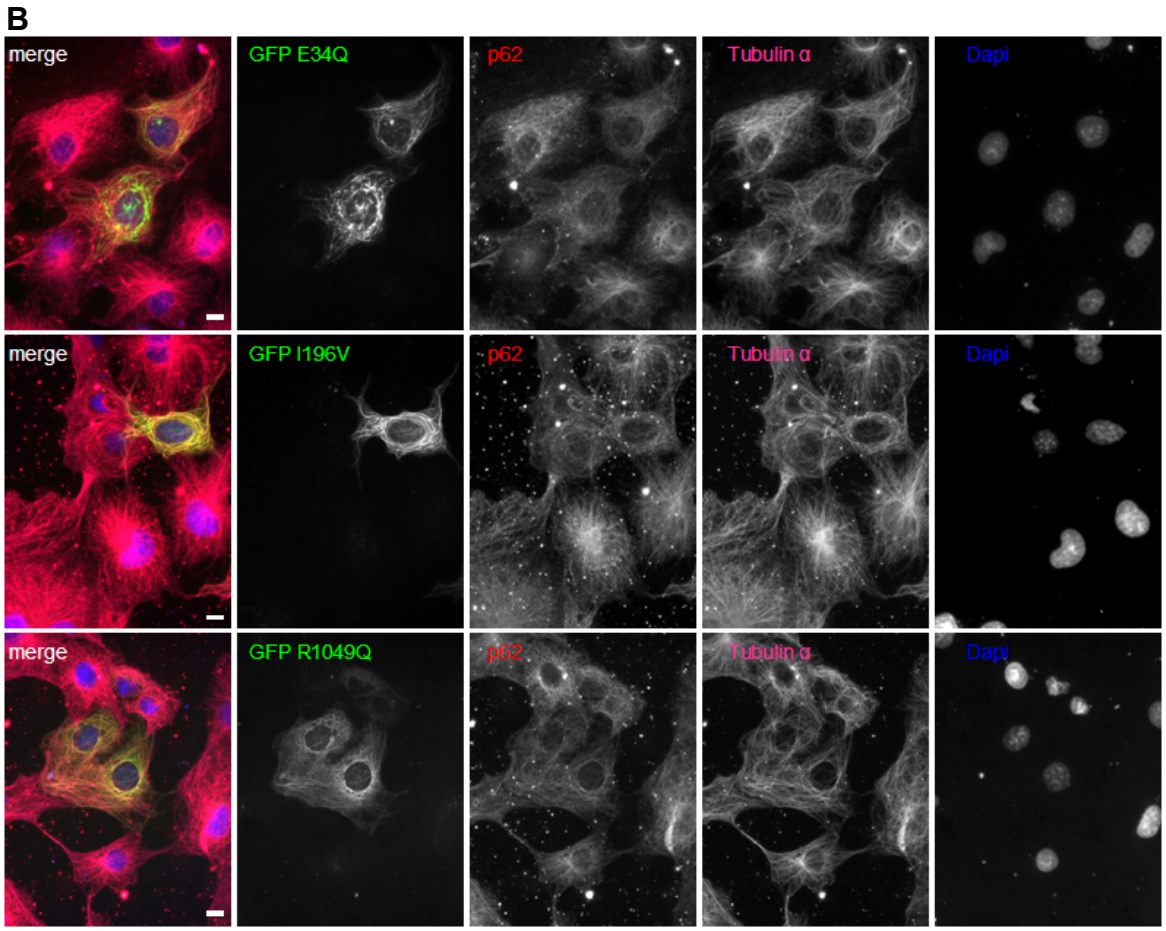

Fig. 20: Distribution of endogenous p62 in p150 transfected Cos-7 cells

scale bar: 10 µm *Dapi: 4',6-diamidino-2-phenylindole*
GFP: green fluorescent protein
Cos-7 cells are transfected with a GFP-tagged p150 construct (green) and then stained against p62 (red) and tubulin-α (magenta). Cell nuclei are stained with Dapi (blue). The distribution of endogenous p62 shows a pattern, co-localizing with the filamentous structures of the tubulin-α cytoskeleton. This distribution is not affected by over expression of any of the modified proteins. (A) The aggregates that are seen in G59S and D63Y do not affect the localization of p62. (B) The aggregates seen in E34Q also have no affect on the localization of p62.

3.4.4. Dynein complex

Since the dynactin complex is the most important factor for dynein mediated movement in the cell, we were interested in the effect the mutations of p150 might have on the interaction between these two transport molecules. Cytoplasmic dynein consists of two heavy chains, two 74 kDa intermediate chains, four light intermediate chains and several light chains. We were especially interested in the heavy chains because of their function of binding to the microtubules and the intermediate chains, which are known to bind to p150 directly. On that account we started to perform morphological studies at first to get to know how the dynein

subunits are distributed in the cell and if the mutated p150 alters the normal arrangement. We performed immunecytochemistry on GFP p150 transfected cells and looked for the dynein heavy chain *(Figure 21)*. The endogenous dynein heavy chain showed a filamentous pattern that co-localized with tubulin-α stainings. The wild type transfected cells also showed a filamentous pattern of p150 and therefore p150 and dynein heavy chain co-localized as well.

The co-localization could be observed for any filamentous structures in the different p150 mutations. So this co-localization was detected in the E34Q mutation in those areas where p150 showed a filamentous distribution, in the I196V mutation and very slightly in the R1049Q mutation with the very few fine filaments that were detectable.

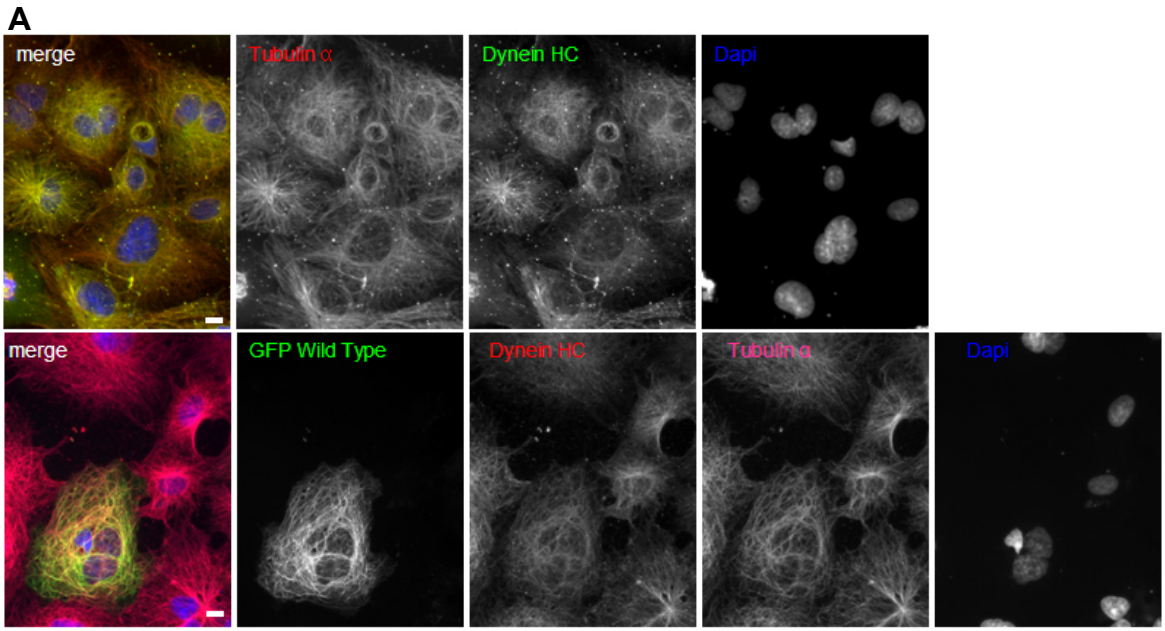

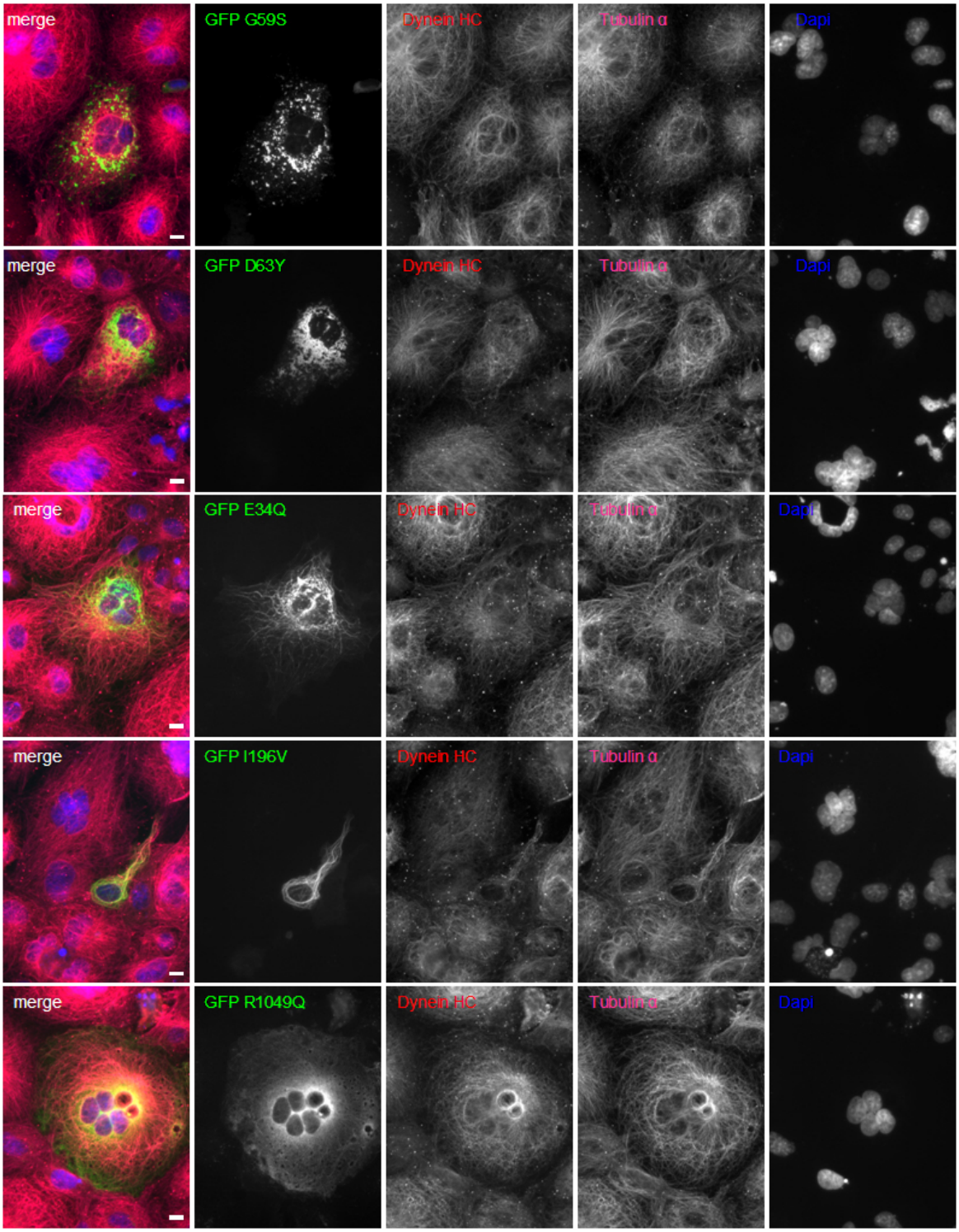

Fig. 21: Distribution of endogenous dynein heavy chain (HC) in p150 transfected Cos-7 cells

scale bar: 10 µm *Dapi: 4',6-diamidino-2-phenylindole*
GFP: green fluorescent protein
Cos-7 cells are transfected with a GFP-tagged p150 construct (green) and stained against dynein HC (red) and tubulin-α (magenta). Cell nuclei are stained with Dapi (blue). The distribution of endogenous dynein HC shows a pattern, co-localizing with the filamentous structures of the tubulin-α cytoskeleton. This distribution is not affected by over expression of any of the modified proteins. (A) Untransfected and wild type transfected cells. (B) Cells transfected with the different mutations.

No co-localization of p150 and dynein heavy chain could be demonstrated for any p150 aggregates. This was true for the gold standard G59S, the D63Y mutation and for those aggregates that could be seen in the E34Q mutation.

A surprisingly different result could be presented for the dynein intermediate chain *(Figure 22)*.

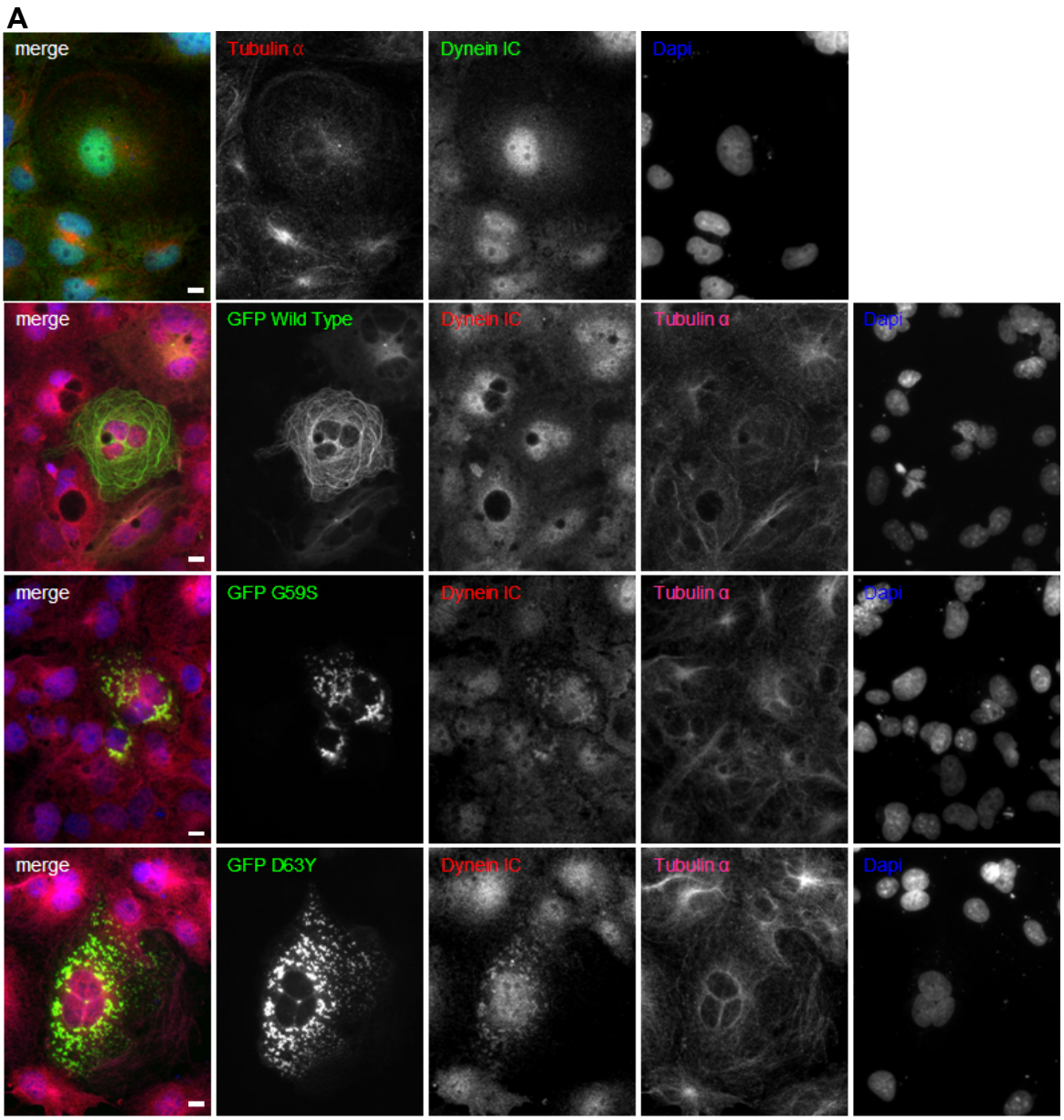

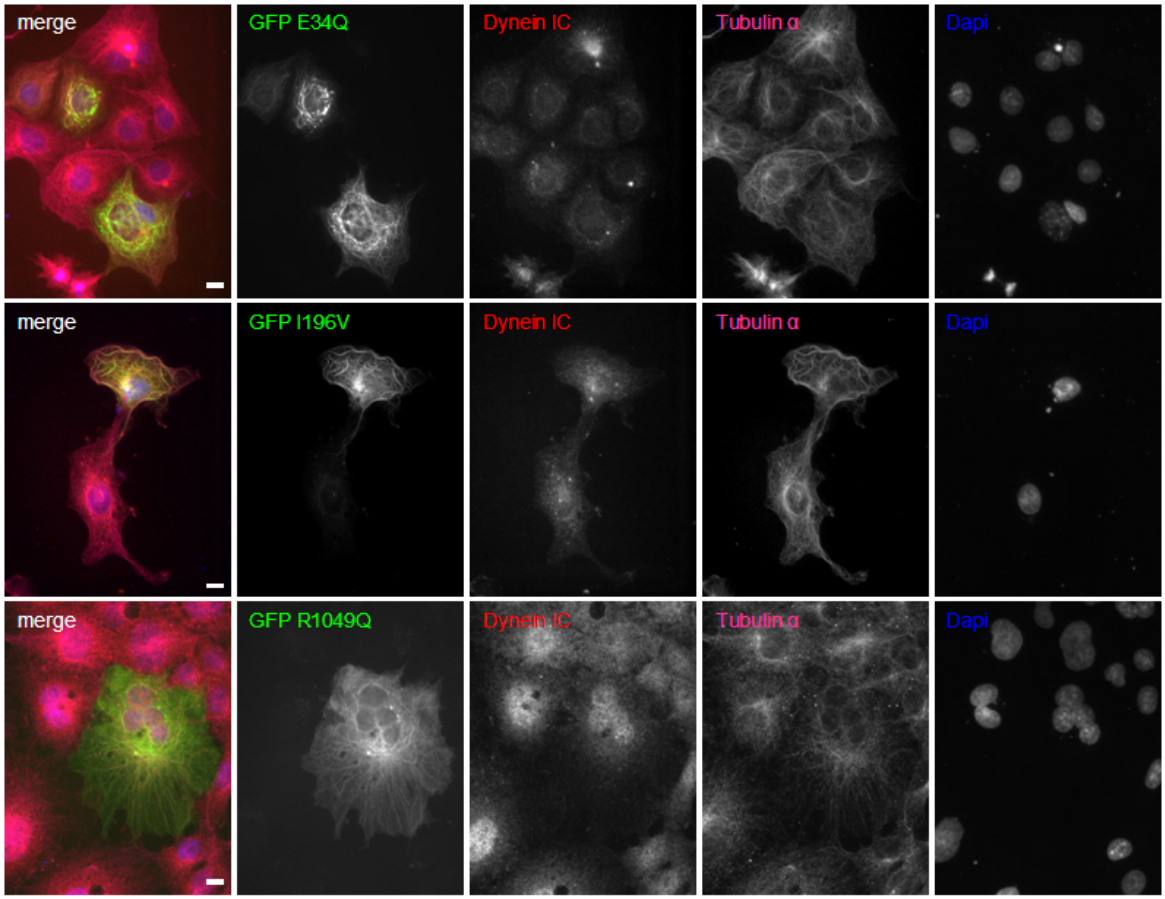
merge
GFP E34Q
Dynein IC
Tubulin α
Dapi
merge
GFP I196V
Dynein IC
Tubulin α
Dapi
merge
GFP R1049Q
Dynein IC
Tubulin α
Dapi

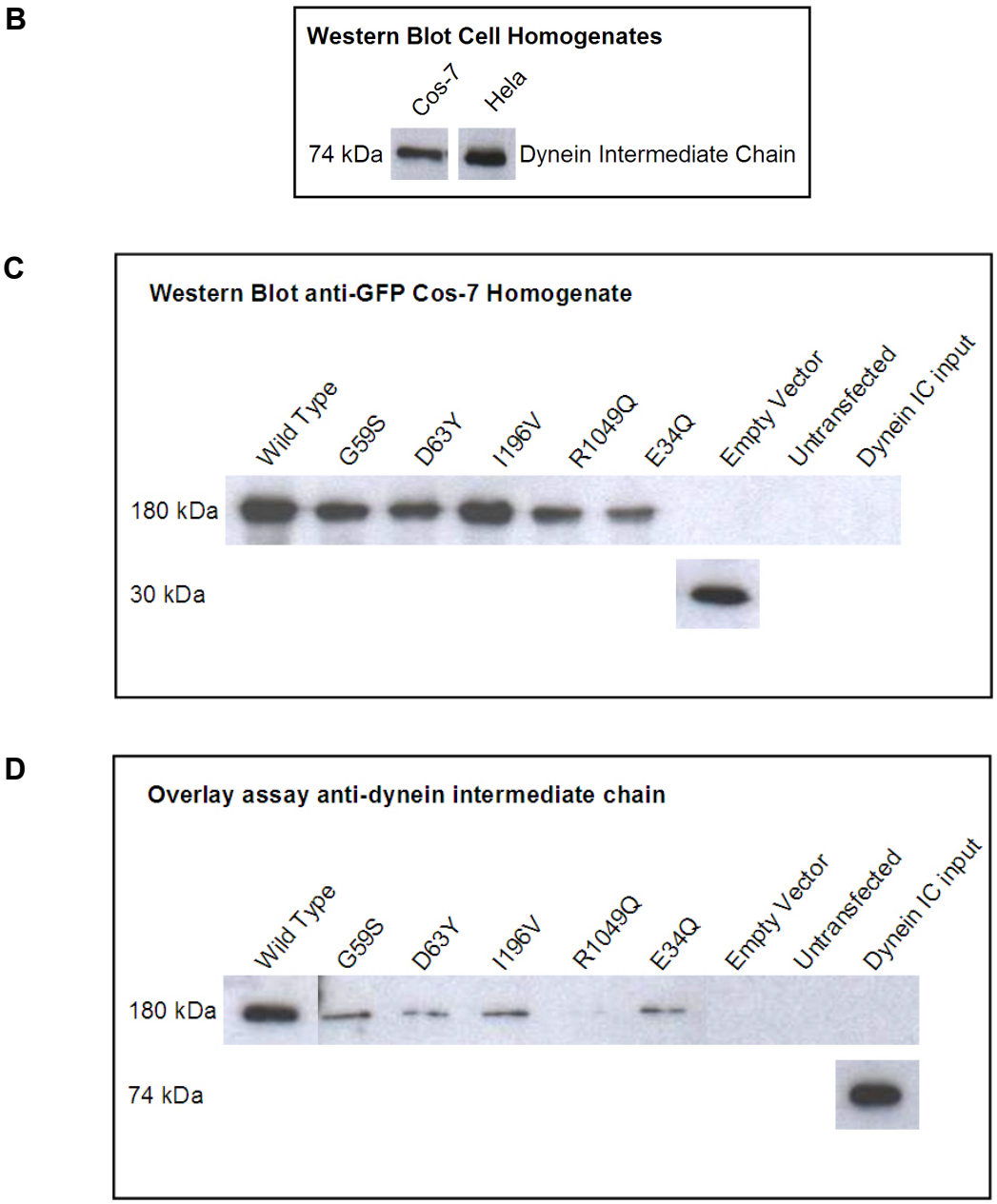

Fig. 22: Distribution of endogenous cytoplasmic dynein intermediate chain (IC) in p150 transfected Cos-7 cells

scale bar: 10 µm *Dapi: 4',6-diamidino-2-phenylindole*
GFP: green fluorescent protein
HeLa cells : Henriette Lacks cells
kDa: kilo Dalton
Cos-7 cells are transfected with a GFP-tagged p150 construct (green) and then stained against dynein intermediate chain (red) and tubulin-α (magenta). Cell nuclei are stained with Dapi (blue). (A) The distribution of endogenous cytoplasmic dynein IC shows an evenly dispersed pattern throughout the cytoplasm in p150 wild type transfected cells. In p150 G59S and D63Y transfected cells, the cytoplasmic dynein IC is not evenly distributed in the cytoplasm but is centralized in the aggregates that are formed by the modified p150. (B) Western blot anti dynein IC shows the expression of dynein IC in Cos-7 and HeLa cells (C) Western blot anti GFP shows the transfection success in Cos-7 cells, which were transfected with p150 wild type, G59S, D63Y, E34Q, I196V, R1049Q and the empty GFP vector. (D) The overlay assay was performed with HeLa cell lysate, which contains the endogenous dynein intermediate chain. The blot was then stained against cytoplasmic dynein intermediate chain. The dynein IC input was obtained from an immunoprecipitation anti dynein IC from HeLa cell lysate.

Unlike the dynein heavy chain, the intermediate chain did not show a filamentous pattern in the cell. It was distributed rather in an amorphous structure. Transfection of the cells with wild type p150 did not change the distribution of dynein intermediate chain and no co-localization of p150 and dynein intermediate chain could be observed. When we transfected the cells with the gold standard G59S or the D63Y mutation, the picture changed completely. We could then observe a complete re-localization of dynein intermediate chain and found a co-localization of the aggregates of p150 and dynein intermediate chain. This phenomenon could not be detected for the aggregates in the E34Q mutation though. In these cells the distribution pattern of dynein intermediate chain rather resembled the pattern in wild type transfected cells. For cells transfected with the 196V and the R1049Q mutation we could not find any co-localization of p150 and dynein intermediate chain either. The distribution pattern of dynein intermediate chain resembled very much that one in wild type transfected cells.

Now that we had discovered this very strong co-localization of dynein intermediate chain with the aggregates of p150 of the G59S and the D63Y mutation, we wanted to investigate the binding ability of p150 and dynein intermediate chain on a more functional level. For that reason we performed an overlay assay using Cos-7 cell lysates from cells transfected with the different p150 constructs and cell lysates from HeLa cells for the endogenous dynein intermediate chain as the binding partner. Before we started this investigation we needed to know if the protein level of dynein intermediate chain is comparable in both cell types. Therefore we performed a Western blot analysis and showed that dynein intermediate chain could be detected in both cell types in a comparable fashion. Before we could move on with the overlay assay we showed in a Western blot that the transfection level of all the constructs is at a similar level. The wild type and the I196V transfection levels are a little higher than the remaining constructs. For controls we also used the GFP empty vector and untransfected cells and performed a blot anti GFP.

Performing the overlay assay, we saw a very peculiar result. It appeared that a binding between the p150 constructs and dynein intermediate chain could be detected for wild type p150, the gold standard G59S and all the other mutations. Only the binding ability of p150 with the R1049Q mutation and dynein intermediate chain seemed to be altered although a comparable transfection level had been

shown for the R1049Q too. No band could be detected on the lane used for the R1049Q construct.

3.4.5. Other risk factor or disease causing candidate proteins

Several other cellular proteins have been suggested as candidate genes for provoking or contributing to the cause of ALS. Two of them are the TAR DNA binding protein-43 (TDP43) and the fused in sarcoma/ translated in liposarcoma protein (FUS/TLS).

We wanted to find out if the mutations in p150 can lead to an altered distribution of these proteins in the cell or if any other conspicuity could be evoked. Both of the proteins are usually localized primarily to the nucleus. To study the morphological characteristics, we used immunecytochemistry in p150 transfected cells *(Figure 23)*.

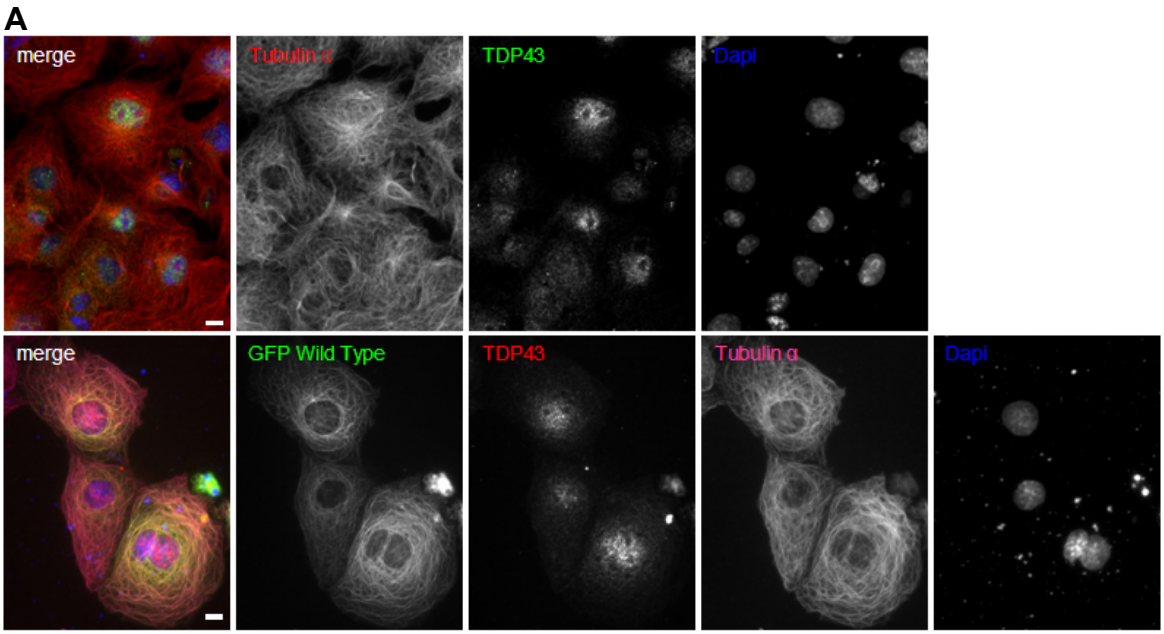

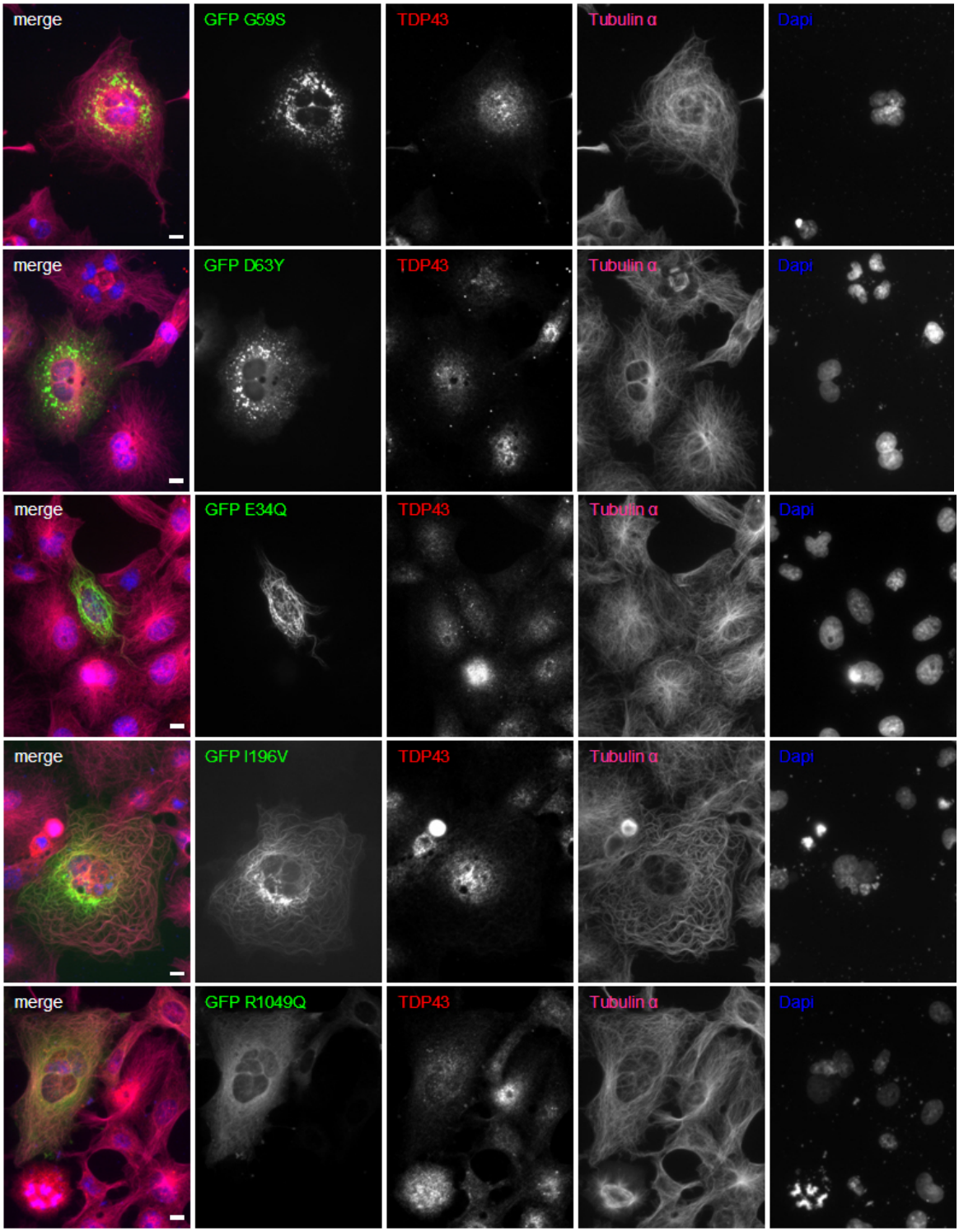

Fig 23: Distribution of endogenous TDP43 in p150-transfected Cos-7 cells.

scale bar: 10 µm *Dapi: 4',6-diamidino-2-phenylindole*
GFP: green fluorescent protein
TDP43: transactive responsive (TAR) DNA binding protein
(A) untransfected Cos-7 and wild type transfected cells are stained for TDP34. (B) Cos-7 cells are transfected with a GFP-tagged p150 construct (green) and then stained against TDP43 (red) and tubulin-α (magenta). Cell nuclei are stained with Dapi (blue). The distribution of the TDP43 is mainly nuclear. This distribution is not affected by over expression of any of the modified p150 proteins.

We also had a look at untransfected cells and found a mainly nuclear localization of TD43 in Cos-7 cells but also a faint distribution of TDP43 around the nucleus. Comparing this arrangement with transfected cells, we could not find any differences between untransfected and p150 transfected cells. Neither did we see an alteration in wild-type p150 transfected cells, nor in any cells transfected with one of the mutations. TDP43 in all cases presented with a nuclear localization with an additional arrangement around the nuclear area. There was also no co-localization observable of TDP43 and any inclusions of p150.

We then focused on FUS and found a very similar result *(Figure 24)*. Immunecytochemistry of FUS in untransfected Cos-7 cells presented a clear nuclear distribution of FUS, sparing the nucleoli. When comparing this to transfected cells, we could not find any deviations from the distribution in untransfected cells. No transfection of Cos-7 cell with wild type or mutated p150 could change the localization of FUS in the cells. We could also not observe any co-localization of FUS and aggregations of mutated p150 in the gold standard mutation, the D63Y mutation, or the E34Q mutation.

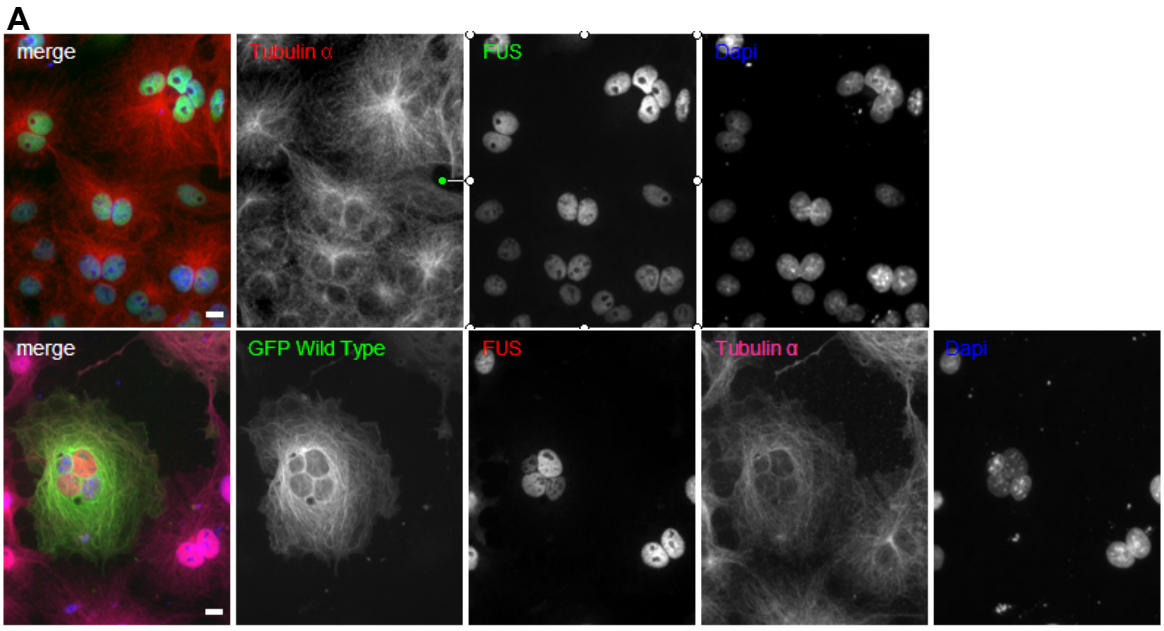

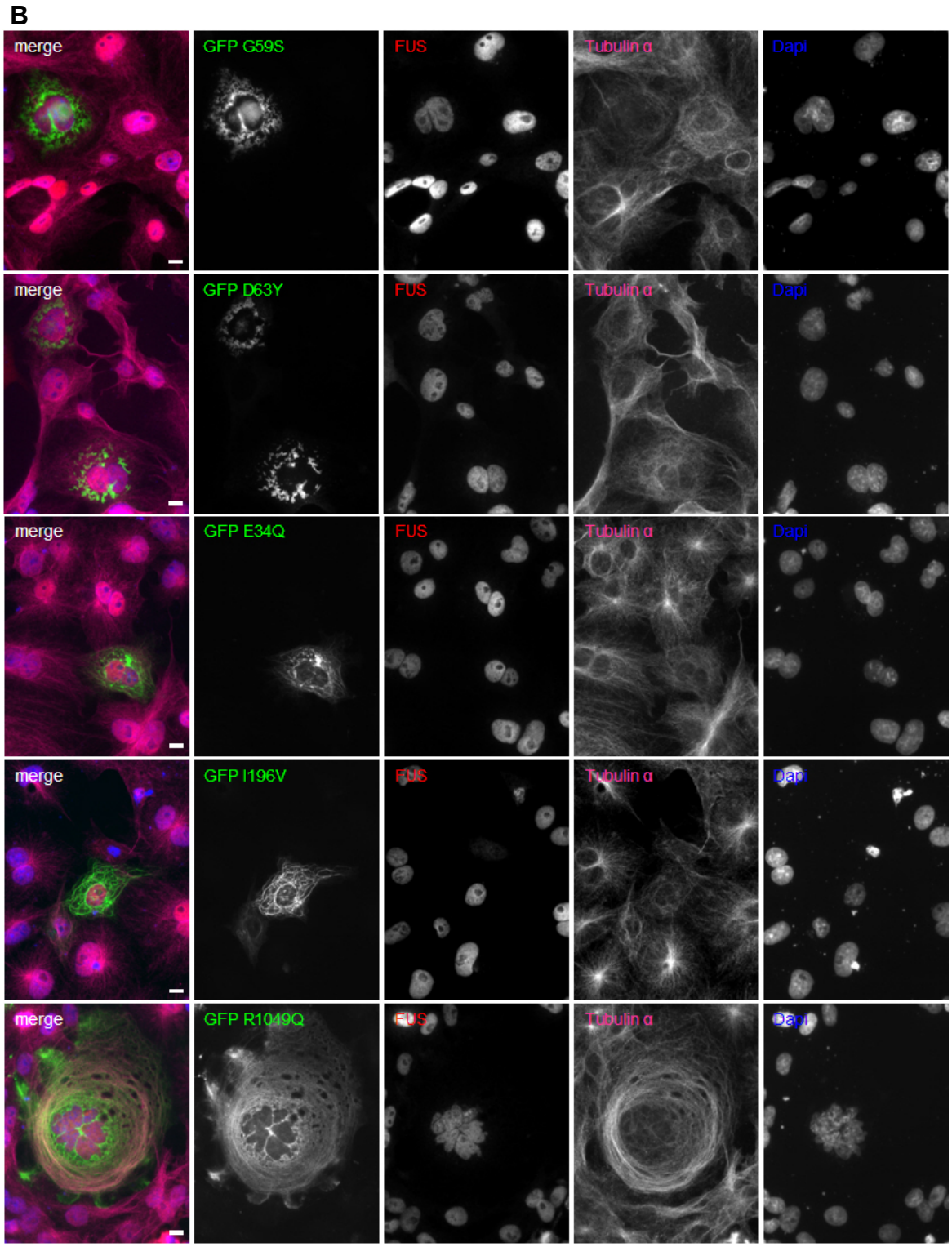

Fig. 24: Distribution of endogenous FUS in p150-transfected Cos-7 cells

scale bar: 10 µm *Dapi: 4',6-diamidino-2-phenylindole*
FUS: fused in liposarcoma
GFP: green fluorescent protein
(A) Untransfected and wild type transfected Cos-7 cells are stained for FUS. (B) Cos-7 cells are transfected with a GFP-tagged p150 construct (green) and then stained against FUS (red) and tubulin-α (magenta). Cell nuclei are stained with Dapi (blue). The distribution of the FUS protein is restricted to the cell nuclei. This distribution is not affected by over expression of any of the modified p150 proteins.

3.5. Transgenic mouse models

On the basis of our morphological studies in different cell systems of four different mutations in the p150 subunit of dynactin, we decided to further investigate the relevance of two mutations in an in vivo model in mice. For these studies, we decided for the D63Y and the I196V mutation because of several reasons. The D63Y looked especially interesting to us because of its location in the Cap-Gly domain of p150 and because of its very close location to the gold standard G59S mutation. In transfection studies it had presented with an astonishing similar phenotype to the G59S mutation, showing the same large inclusions of aggregated p150 in the cytoplasm with no co-localization to the microtubules either.

The I196V on the other hand had no phenotypical similarities with the G59S. No inclusions were found in cells transfected with this mutation but instead we observed a complete co-localization with tubulins, which were remarkably thicker than in wild type transfected or untransfected cells. Furthermore, the mutation is positioned in an interesting region in the DCTN1 gene. It results in an amino acid change shortly before the dynein intermediate chain binding site.

4. Discussion

4.1. Establishment of primary motor neurons

With the establishment of primary motor neurons, we then had a cell system that could possibly mimic the pathomechanism of mutated p150 in motor neurons in vivo. The aim was to establish viable motor neuron cultures that could be used for transfection studies. Therefore, it was very important to establish a culture that reaches a high purity of motor neurons so we could study the impact of the p150 mutations in motor neurons that interact with each other and not in any neurons. Having shown that the motor neuron cultures develop into a stable synaptic interacting network (*Figure 06*), expressing different synaptic markers like synaptophysin or ProSAP2, we used the motor neurons for transfection studies. ProSAP2 is a postsynaptic scaffolding molecule [7]. We soon discovered that transfection of motor neurons worked with the procedure described in *2.2.1.2 Transfections.* But we also noticed that the transfection rate was rather low with this procedure and that transfection has a toxic effect on the culture, leading to a higher amount of dying cells. Probably, a viral transfection procedure would lead to a higher transfection rate.

4.2. Significance of four mutations in the p150 subunit of dynactin

We found that all four analysed mutations of the dynactin p150 subunit show a very distinct morphological feature. Using the G59S mutation as a gold standard because of it being a causal mutation of slowly progressive motor neuron disease, proclaimed by Puls et al. [71], we wanted to compare our findings to an example, in which aggregation of misfolded proteins can lead to motor neuron disease. We then over expressed all of the four mutations, the wild type and the G59S mutation with a GFP-labelled construct in Cos-7 cells and showed that mutations, expressing a filamentous pattern of p150, co-localized with tubulin-α and other filamentous distributed dynactin subunit proteins. These include Arp1, p50, and p62, which also co-localize with tubulins. Those mutations, which presented with a phenotype similar to the gold standard with massive accumulations of p150 showed no co-localization with any filamentous structures in the cell. On the contrary, we could show that dynein IC co-localized with the aggregates that we saw in the gold standard and the D63Y, whereas no co-localization of endogenous dynein IC was observed for the wild type or any other of the mutations. The

opposite impression was then given for the dynein heavy chain, which distributed in a filamentous pattern and therefore showed co-localization with the wild-type and all filamentous distributed mutations, but not with any aggregates.

4.3. Expression pattern of four mutations in p150 in cell lines

Transfection studies were designed to morphologically characterize the different mutations found in an ALS patient collective. Laird et al. [47] had shown that not only in transfected cell systems as shown by Levy et al. [51] but also in a transgenic mice expressing the G59S mutation in p150, massive accumulation of mutated p150 in the cytoplasm of motor neurons could be found. Based on these findings, we wanted to compare the morphological features of four other mutations affecting the p150 subunit. Of course we also included a wild type GFP-labelled p150 construct to be able to compare the distribution of endogenous p150 with the over expressed protein. Although endogenous dynactin generally has a punctate cellular localization *(Figure 09)*, over expression of GFP-labelled p150 results in the decoration of the microtubule cytoskeleton [51]. This is consistent with our findings, when we transfected Cos-7 cells with the wild type GFP-labelled p150.
We had found very distinct different phenotypes for each mutation *(Figure 10)*. Transfected cells with the G59S mutated GFP-labelled construct, which we wanted to use as gold standard, resembled very much the transfected cells with the GFP-labelled construct used by Levy et al. [51] and Dixit et al. [16]. We additionally observed cells that showed very massive inclusions, which could be due to a longer transfection period. Levy et al. [51] had speculated that the perinuclear localization of inclusions may correspond to aggresomes of misfolded protein described by Johnston et al. [35].

A patient, in whom the D63Y mutation was discovered, presented with progressive muscle atrophy with an age of onset of 62 and a following live span of 29 months, compared to the average life span of seventeen years in patients affected by the G59S mutation. Also in contrast to the G59S mutation, this case was an apparently sporadic case of ALS, for which no co-segregation could be shown. Nevertheless, morphologically, the mutation very much mimicked the cellular phenotype of the G59S mutation. We observed the same pattern of inclusions as in the G59S. These inclusions were also scattered throughout the entire cytoplasm

or concentrated perinuclear, especially after a longer transfection period. The inclusions were positive for p150 *(Figure 11)* and showed no co-localization with the microtubule cytoskeleton. This finding suggests that the D63Y mutation might behave in a very similar way to the G59S, with impaired affinity to microtubules as shown for the G59S by Levy et al. [51]. With this mutation being found in a patient that presented with different clinical features from the G59S affected patients, the question arises of how precisely the morphology in cells reflects the pathogenetic relevance. The patient carrying the D63Y mutation presented with PMA, indicating that in this case, primarily the second motor neuron is affected. Patients carrying the G59S mutation also presented with primarily lower motor neuron signs.

The morphological appearance of the E34Q mutation resembled very much the wild type but with a feature that clearly distinguishes it from the wild type though. In cells transfected with the GFP-labelled E34Q p150 mutation, we also found a very high tendency of the p150 to form protein inclusions and to aggregate. The E34Q mutation is also a non co-segregating mutation that was found in one patient and one healthy control. The patient had presented with classical ALS with an age of onset of 61 years and the duration of illness of fourteen months. The clinical signs with pseudo bulbar dysarthria, dysphagia, followed by pareses in the upper and lower extremities, represent a mixed involvement of the upper and lower motor neuron.

We detected that the E34Q mutated protein showed decoration of microtubules, as assessed by co-localization with tubulin-α. This decoration was inconsistent though, as part of the over expressed protein had a very high tendency to form inclusions in the cytoplasm, whereas a co-localization with tubulin of non aggregated protein was existent at the same time. This leads to the conclusion that the mutated protein might have a lowered affinity to the microtubules compared to the wild type and is therefore prone to aggregate. With this mutation being found in a healthy control and a higher percentage in the controls, we have to presume that this mutation is rather a contributory factor than a disease causing mutation.

The I196V mutation was a little harder to assess. This mutation had not only been found in ALS patients but in a lesser number could also be discovered in healthy controls and in a similar percentage also in neurological controls. Patients

suffering from ALS carrying this mutation presented with very heterogeneous phenotypes. Most of the patients suffered primarily from symmetrical and asymmetrical flaccid paresis of the upper or lower limbs. One patient also showed signs of parkinsonism additionally to classical signs of motor neuron disease. Neurological controls presented with MSA and PSP as well as FTD [29]. This fact indicates that mutations in p150 do not solely contribute to ALS but probably also play a role in the generation of other neurodegenerative diseases. But the pathomechanism and the coherence with motor neuron diseases still remain to be discovered.

During our decision finding process on which mutation to study further, we decided on the I196V mutation for two reasons. First of all, this mutation lies very close to the dynein intermediate chain binding site, which was particularly interesting to us, and secondly this mutation presented with such a peculiar phenotype in the transfection studies. We could show that the over expressed mutated p150 protein co-localized completely with the microtubules, detected by tubulin-α. Interestingly, the tubular structures seemed to be thickened in comparison to non transfected cells or the wild type protein. The formation of inclusions could only be detected after a very long transfection time, probably due to degradation of redundant protein amounts, as it could also be shown for the wild type *(Figure 12)*. Because of these thickened appearing tubular structures, we assumed a bundling of microtubules could appear due to a higher affinity of I196V mutated p150 to the microtubules. This probable increase in affinity needs to be proven in binding studies.

Even more puzzling was the appearance of R1049Q p150 transfected cells. This mutation had also been detected in ALS patients as well as controls. It was found in one neurological and several healthy controls. The MND patients carrying this mutation presented with ALS, as well as PLS and therefore with a mixed dominance of the upper and lower motor neuron [29]. The neurological control patient was diagnosed with PMA, another hint that p150 mutations may affect not only motor neurons, but rather contribute to a multi system disease. This mutation is located in a very different region on the p150 subunit than all the other analysed mutations. It was found in exon 26 in the second coiled coil domain. This gave us an idea of how this mutation could affect the inter subunit interaction, leading to a

destabilised dynactin complex. This hypothesis was undermined by the transfection pattern of the mutated p150 in Cos-7 cells as a bigger part of the p150 seemed to be diffusely distributed in the cell compared to the relatively small amount that showed a fine co-localization with tubulin-α. The diffusely scattered p150 pattern was never found to co-localize with any of the dynactin subunits like Arp1, p50, and p62, suggesting that the whole dynactin complex might be disrupted because of aberrant inter subunit interaction. Also for this mutation, binding studies need to be performed to show the binding ability of mutated p150 to subcellular structures like the cytoskeleton or other parts of the dynactin complex, and especially the effective motor protein dynein (Figure 22).

What was striking in the comparison of clinical features and cellular phenotypes was that in most patients the clinical features were consistent with the primary degeneration of the second motor neuron. This observation applies to patients carrying the G59S, D63Y, and most of the patients carrying the I196V mutation. Given that the second motor neuron is the executing neuron, ending in the neuromuscular end plate and covering a longer distance, the question is, whether this longer expansion may lead to a greater vulnerability of the neuron. Having to cover a longer distance, the axons of the neurons are more extensive, and therefore transport mechanisms probably take longer and maybe are even more susceptible to disturbances. Also, the question is, whether different toxic substances accumulate in the periphery in the second motor neuron compared to substances in the upper motor neuron, which could also lead to a greater vulnerability, if these substances are not being transported to their place of degradation.

4.3.1. Cellular inclusions of aggregated p150

One very striking trait of any transfected cell was that after a longer period of transfection, all cells would show aggregates of p150. This was also true for the wild type p150 construct. This observation lead to the assumption that not only the mutations, and the therewith eventual defect in the protein function, may result in the formation of inclusions. The transfection of a GFP-labelled constructs causes two side effects that need to be considered. Firstly, the recombinant protein is much higher expressed than the endogenous protein which leads to much higher amounts of recombinant protein than the natural level and secondly, the over

expressed protein carries a GFP-tag, which itself is a non-endogenous protein, regardless of its small size. To take these effects into consideration, we compared two different transfection periods with regard to the amount of cells that showed some form of aggregated protein *(Figure 12)*. This experiment revealed that the formation of aggregates is time dependent, meaning that after sixteen hours of transfection in all mutations and the wild type a higher amount of cells displaying aggregates could be detected than after six hours. But this result was not uniformly applicable, as in some mutations the percental increase differed a lot from others. In the wild type the percental increase amounted 19 %. A very similar result with a percental increase of 18 % was seen only in the I196V. The R1049Q and the E34Q transfected cells showed a much higher increase of 38 % respectively 48 %, whereas the G59S and D63Y transfected cells, which had presented with a percentage of 100 % alternatively 96 % after six hours only showed an increase of 0 % and 4 %, since the percentage of cells showing aggregates had been so high from the beginning on. These results implicate that any transfected construct, which leads to over expression of the p150 protein, results in the formation of clustered protein aggregates because of the unnatural high amount of the protein. But regarding the exact percentages of the different constructs, it is obvious that the formation of aggregates is a specific trait of the G59S and D63Y mutated proteins, as cells transfected with these constructs exhibit a rate of nearly 100 % even after a very short transfection time. The assumption of formation of aggregates being a specific characteristic of these mutations is also undermined by the observation that in these cells a decoration of microtubules has never been seen, so the existence of functionally intact protein is very doubtful. However, for E34Q and R1049Q transfected cells, another explanation has to be found. Since a percental increase of about 19 % seems to be the normal rate for over expressed p150, as this is the rate observed in wild type transfected cells, the E34Q and the R1049Q showed a higher rate of aggregation formation. The E34Q presented with 13 % of cells with aggregates after six hours and 61 % after sixteen hours with an increase of 48 %. This strong increase suggests that the formation of aggregates is not only due to a normal process when over expressing p150, but also to some degree to an attempt of the cell to degrade the misfunctional protein. This process has been explained by Johnston et al. [36] as aggresome formation is a general response of cells, which

occurs when the capacity of the proteasome is exceeded by the production of aggregation-prone misfolded proteins. Since most of the inclusions of aggregated p150 are seen perinuclear, especially after longer transfection periods, this explanation could be applicable to these transfection studies. In R1049Q transfected cells, the morphological characteristic of over expressed p150 is the diffuse amorphous pattern with some fine filamentous structures. Nevertheless, the formation of aggregates could also be observed in R1049Q transfected cells. After six hours the percentage resembled very much the wild type transfected cells with 4 % of cells with aggregates. After sixteen hours of transfection a relatively higher amount of cells with aggregates, compared to the wild type, was found with a percentage of 38 % as compared to 19 % in the wild type. This leads to the assumption that the R1049Q mutation results in a defect in the protein, which induces intensified accumulation and aggregation of the protein. This could be due to the disruption of the dynactin complex, because of the mutation being positioned in the coiled coil domain II, that is most important for inter subunit interactions. Disengaged p150 could therefore be dispersed amorphously in the cell, not being able to bind to its interacting subunits and after a while aggregate, forming visible inclusions in the cytoplasm.

The results seen in I196V transfected cells mirror nearly the percentages seen in wild type transfected cells so it suggests itself that the aggregates seen in these cells result from normal over expression and are not subject of some functional defect. We would rather suggest an increased binding affinity to microtubules as we have observed thickened filaments that suggest the bundling of microtubules as described above.

Johnston et al. [35] have suggested a mechanism of formation of an aggresome, the perinuclear accumulation of misfolded proteins, when the cellular degradation pathway is overwhelmed. To further investigate what the inclusions exactly consist of, where they are located and if they are being degraded by the cell, one should consider checking the aggregates for being ubiquitinated by the means of Western blots or immunecytochemistry. Furthermore, the existence of autophagosomes should be tested and if the proteasome is localized or trapped in the inclusions. Another interesting feature would be how the Golgi apparatus reacts, as the main processing and packaging apparatus of proteins, after over expressing the different p150 mutated proteins.

4.4. Comparability of the expression in primary motor neurons

The aim was to asses, whether the morphological characteristics of each mutation were comparable reproducible in another cell system, in primary motor neurons. The motor neurons are more likely to reflect the impact of the mutations in a better comparable fashion to the actual process in motor neurons of affected people.

Therefore, we over expressed the different mutated forms of p150 as well as wild type p150 as a GFP-labelled protein in the motor neurons by means of transfection.

The transfection pattern of p150 resembled very much the pattern in Cos-7 cells. Since Cos-7 cells display no extended cell processes, we had the chance to analyse, if the neurites would be affected in a different way than the cell body. In contrary to previous studies by Laird et al. [47], Levy et al. [51], or Puls et al. [71], we could show that the inclusions of G59S mutated p150 were not only be detectable in the cell body of the motor neurons but were also located in the neurites *(Figure 14).* The same applied to the D63Y mutation, in which we also detected typical inclusions in the extended processes of motor neurons. Since the transport along microtubules is mediated by cytoplasmic dynein and its enhancer dynactin, defects in either one of the proteins may lead to a defect in the transport process. Therefore it is presumable that especially in the neurites, where transport needs to be performed over a long distance, non functional p150 protein may accumulate and form visible aggregates.

Transfection patterns of the other mutated protein constructs could also be reconstructed in the primary motor neuron cell system. In The E34Q transfected motor neurons a filamentous pattern co-localizing with tubulin together with some aggregates could be detected. The I196V transfected cells displayed thickened appearing filaments just as in Cos-7 cells and also the R1049Q showed a similar pattern to what had been observed in Cos-7 cells, a diffuse pattern of p150 with some filaments co-localizing with tubulins. All these observations lead to the conclusion that the transfection patterns observed in Cos-7 cells were not specific to this cell system but must be actual traits of the mutations. Therefore, the results seen in Cos-7 cells can be directly compared to any results found in transfection studies with primary motor neurons.

4.5. The effect of p150 mutations on the cytoskeleton and important organelles

The cytoskeleton is composed of the three major components, the microfilaments particularly actin, the intermediate filaments and the microtubules [11]. All three elements play an important role in the structural support, in maintaining the cell shape, and provide the main component for intracellular transport and cell division. The cytoskeleton remains dynamic, allowing the cell to grow or change in size and shape over time.

Thus, we studied all three components of the cytoskeleton regarding the impact of the mutated p150 on the cytoskeletal set up. In addition to their structural roles, both microtubules and actin filaments function as active tracks for directed motility within the cell [50].

4.5.1. Microtubules

We observed a decoration of microtubules, as assessed by co-localization with tubulin-α for the wild type p150 transfected cells. As described earlier, endogenous p150 is distributed in a punctate pattern in the entire cell, but shows co-localization with microtubules when it is over expressed. This co-localization could be detected for all mutations that showed morphological features of filamentous distribution of p150 *(Figure 10)*. For any aggregates of p150, no co-localization with the microtubule cytoskeleton was observable, indicating the loss of function of protein as Levy et al. [51] had described for the G59S mutation. Levy et al. [51] had suggested a model for the G59S p150 mediated cell death, which describes the mechanism by which the mutation causes a loss and at the same time toxic gain of function of p150. The mutation is said to cause impaired microtubule binding, which then leads to disrupted dynein/dynactin-based transport. Additionally, misfolding of the Cap-Gly domain is caused by the G59S mutation which causes aberrant self-association and aggregation. This gain of function may induce further impairment in minus end directed transport, either by physical blockage caused by the aggregates, or by sequestration of trapped dynein and dynactin. Since the D63Y mutation is morphologically not distinguishable from the G59S and is located so closely to the gold standard in the Cap-Gly domain, we assume that the same pathomechanism is applicable also to this mutation. The morphology of the E34Q mutation however is not easily explicable with this model as some

characteristics still resemble the wild type with partly decorated microtubules. Therefore, we assume that the microtubule binding ability might only be slightly affected and only a little amount of the misfolded protein aggregates.

The I196V mutation showed complete decoration of microtubules with no protein aggregation. Since the filaments in this mutation appeared thickened compared to wild type transfected cells or untransfected cells, we hypothesized that the binding of I196V mutated p150 might be increased and that bundling of the microtubules appears because of the aggravated binding ability of p150. This hypothesis needs to be confirmed in microtubule binding studies.

The impact, which the R1049Q mutation had on the cells, was not comparable with any of the other mutations. The mutated p150 was diffusely distributed in the cytoplasm and additionally, a faint decoration of the microtubules could be detected. Based on this observation, we assumed that the microtubule binding ability could be also reduced in this mutation and the p150 then redistributes in the cell. After a longer period of transfection, the formation of aggregates could also be detected in cells transfected with the R1049Q mutated protein consistent with the view that misfunctional protein aggregates and forms inclusions in the cytoplasm.

4.5.2. Actin filaments

The actin cytoskeleton, which is mainly responsible for short distance movements, provides the tracks for another cellular motor protein, myosin. Since the dynein/dynactin complex operates independently from the actin cytoskeleton, it is not remarkable that the actin filaments seemed not to be affected by over expression of any of the mutated p150 proteins compared to wild type or untransfected cells *(Figure 15).*

4.5.3. Intermediate filaments

Intermediate filaments serve primarily to provide structural stabilisation to the cell and in neuronal cells neurofilaments, which are the neuronal specific intermediate filaments, help to regulate the radial growth of axons [11].

Johnston et al. [36] had described that aggresome formation, an aggregation of misfolded multi-ubiquitinated protein, is accompanied by redistribution of the

intermediate filament protein vimentin, which forms a cage surrounding the aggresome.

We observed that there was a redistribution of the intermediate filaments in Cos-7 cells after transfection of p150 mutated constructs *(Figure 16 vimentin)*. This redistribution was mainly found in the G59S and D63Y p150 transfected cells, in which large cytoplasmic inclusions of aggregated p150 could be observed. We saw a circular rearrangement of vimentin, enclosing the nucleus and partly the inclusions but never did we see the complete caging of all aggregates. Therefore, we suppose that not all aggregates of misfolded protein are being transported to the perinuclear aggresome, as the defective dynein/dynactin motor is not capable of carrying all aggregates to the cell centre. In those cells, transfected with D63Y p150, which display small scattered inclusions, we did not see a rearrangement of intermediate filaments. This observation suggests that the rearrangement only appears after a true compilation of an aggresome, probably in a time dependent manner. In wild type and other mutated p150 transfected cells, we did not observe a redistribution of vimentin, but saw an arrangement that resembled that seen in untransfected cells. So the p150 mutations besides the D63Y and the G59S did not interfere with the arrangement of intermediate filaments in the cell.

4.5.4. Mitochondria

Mitochondria are one of several organelle types that are transported by the dynein/dynactin motor. Levy et al. [51] had shown that mitochondria are associated with inclusions of aggregated p150. They found mitochondria within and surrounding the G59S p150 positive inclusions. They had also demonstrated that mitochondria in cells transfected with G59S p150 were less widely distributed than in cells transfected with wild type protein assuming that loss of dynein/dynactin transport causes mitochondrial mislocalization and mitochondria can not be transported to the cell periphery because of aberrant interaction with the aggregated G59S p150. We could not reinforce these observations. We also looked at untransfected cells and found that there are different distribution patterns of mitochondria in Cos-7 cells. In some cells mitochondria were loosely distributed in the entire cell with long tubular mitochondria, in other cells we saw a concentration of densely packed mitochondria focused around the perinuclear region, leaving out the periphery of the cell completely *(Figure 17)*. When we then

transfected the cells with the different mutations, we also saw the mitochondria differently distributed in the cytoplasm. In wild type protein transfected cells the mitochondria were relatively evenly distributed among the cell with a lower density in the cell periphery, whereas in G59S and D63Y p150 transfected cells, the mitochondria were distributed also in the cell periphery, mingled with the aggregations, but not co-localizing with them, meaning not being entrapped in the inclusions. The distribution of mitochondria resembled very much the one seen in wild type protein transfected cells in E34Q and R1049Q p150 transfected cells. In I196V p150 transfected cells, we saw a mitochondrial distribution that resembled very much the untransfected cells which displayed their mitochondria perinuclear.
Because of our results we could not clearly argue that mitochondrial dispersion is affected by the mutations as it is very variable in untransfected cells as well. To draw a conclusion if mitochondrial transport and therefore distribution is affected one would have to perform for example life cell imaging studies to measure the movement distance and velocity of mitochondria along neuronal axons.

4.6. The effect of p150 mutations on the dynein/dynactin complex

As previously shown by Johnston et al. [35], cytoplasmic dynein exhibits a diffuse, somewhat punctate distribution throughout the cytoplasm of untransfected cells. We found the same pattern for the cytoplasmic dynein intermediate chain in Cos-7 cells *(Figure 22A)*.
Johnston et al. [35] have also shown that cytoplasmic dynein is present in the so called aggresome. Comparing this to our finding of co-localization of dynein intermediate chain with the aggregates of G59S and D63Y mutated p150, we find a very similar result. The observed redistribution of dynein into the aggresomes may reflect an increase net retrograde transport of dynein attached to the misfolded substrate, in this case to p150. Johnston et al. [35] further suggest that dynein present in aggresomes could reflect a change in steady state distribution of dynein as a result of an increase flux of misfolded protein to the aggresome, rather than dynein itself becoming a substrate of the aggresome pathway. This theory would imply that dynein could still function properly without or just very little functional dynactin at its help as dynactin p150 in this case is the transported substrate itself.
To detect, whether the binding ability of p150 to the dynein intermediate chain might be altered by any of the mutations, we had performed immunoprecipitations

with a subsequent overlay assay *(Figure 22B)*. We found that the binding did not seem to be altered with the exception of the R1049Q mutation. In this mutation the binding to the dynein intermediate chain was not detectable. In the transfection studies, we had not noticed a strong conspicuity for the R1049Q, as the dynein intermediate chain was distributed in a punctate pattern that did not seem to co-localize with wild type p150 or any other non aggregating mutation and behaved in the same way in R1049Q p150 transfected cells. The experiment was very hard to repeat because very often no bands at all would show, regardless of the quantity of precipitated GFP-tagged p150. Demonstrated by Vaughan et al. [90], who had also performed overlay assays, the binding ability of the dynein intermediate chain to p150 is regulated by phosphorylation of the serine residue in position 84 in the dynein intermediate chain. We assumed that our trouble repeating the overlay experiment could have been impacted by the phenomenon of the p150 not being able to bind to phosphorylated dynein intermediate chains.

In contrast to the work by Laird et al. [47] on a transgenic mouse model with the G59S mutation, we could not show that other parts of the dynactin complex like p50 or Arp1 were found in the inclusions. What we did find was the dynein intermediate chain in the inclusions as described above but never did we see the heavy chain co-localizing with any protein aggregations. The dynein heavy chain distribution was not affected by any mutation of p150. It co-localized with the microtubules as assessed by tubulin-α stainings. We did not see any co-localization of p150 aggregates and dynein heavy chain, suggesting that the dynein complex is disrupted by the G59S, D63Y and partly the E34Q p150 mutation as the dynein intermediate chain co-localized with the aggregates of p150. This finding implicates even more that dynein/dynactin function is impaired by the mutations. As described above, we also found no co-localization of other dynactin subunits with the p150 aggregates, which leads to the conclusion that only the misfolded part of dynactin, namely p150, forms the cytoplasmic inclusions.

Expression levels are very likely to be tightly regulated in the cell. Both depletion and over expression of p150 may be predicted to have a negative effect on axonal transport and cellular trafficking. Therefore, mutations that alter the expression level of this protein may be considered as a potential risk factor for motor neuron disease. While the ALS associated mutations, I196V did not noticeably affect

protein stability or protein aggregation, these aspects may be as important as direct disturbances in binding domains within p150.

As expression levels of by means of transfection over expressed proteins are generally very much higher than the endogenous protein levels, one has to be very careful with drawing direct conclusions from effects the over expression might have on the cell in regards to the pathomechanism of motor neuron disease. Therefore, it would be wise to down regulate the expression level of the protein by using for example viral transfections, which results in better transfection rates and better comparable expression levels of the protein. Furthermore, the GFP-tag of the recombinant protein might also impact the cellular degradative pathways, so one could use other vectors without a GFP-tag, which then entails that the over expressed construct would have to be stained to make it visible.

4.7. The effect of p150 mutations on nuclear proteins

Several other cellular proteins have been suggested to be capable of causing or at least contributing to the development of ALS. Two of these are FUS and TDP-43, both nuclear proteins that are engaged in regulating the transcription process [88]. Several studies of cases of ALS in which cytoplasmic FUS and TDP-43 positive inclusions were found, have been performed [64, 88]. Mutations in FUS and TDP-43 have been suggested to be causative for ALS [45, 85]. Recently, it has also been shown by Wils et al. [97] that TDP-43 mutations in mice can cause ALS and frontotemporal lobar degeneration (FTLD).

Because of these findings, we wanted to investigate, whether the p150 mutations may be connected with pathology in FUS and TDP-43. We wanted to find out, whether the p150 mutations have an impact on the localization and distribution of those two proteins. Therefore, we over expressed the wild type and different mutated p150 constructs in Cos-7 cells and studied the distribution of FUS and TDP-43 by immunecytochemistry *(Figure 23 and 24)*. We found that none of the p150 mutations have an effect of either one of the proteins. The distribution remains nuclear just as in untransfected cells. Hence, we supposed that the malfunctions due to p150 mutations and defects in TDP43 and FUS do not have interrelated pathways, and that mutations in either p150 or in the nuclear transcription regulating proteins contribute in a different manner to the development of ALS.

4.8. Transgenic mouse models

The generation and characterization of transgenic mouse models was not subject of my thesis and was performed in the laboratory of Prof. PhD Philip Wong, Department of Neuroscience, Johns Hopkins University of Baltimore, Maryland. We have got evidence that so far the I196V p150 transgenic mice present with a neurological phenotype. Therefore, this mutation gains more importance, suggesting that it could be a causative mutation for neurodegeneration.

4.9. Conclusions

ALS is a disease, which manifests most prominently in the degeneration of motor neurons, although it is regarded as a multisystem disease [82]. Given all different cases of sporadic but also familial ALS, not one single gene or one single causative factor could be delineated that leads to motor neuron disease. Especially when we look at all the different factors including genetic factors, oxidative stress, excitotoxicity, protein aggregation and damage to transport processes that have been suggested to cause or to contribute to the development of ALS, one has to conclude that the primary pathogenic processes underlying ALS are very likely to be multifactorial. In this thesis we tried to ponder on which role dynactin, especially four different mutations in its microtubule binding p150 subunit, might play in the manifestation of ALS. Dynactin being the protein that provides a further docking site for many dynein cargoes and that enhances the processivity of the dynein motor, we hypothesized that mutations in dynactin can contribute to a disruption of normal dynein function.

Disruption of cellular transport is implicated in multiple neurodegenerative diseases. Neurons are especially vulnerable to impaired transport mechanisms, as long range movement is absolutely necessary along its extended processes, namely axons and dendrites. In axons, the microtubules are aligned in one direction with the minus end directed towards the cell body and the plus end towards the periphery, whereas in dendrites the microtubule arrangement is alternated with some microtubules directing their minus end towards the nucleus and some towards the periphery, so a mixed polarity is found in dendrites [11]. This cytoskeletal set up leads to a unidirectional movement of the dynein motor towards the cell body, making it a retrograde transport in the axon. Neurons, especially motor neurons with their uniquely long axons, depend on axonal

transport for their cell homeostasis, as well as communication between the cell body and periphery. Dynein, in cooperation with its enhancer dynactin, is the major motor driving retrograde axonal transport. This function makes it so important, as various cargoes have to be transported along the axon towards the cell centre. These cargoes include neurotrophic factors, injury signals, organelles like mitochondria and endosomes, RNA granules, neurofilaments, and many others.

Some of the most critical cargoes, that the dynein/dynactin complex has to transport in neurons, are the various neurotrophic factors and signalling factors. Neuronal differentiation and survival depends on transport of trophic factors from the periphery to the cell body [11]. Neurotrophic factors such as nerve growth factor (NGF), neurotrophin 3 (NT-3), neurotrophin 4 (NT-4), and brain derived neurotrophic factor (BDNF) bind to membrane associated receptors and after internalisation are actively transported via dynein/dynactin to the cell body to elicit their full cellular response [11]. Heerssen et al. [28] showed that the inhibition of dynein transport blocks neurotrophin-stimulated survival of cultured neurons, consistent with a critical role for active retrograde transport in the maintenance of healthy neurons. The dynein/dynactin motor is also responsible for injury signalling as signals from the injury site must be transported to the cell body. The activated microtubule associated protein (MAP) kinase extracellular signal-regulated kinase (Erk) is also retrogradely transported by dynein [68]. After cell injury, local protein expression is involved in axon regeneration. For this expression, RNA particles need to be transported to the place of need, which is performed by dynein mediated transport. Many of the mRNAs localized within axons encode cytoskeletal proteins including β-actin, tau, and neurofilament subunits and vimentin [68]. When this task of local protein expression at the place of injury can not be performed, one can easily imagine how the neurons will have trouble regenerating and eventually degenerate.

One of the most crucial roles though of the dynein/dynactin complex might be the removal of misfolded or degraded proteins from the periphery to the cell body, where damaged proteins can be degraded in their normal pathway. This is performed by dynein by transporting vesicles to the lysosome but also by driving lysosomal motility along microtubules. Even more importantly, dynein is involved in the accumulation of misfolded proteins into aggresomes [35], perinuclear accumulations of misfunctional proteins, that are built when the degradative

machinery of the cell is overwhelmed. One can argue whether the formation of aggresomes may have a cyto-protective function as suggested by Taylor et al. [86], or if these massive aggregations of defective misfolded proteins may lead to the overstraining of the proteasome, causing the accumulation of even more defective proteins including others that would underlie the normal cellular degradative pathway.

Impaired axonal transport by disruption of the dynein/dynactin complex can lead to the clumping of neurofilaments [48]. Aggregation of neurofilaments is a common marker of neurodegenerative disease, as neurofilaments are one of many cargoes of the dynein/dynactin complex [93]. The aggregation of neurofilaments has been observed by Lai et al. [46] and Laird et al. [47] in heterozygous p150 G59S knock in mice as a result of inhibition of normal dynein/dynactin function.

Furthermore, dynein's function is to retrogradely transport mitochondria along the axon to the cell body, mainly for degradation purposes. But several studies indicate that mitochondria are distributed preferentially to areas with high metabolic demands [60], suggesting that mitochondria need to be redistributed, which is performed by kinesin, the anterograde motor, and dynein alike. Mitochondria are not only the most important energy supply of the cell but also play an important role by meeting cellular metabolic demands, maintaining Ca^{2+} homeostasis, and regulating apoptosis. Therefore, mitochondrial dysfunction by mislocalization can contribute to excitotoxicity and oxidative stress. These mechanisms have also been implicated in several neurodegenerative diseases, including ALS [57].

But the dynein/dynactin complex is not only required for long distance axonal transport, but functions in many essential cellular processes including ER to Golgi trafficking, endosome and lysosome motility, and spindle assembly. Therefore, the impairment of cytoplasmic trafficking processes would lead to an even wider range of misfunctions in the cell that could affect the degradative pathways and the metabolic function.

The progressive accumulation of intracellular membrane vesicles in motor neurons of mutant G59S p150 mice, as described by Laird et al. [47], is consistent with the view that mutant dynactin p150 causes aberrant membrane trafficking leading to the "poisoning" of the bidirectional transport of vesicles between the ER and Golgi

apparatus within motor neurons. Such membrane trafficking have been shown to involve dynein/dynactin mediated transport Lee et al. [49].

Translocation from the cytoplasm to the nucleus of the nuclear factor kappa B (NF-κB) after stimulation has also been shown by Shrum et al. [84] to be dependent on the dynein/dynactin complex. NF-κB is a transcription factor that is essential for physiological processes ranging from innate and adaptive immunity to learning and memory. Both disruption of dynactin by over expression of dynamitin, and loss of endogenous dynein by knockdown, using short hairpin RNA (shRNA), lead to the inhibition of NF-κB translocation [84].

Various lines of evidence support the idea that dysfunction of the dynein operation can lead to neuronal misfunction and cell death. In Cramping (Cra1) and Legs at odd angle (Loa) mice, point mutations in the dynein heavy chain lead to a neurodegenerative phenotype [27]. But Dupuis et al. [17] could disprove that Cra1 transgenic mice display a motor neuron disease phenotype but rather a sensory neuropathy due to a degeneration of sensory neurons associated with a loss of muscle spindles. As described by La Monte et al. [48], also disruption of the association of dynein with dynactin by over expression of dynamitin results in progressive neurodegeneration in mice. This disruption is a graded function of the expression levels of dynamitin [77].

The question is what the relative contribution of loss of normal dynein/dynactin function and toxic gain of function, due to protein misfolding and aggregation may be to the primary pathogenesis. It is probably a combination of both mechanisms, as one contributes to the other. Aggregation of misfunctional proteins along the microtubule tracks can lead to a mechanic blockage and therefore inhibit transport capacity. On the other hand, the loss of normal dynein/dynactin transport function can result in the aggregation of misfolded proteins, closing the vicious circle.

Given all the above mentioned functions of the dynein/dynactin complex, in which these proteins play a fundamental role, one clearly has to argue that the pathomechanism of ALS with mutations in p150 has to be connected to the misfunction of dynein/dynactin dependent transport.

The G59S mutation in the DCTN1 gene encoding the dynactin p150 subunit results in motor neuron degeneration. Affected patients develop adult onset vocal fold paralysis, facial weakness, and distal limb muscle weakness and atrophy and

it was shown that the mutation results in the selective loss or motor neurons [71]. Levy et al. [51] have suggested the following pathomechanism for the G59S mutation. Three intersecting pathways are proposed to cause motor neuron toxicity followed by cell death. Since the mutation causes impaired microtubule binding, the dynein/dynactin based transport is disrupted. Additionally, the mutation results in misfolding of the Cap-Gly domain, which in response leads to aberrant self-association and the large proportion of unbound p150, along with the high expression levels of the p150 in neurons, leads to a high cytosolic concentration of misfolded mutant protein. This protein proportion forms aggregates, which may induce further impairment in axonal transport by physical blockage or by sequestration of dynein and dynactin, finally leading to motor neuron specific degeneration.

The D63Y mutation presented with a very similar cellular phenotype to the G59S. Therefore, we assume that the pathomechanism could be the same as for the G59S, impairing the retrograde axonal transport by mechanical blockage and the formation of large scale aggregates. This impaired transport brings all different problems to the cell, which then lacks trophic factors, evacuation of toxic products to the cell centre, mislocalization of mitochondria and many more as explicated above.

The defects caused by the E34Q mutation are probably subject to a similar mechanism, but to a lesser extend. We could not show the complete loss of microtubule decoration. Therefore, E34Q has to be considered rather as a contributory than a causative factor for ALS, given also the fact that this E34Q mutation has been discovered in a healthy control as well.

The pathomechanism underlying the I196V mutation might be even more complicated. The I196V mutation has not only been detected in ALS patients but also in neurological, as well as healthy controls. This fact leads to the idea that this mutation is also a contributory factor to the development of ALS. The potential increased binding ability of p150 to the microtubules could lead to an aberrant microtubule bundling, which is consistent with the thickened filaments seen in transfected cells and could negatively impact the axonal transport, decelerating the speed of the dynactin/dynein complex. This defect alone may not lead to the development of motor neuron disease, as also a number of healthy controls have been found to carry this mutation. But other unknown contributory factors could

lead to the breakdown of the axonal transport machinery causing motor neuron degeneration. Other factors could also impact on the degeneration of other cell systems, leading to parkinsonism and frontotemporal dementia as detected in neurological controls.

A similar contributory position could be accredited to the R1049Q mutation. This mutation has been detected with even a higher percentage in healthy and neurological controls as well. In overlay assays we showed that the R1049Q mutation leads to a loss of dynein intermediate chain interaction. This could be due to the disruption of the whole dynactin complex, caused by the mutation being located in the second coiled coil domain. A neurological control carrying the R1049Q mutation has been diagnosed with MSA, suggesting a somewhat related pathomechanism of ALS and parkinsonism, as MSA and PSP patients have been found to carry various different p150 mutations [29]. Vilerino-Guell et al. [92] have also identified the I196V and the R1049Q mutation in their studies and have claimed that these are non-segregating and therefore non disease causing variants of the p150 subunit. These findings are consistent with our studies, which suggest that both of these mutations are rather contributory modulating factors than primarily disease causing.

Although these four mutations might not be disease causing, as several of them have also been found in healthy controls and showed no clear peculiarities concerning loss of binding abilities, but they clearly are contributory factors to cause neuronal degeneration. The extended axons make neurons uniquely vulnerable to defects in active transport, so it is reasonable to propose that even when subtle defects are present, which not alone may cause ALS directly, they may cumulatively lead to motor neuron degeneration. One could argue that multiple insults to the neuron, of genetic and environmental nature, lingeringly add up until the final point of neurodegeneration. This could also explain the late onset of ALS. To explain how impaired retrograde transport could lead to very severe defects that are capable of leading to neurodegeneration, I will sum up the mechanisms, whose downstream effect could have such an immense impact on the neurons. A very critical role of the dynein/dynactin complex is to transport defective or damaged proteins to the cell centre for degradation. The failure to degrade those proteins could lead to an accumulation of toxic substances in the distal end of the axon.

Alternatively, another reason for degeneration and cell death could be the lack of neurotrophic factors that are not transported to the cell centre anymore, where they evoke the full necessary cellular response. Therefore essential signalling pathways are inhibited. But not only trophic factors but also protective injury signals need to be retrogradely transported to the cell centre. For example NF-κB, which is necessary for the cellular response to stress signals, is also dependent on dynein/dynactin mediated transport to the nucleus. Loss of signalling of any kind could thus lead to the activation of programmed cell death pathways or at least lead to an impaired ability of the motor neuron to recover from cellular stress.

Since the transport of organelles is likewise damaged in impaired retrograde transport, mitochondrial mislocalization could lead to mitochondrial misfunction. This in turn may lead to an abased energy supply, alter Ca^{2+} homeostasis, and activate the apoptotic pathway. In the same manner as organelles, the fusion of autophagosomes and lysosomes also depends on the active transport of dynein/dynactin along microtubules. With a disturbed function of the motor, enlarged autophagosomes accumulate and the aggregation of autophagosome substrate is enhanced [74].

Also, impaired transport of neurofilaments can lead to aggregation of filaments along the microtubule tracks and mechanically block the transport of organelles or other cargoes.

Furthermore, dynactin has been suggested to be essential in maintaining the stability of the neuromuscular junction [18]. Misfunctional dynactin could therefore destabilise the neuromuscular junction, leading to an incomplete synaptic transmission and therefore defective neuromuscular signalling.

Finally, motor neurons, which may be affected by any of the above described effects, are more likely to be susceptible to other stresses, so different effects can add up leading finally to degeneration and cell death.

Interestingly, motor neuron degeneration can also occur in patients with fronto-temporal dementia and Parkinson's disease, associated with mutations in the microtubule associated protein tau [82]. But some patients with familial fronto-temporal dementia, parkinsonism, and ALS do not have identified mutations in tau [41, 96]. This suggests that other factors or genes causing this triad remain to be identified. Another very peculiar correlation is the location of dynactin p150

mutations causing Perry syndrome. Farrer et al. [22] have described several mutations in the p150 subunit in patients with Perry syndrome that are all very closely located to the G59S mutation. Intriguingly, the ubiquitin immuno-positive inclusions resemble very much those found in patients suffering from ALS or fronto-temporal dementia but spare both motor neurons and cortical regions and instead affect the extrapyramidal system. Perry syndrome is a rapidly progressive neurodegenerative disorder with an onset between the fifth and sixth decade of life. Pathologically, Perry syndrome has been recognized as a TDP-43 proteinopathy, although the physiological relevance remains unclear [22]. Altogether, these findings suggest a somewhat related pathologic mechanism for these different neurodegenerative diseases as all present with a progressive adult onset and all of them display similar identified pathologic features like dynactin p150 mutations, ubiquitin positive cytoplasmic inclusions, and TDP-43 protein mislocalization, just to name some of them. Therefore, a combined pathway leading to neurodegeneration is possible in these different diseases. Hence, ALS should possibly be classified as a multisystem neurodegenerative disease instead of ranking it as a pure motor neuron degenerative disease.

5. Summary

Amyotrophic lateral sclerosis (ALS) is an adult onset neurodegenerative disease, which manifests in the degeneration of the upper and lower motor neuron, ultimately leading to death of a diseased person within three to five years. The pathomechanism of this disease still remains unclear, although several mechanisms have been suggested to cause the selective death of motor neurons.

Based on the observation that mutations in the dynactin p150 gene (DCTN1) can be frequently found in ALS patients after sequencing the DCTN1 gene in ALS patients and controls, this study tried to investigate the potential pathogenetic impact of this finding. We concentrated on four mutations that appeared to be more interesting than others based on morphological criteria and their position in the gene. All of them showed a very distinct phenotype. A previously described disease causing point mutation, G59S, in the cytoskeleton-associated protein, glycine-rich (Cap-Gly) domain was used as gold standard. It was shown to form large scale cytoplasmic inclusions of misfolded p150. After transfection of non-neuronal as well as primary motor neurons from rat embryos with the different mutated constructs, we concluded that there are no major differences in the distribution pattern of transfected p150 in *Cercopithecus aethiops, origin-defective SV-40* kidney fibroblasts from African green monkey (Cos-7) cells and motor neurons. The morphological hallmark consists of a time-dependent formation of cellular aggregates of p150 for all the mutations in different degrees. The D63Y mutation, being the closest to the gold standard and also located in the Cap-Gly domain, presented very similar to the G59S with the formation of aggregates even after very short transfection period. The E34Q, another mutation located in the Cap-Gly domain, also presented with the formation of aggregates but to a lesser extent and showed a simultaneous microtubular decoration. The I196V, closely located to the dynein binding site, showed thickened filamentous structures, co-localizing with microtubules. Very differently presented the R1049Q mutation, which lies in the second coiled coil domain. The transfected p150 distributed amorphously in the cells with a very faint co-localization with some microtubules.

Other dynactin subunits were not affected in their localization by the over expression of mutated p150. We also studied the cytoskeletal set up in transfected cells and found that neither the microtubules nor the actin cytoskeleton was

affected, whereas the intermediate filaments were rearranged in cells transfected with the G59S and the D63Y, forming an oval rim around perinuclear aggregates. The distribution of dynein, as the most important partner for minus end directed transport, was also investigated. We did not see any differences in the distribution compared to wild type transfected cells for the dynein heavy chain, but the dynein intermediate chain co-localized with the aggregates in G59S and D63Y transfected cells.

Based on these results, we decided to develop transgenic mouse models carrying the D63Y and the I196V mutation. We can so far report that the animals carrying the I196V mutation develop a neurological phenotype, which is currently being investigated in depth.

6. References

References

1. Askham JM, Vaughan KT, Goodson HV, Morrison EE. Evidence that an interaction between EB1 and p150(Glued) is required for the formation and maintenance of a radial microtubule array anchored at the centrosome. Mol Biol Cell 13: 3627-3645, 2002.
2. Azzouz M, Ralph GS, Storkebaum E, Walmsley LE, Mitrophanous KA, Kingsman SM, Carmeliet P, Mazarakis ND. VEGF delivery with retrogradely transported lentivector prolongs survival in a mouse ALS model. Nature 429: 413-417, 2004.
3. Banks GT, Fisher EM. Cytoplasmic dynein could be key to understanding neurodegeneration. Genome Biol 9: 214, 2008.
4. Battistini S, Giannini F, Greco G, Bibbo G, Ferrera L, Marini V, Causarano R, Casula M, Lando G, Patrosso MC, Caponnetto C, Origone P, Marocchi A, Del Corona A, Siciliano G, Carrera P, Mascia V, Giagheddu M, Carcassi C, Orru S, Garre C, Penco S. SOD1 mutations in amyotrophic lateral sclerosis. Results from a multicenter Italian study. J Neurol 252: 782-788, 2005.
5. Berrueta L, Tirnauer JS, Schuyler SC, Pellman D, Bierer BE. The APC-associated protein EB1 associates with components of the dynactin complex and cytoplasmic dynein intermediate chain. Curr Biol 9: 425-428, 1999.
6. Blangy A, Arnaud L, Nigg EA. Phosphorylation by p34cdc2 protein kinase regulates binding of the kinesin-related motor HsEg5 to the dynactin subunit p150. J Biol Chem 272: 19418-19424, 1997.
7. Boeckers TM. The postsynaptic density. Cell Tissue Res 326: 409-422, 2006.
8. Brooks BR. Natural history of ALS: symptoms, strength, pulmonary function, and disability. Neurology 47: S71-81; discussion S81-72, 1996.
9. Bu W, Su LK. Characterization of functional domains of human EB1 family proteins. J Biol Chem 278: 49721-49731, 2003.
10. Burkhardt JK, Echeverri CJ, Nilsson T, Vallee RB. Overexpression of the dynamitin (p50) subunit of the dynactin complex disrupts dynein-dependent maintenance of membrane organelle distribution. J Cell Biol 139: 469-484, 1997.

11. Chevalier-Larsen E, Holzbaur EL. Axonal transport and neurodegenerative disease. Biochim Biophys Acta 1762: 1094-1108, 2006.
12. Chevalier-Larsen ES, Wallace KE, Pennise CR, Holzbaur EL. Lysosomal proliferation and distal degeneration in motor neurons expressing the G59S mutation in the p150Glued subunit of dynactin. Hum Mol Genet 17: 1946-1955, 2008.
13. Chio A, Restagno G, Brunetti M, Ossola I, Calvo A, Mora G, Sabatelli M, Monsurro MR, Battistini S, Mandrioli J, Salvi F, Spataro R, Schymick J, Traynor BJ, La Bella V. Two Italian kindreds with familial amyotrophic lateral sclerosis due to FUS mutation. Neurobiol Aging 30: 1272-1275, 2009.
14. Culver-Hanlon TL, Lex SA, Stephens AD, Quintyne NJ, King SJ. A microtubule-binding domain in dynactin increases dynein processivity by skating along microtubules. Nat Cell Biol 8: 264-270, 2006.
15. Deacon SW, Serpinskaya AS, Vaughan PS, Lopez Fanarraga M, Vernos I, Vaughan KT, Gelfand VI. Dynactin is required for bidirectional organelle transport. J Cell Biol 160: 297-301, 2003.
16. Dixit R, Levy JR, Tokito M, Ligon LA, Holzbaur EL. Regulation of dynactin through the differential expression of p150Glued isoforms. J Biol Chem 283: 33611-33619, 2008.
17. Dupuis L, Fergani A, Braunstein KE, Eschbach J, Holl N, Rene F, Gonzalez De Aguilar JL, Zoerner B, Schwalenstocker B, Ludolph AC, Loeffler JP. Mice with a mutation in the dynein heavy chain 1 gene display sensory neuropathy but lack motor neuron disease. Exp Neurol 215: 146-152, 2009.
18. Eaton BA, Fetter RD, Davis GW. Dynactin is necessary for synapse stabilization. Neuron 34: 729-741, 2002.
19. Ebneth A, Godemann R, Stamer K, Illenberger S, Trinczek B, Mandelkow E. Overexpression of tau protein inhibits kinesin-dependent trafficking of vesicles, mitochondria, and endoplasmic reticulum: implications for Alzheimer's disease. J Cell Biol 143: 777-794, 1998.
20. Eckley DM, Gill SR, Melkonian KA, Bingham JB, Goodson HV, Heuser JE, Schroer TA. Analysis of dynactin subcomplexes reveals a novel actin-related protein associated with the arp1 minifilament pointed end. J Cell Biol 147: 307-320, 1999.

21. Engelender S, Sharp AH, Colomer V, Tokito MK, Lanahan A, Worley P, Holzbaur EL, Ross CA. Huntingtin-associated protein 1 (HAP1) interacts with the p150Glued subunit of dynactin. Hum Mol Genet 6: 2205-2212, 1997.
22. Farrer MJ, Hulihan MM, Kachergus JM, Dachsel JC, Stoessl AJ, Grantier LL, Calne S, Calne DB, Lechevalier B, Chapon F, Tsuboi Y, Yamada T, Gutmann L, Elibol B, Bhatia KP, Wider C, Vilarino-Guell C, Ross OA, Brown LA, Castanedes-Casey M, Dickson DW, Wszolek ZK. DCTN1 mutations in Perry syndrome. Nat Genet 41: 163-165, 2009.
23. Gaglio T, Dionne MA, Compton DA. Mitotic spindle poles are organized by structural and motor proteins in addition to centrosomes. J Cell Biol 138: 1055-1066, 1997.
24. Gennerich A, Carter AP, Reck-Peterson SL, Vale RD. Force-induced bidirectional stepping of cytoplasmic dynein. Cell 131: 952-965, 2007.
25. Greenway MJ, Andersen PM, Russ C, Ennis S, Cashman S, Donaghy C, Patterson V, Swingler R, Kieran D, Prehn J, Morrison KE, Green A, Acharya KR, Brown RH, Jr., Hardiman O. ANG mutations segregate with familial and 'sporadic' amyotrophic lateral sclerosis. Nat Genet 38: 411-413, 2006.
26. Habermann A, Schroer TA, Griffiths G, Burkhardt JK. Immunolocalization of cytoplasmic dynein and dynactin subunits in cultured macrophages: enrichment on early endocytic organelles. J Cell Sci 114: 229-240, 2001.
27. Hafezparast M, Klocke R, Ruhrberg C, Marquardt A, Ahmad-Annuar A, Bowen S, Lalli G, Witherden AS, Hummerich H, Nicholson S, Morgan PJ, Oozageer R, Priestley JV, Averill S, King VR, Ball S, Peters J, Toda T, Yamamoto A, Hiraoka Y, Augustin M, Korthaus D, Wattler S, Wabnitz P, Dickneite C, Lampel S, Boehme F, Peraus G, Popp A, Rudelius M, Schlegel J, Fuchs H, Hrabe de Angelis M, Schiavo G, Shima DT, Russ AP, Stumm G, Martin JE, Fisher EM. Mutations in dynein link motor neuron degeneration to defects in retrograde transport. Science 300: 808-812, 2003.
28. Heerssen HM, Pazyra MF, Segal RA. Dynein motors transport activated Trks to promote survival of target-dependent neurons. Nat Neurosci 7: 596-604, 2004.

29. Hendrich. Geno- und Phänotypische Analyse von Motoneuronpatienten mit Mutationen in der p150-Untereinheit des Dynactingens, University of Ulm, 2010.
30. Hermann A, Gastl R, Liebau S, Popa MO, Fiedler J, Boehm BO, Maisel M, Lerche H, Schwarz J, Brenner R, Storch A. Efficient generation of neural stem cell-like cells from adult human bone marrow stromal cells. J Cell Sci 117: 4411-4422, 2004.
31. Holleran EA, Ligon LA, Tokito M, Stankewich MC, Morrow JS, Holzbaur EL. beta III spectrin binds to the Arp1 subunit of dynactin. J Biol Chem 276: 36598-36605, 2001.
32. Hoogenraad CC, Akhmanova A, Howell SA, Dortland BR, De Zeeuw CI, Willemsen R, Visser P, Grosveld F, Galjart N. Mammalian Golgi-associated Bicaudal-D2 functions in the dynein-dynactin pathway by interacting with these complexes. Embo J 20: 4041-4054, 2001.
33. Hoogenraad CC, Wulf P, Schiefermeier N, Stepanova T, Galjart N, Small JV, Grosveld F, de Zeeuw CI, Akhmanova A. Bicaudal D induces selective dynein-mediated microtubule minus end-directed transport. Embo J 22: 6004-6015, 2003.
34. Jackson M, Al-Chalabi A, Enayat ZE, Chioza B, Leigh PN, Morrison KE. Copper/zinc superoxide dismutase 1 and sporadic amyotrophic lateral sclerosis: analysis of 155 cases and identification of a novel insertion mutation. Ann Neurol 42: 803-807, 1997.
35. Johnston JA, Illing ME, Kopito RR. Cytoplasmic dynein/dynactin mediates the assembly of aggresomes. Cell Motil Cytoskeleton 53: 26-38, 2002.
36. Johnston JA, Ward CL, Kopito RR. Aggresomes: a cellular response to misfolded proteins. J Cell Biol 143: 1883-1898, 1998.
37. Kabashi E, Valdmanis PN, Dion P, Spiegelman D, McConkey BJ, Vande Velde C, Bouchard JP, Lacomblez L, Pochigaeva K, Salachas F, Pradat PF, Camu W, Meininger V, Dupre N, Rouleau GA. TARDBP mutations in individuals with sporadic and familial amyotrophic lateral sclerosis. Nat Genet 40: 572-574, 2008.
38. Karki S, LaMonte B, Holzbaur EL. Characterization of the p22 subunit of dynactin reveals the localization of cytoplasmic dynein and dynactin to the midbody of dividing cells. J Cell Biol 142: 1023-1034, 1998.

39. King SJ, Brown CL, Maier KC, Quintyne NJ, Schroer TA. Analysis of the dynein-dynactin interaction in vitro and in vivo. Mol Biol Cell 14: 5089-5097, 2003.
40. King SJ, Schroer TA. Dynactin increases the processivity of the cytoplasmic dynein motor. Nat Cell Biol 2: 20-24, 2000.
41. Kowalska A, Konagaya M, Sakai M, Hashizume Y, Tabira T. Familial amyotrophic lateral sclerosis and parkinsonism-dementia complex--tauopathy without mutations in the tau gene? Folia Neuropathol 41: 59-64, 2003.
42. Krueger KA, Tsuji S, Fukuda Y, Takahashi Y, Goto J, Mitsui J, Ishiura H, Dalton JC, Miller MB, Day JW, Ranum LP. SNP haplotype mapping in a small ALS family. PLoS ONE 4: e5687, 2009.
43. Kwiatkowski TJ, Jr., Bosco DA, Leclerc AL, Tamrazian E, Vanderburg CR, Russ C, Davis A, Gilchrist J, Kasarskis EJ, Munsat T, Valdmanis P, Rouleau GA, Hosler BA, Cortelli P, de Jong PJ, Yoshinaga Y, Haines JL, Pericak-Vance MA, Yan J, Ticozzi N, Siddique T, McKenna-Yasek D, Sapp PC, Horvitz HR, Landers JE, Brown RH, Jr. Mutations in the FUS/TLS gene on chromosome 16 cause familial amyotrophic lateral sclerosis. Science 323: 1205-1208, 2009.
44. Laemmli UK. Cleavage of structural proteins during the assembly of the head of bacteriophage T4. Nature 227: 680-685, 1970.
45. Lagier-Tourenne C, Cleveland DW. Rethinking ALS: the FUS about TDP-43. Cell 136: 1001-1004, 2009.
46. Lai C, Lin X, Chandran J, Shim H, Yang WJ, Cai H. The G59S mutation in p150(glued) causes dysfunction of dynactin in mice. J Neurosci 27: 13982-13990, 2007.
47. Laird FM, Farah MH, Ackerley S, Hoke A, Maragakis N, Rothstein JD, Griffin J, Price DL, Martin LJ, Wong PC. Motor neuron disease occurring in a mutant dynactin mouse model is characterized by defects in vesicular trafficking. J Neurosci 28: 1997-2005, 2008.
48. LaMonte BH, Wallace KE, Holloway BA, Shelly SS, Ascano J, Tokito M, Van Winkle T, Howland DS, Holzbaur EL. Disruption of dynein/dynactin inhibits axonal transport in motor neurons causing late-onset progressive degeneration. Neuron 34: 715-727, 2002.

49. Lee MC, Miller EA, Goldberg J, Orci L, Schekman R. Bi-directional protein transport between the ER and Golgi. Annu Rev Cell Dev Biol 20: 87-123, 2004.
50. Levy JR, Holzbaur EL. Cytoplasmic dynein/dynactin function and dysfunction in motor neurons. Int J Dev Neurosci 24: 103-111, 2006.
51. Levy JR, Sumner CJ, Caviston JP, Tokito MK, Ranganathan S, Ligon LA, Wallace KE, LaMonte BH, Harmison GG, Puls I, Fischbeck KH, Holzbaur EL. A motor neuron disease-associated mutation in p150Glued perturbs dynactin function and induces protein aggregation. J Cell Biol 172: 733-745, 2006.
52. Li SH, Gutekunst CA, Hersch SM, Li XJ. Interaction of huntingtin-associated protein with dynactin P150Glued. J Neurosci 18: 1261-1269, 1998.
53. Liebau S, Proepper C, Schmidt T, Schoen M, Bockmann J, Boeckers TM. ProSAPiP2, a novel postsynaptic density protein that interacts with ProSAP2/Shank3. Biochem Biophys Res Commun 385: 460-465, 2009.
54. Liebau S, Propper C, Bockers T, Lehmann-Horn F, Storch A, Grissmer S, Wittekindt OH. Selective blockage of Kv1.3 and Kv3.1 channels increases neural progenitor cell proliferation. J Neurochem 99: 426-437, 2006.
55. Liebau S, Vaida B, Proepper C, Grissmer S, Storch A, Boeckers TM, Dietl P, Wittekindt OH. Formation of cellular projections in neural progenitor cells depends on SK3 channel activity. J Neurochem 101: 1338-1350, 2007.
56. Ligon LA, Shelly SS, Tokito M, Holzbaur EL. The microtubule plus-end proteins EB1 and dynactin have differential effects on microtubule polymerization. Mol Biol Cell 14: 1405-1417, 2003.
57. Manfredi G, Xu Z. Mitochondrial dysfunction and its role in motor neuron degeneration in ALS. Mitochondrion 5: 77-87, 2005.
58. Martinou JC, Le Van Thai A, Cassar G, Roubinet F, Weber MJ. Characterization of two factors enhancing choline acetyltransferase activity in cultures of purified rat motoneurons. J Neurosci 9: 3645-3656, 1989.
59. Matanis T, Akhmanova A, Wulf P, Del Nery E, Weide T, Stepanova T, Galjart N, Grosveld F, Goud B, De Zeeuw CI, Barnekow A, Hoogenraad CC. Bicaudal-D regulates COPI-independent Golgi-ER transport by recruiting the dynein-dynactin motor complex. Nat Cell Biol 4: 986-992, 2002.

60. Morris RL, Hollenbeck PJ. The regulation of bidirectional mitochondrial transport is coordinated with axonal outgrowth. J Cell Sci 104 (Pt 3): 917-927, 1993.
61. Munch C, Rosenbohm A, Sperfeld AD, Uttner I, Reske S, Krause BJ, Sedlmeier R, Meyer T, Hanemann CO, Stumm G, Ludolph AC. Heterozygous R1101K mutation of the DCTN1 gene in a family with ALS and FTD. Ann Neurol 58: 777-780, 2005.
62. Munch C, Sedlmeier R, Meyer T, Homberg V, Sperfeld AD, Kurt A, Prudlo J, Peraus G, Hanemann CO, Stumm G, Ludolph AC. Point mutations of the p150 subunit of dynactin (DCTN1) gene in ALS. Neurology 63: 724-726, 2004.
63. Murray LM, Talbot K, Gillingwater TH. Neuromuscular Synaptic Vulnerability in Motor Neuron Disease: Amyotrophic Lateral Sclerosis and Spinal Muscular Atrophy. Neuropathol Appl Neurobiol.
64. Neumann M, Sampathu DM, Kwong LK, Truax AC, Micsenyi MC, Chou TT, Bruce J, Schuck T, Grossman M, Clark CM, McCluskey LF, Miller BL, Masliah E, Mackenzie IR, Feldman H, Feiden W, Kretzschmar HA, Trojanowski JQ, Lee VM. Ubiquitinated TDP-43 in frontotemporal lobar degeneration and amyotrophic lateral sclerosis. Science 314: 130-133, 2006.
65. Nishimura AL, Mitne-Neto M, Silva HC, Richieri-Costa A, Middleton S, Cascio D, Kok F, Oliveira JR, Gillingwater T, Webb J, Skehel P, Zatz M. A mutation in the vesicle-trafficking protein VAPB causes late-onset spinal muscular atrophy and amyotrophic lateral sclerosis. Am J Hum Genet 75: 822-831, 2004.
66. Park. Roles for the dynactin complex in the glucocorticoid receptor signaling pathway. PhD thesis, The Johns Hopkins University, 2003.
67. Pasinelli P, Brown RH. Molecular biology of amyotrophic lateral sclerosis: insights from genetics. Nat Rev Neurosci 7: 710-723, 2006.
68. Perlson E, Hanz S, Ben-Yaakov K, Segal-Ruder Y, Seger R, Fainzilber M. Vimentin-dependent spatial translocation of an activated MAP kinase in injured nerve. Neuron 45: 715-726, 2005.

69. Pfister KK, Shah PR, Hummerich H, Russ A, Cotton J, Annuar AA, King SM, Fisher EM. Genetic analysis of the cytoplasmic dynein subunit families. PLoS Genet 2: e1, 2006.
70. Puls I, Jonnakuty C, LaMonte BH, Holzbaur EL, Tokito M, Mann E, Floeter MK, Bidus K, Drayna D, Oh SJ, Brown RH, Jr., Ludlow CL, Fischbeck KH. Mutant dynactin in motor neuron disease. Nat Genet 33: 455-456, 2003.
71. Puls I, Oh SJ, Sumner CJ, Wallace KE, Floeter MK, Mann EA, Kennedy WR, Wendelschafer-Crabb G, Vortmeyer A, Powers R, Finnegan K, Holzbaur EL, Fischbeck KH, Ludlow CL. Distal spinal and bulbar muscular atrophy caused by dynactin mutation. Ann Neurol 57: 687-694, 2005.
72. Quintyne NJ, Gill SR, Eckley DM, Crego CL, Compton DA, Schroer TA. Dynactin is required for microtubule anchoring at centrosomes. J Cell Biol 147: 321-334, 1999.
73. Quintyne NJ, Schroer TA. Distinct cell cycle-dependent roles for dynactin and dynein at centrosomes. J Cell Biol 159: 245-254, 2002.
74. Ravikumar B, Acevedo-Arozena A, Imarisio S, Berger Z, Vacher C, O'Kane CJ, Brown SD, Rubinsztein DC. Dynein mutations impair autophagic clearance of aggregate-prone proteins. Nat Genet 37: 771-776, 2005.
75. Riehemann K, Sorg C. Sequence homologies between four cytoskeleton-associated proteins. Trends Biochem Sci 18: 82-83, 1993.
76. Rosen DR. Mutations in Cu/Zn superoxide dismutase gene are associated with familial amyotrophic lateral sclerosis. Nature 364: 362, 1993.
77. Ross JL, Wallace K, Shuman H, Goldman YE, Holzbaur EL. Processive bidirectional motion of dynein-dynactin complexes in vitro. Nat Cell Biol 8: 562-570, 2006.
78. Rothstein JD. Current hypotheses for the underlying biology of amyotrophic lateral sclerosis. Ann Neurol 65 Suppl 1: S3-9, 2009.
79. Salina D, Bodoor K, Eckley DM, Schroer TA, Rattner JB, Burke B. Cytoplasmic dynein as a facilitator of nuclear envelope breakdown. Cell 108: 97-107, 2002.
80. Schafer DA, Gill SR, Cooper JA, Heuser JE, Schroer TA. Ultrastructural analysis of the dynactin complex: an actin-related protein is a component of a filament that resembles F-actin. J Cell Biol 126: 403-412, 1994.
81. Schroer TA. Dynactin. Annu Rev Cell Dev Biol 20: 759-779, 2004.

82. Shaw PJ. Molecular and cellular pathways of neurodegeneration in motor neurone disease. J Neurol Neurosurg Psychiatry 76: 1046-1057, 2005.
83. Short B, Preisinger C, Schaletzky J, Kopajtich R, Barr FA. The Rab6 GTPase regulates recruitment of the dynactin complex to Golgi membranes. Curr Biol 12: 1792-1795, 2002.
84. Shrum CK, Defrancisco D, Meffert MK. Stimulated nuclear translocation of NF-kappaB and shuttling differentially depend on dynein and the dynactin complex. Proc Natl Acad Sci U S A 106: 2647-2652, 2009.
85. Sreedharan J, Blair IP, Tripathi VB, Hu X, Vance C, Rogelj B, Ackerley S, Durnall JC, Williams KL, Buratti E, Baralle F, de Belleroche J, Mitchell JD, Leigh PN, Al-Chalabi A, Miller CC, Nicholson G, Shaw CE. TDP-43 mutations in familial and sporadic amyotrophic lateral sclerosis. Science 319: 1668-1672, 2008.
86. Taylor JP, Tanaka F, Robitschek J, Sandoval CM, Taye A, Markovic-Plese S, Fischbeck KH. Aggresomes protect cells by enhancing the degradation of toxic polyglutamine-containing protein. Hum Mol Genet 12: 749-757, 2003.
87. Ton CC, Hirvonen H, Miwa H, Weil MM, Monaghan P, Jordan T, van Heyningen V, Hastie ND, Meijers-Heijboer H, Drechsler M, et al. Positional cloning and characterization of a paired box- and homeobox-containing gene from the aniridia region. Cell 67: 1059-1074, 1991.
88. Vance C, Rogelj B, Hortobagyi T, De Vos KJ, Nishimura AL, Sreedharan J, Hu X, Smith B, Ruddy D, Wright P, Ganesalingam J, Williams KL, Tripathi V, Al-Saraj S, Al-Chalabi A, Leigh PN, Blair IP, Nicholson G, de Belleroche J, Gallo JM, Miller CC, Shaw CE. Mutations in FUS, an RNA processing protein, cause familial amyotrophic lateral sclerosis type 6. Science 323: 1208-1211, 2009.
89. Vandenberghe W, Van Den Bosch L, Robberecht W. Glial cells potentiate kainate-induced neuronal death in a motoneuron-enriched spinal coculture system. Brain Res 807: 1-10, 1998.
90. Vaughan PS, Leszyk JD, Vaughan KT. Cytoplasmic dynein intermediate chain phosphorylation regulates binding to dynactin. J Biol Chem 276: 26171-26179, 2001.

91. Vaughan PS, Miura P, Henderson M, Byrne B, Vaughan KT. A role for regulated binding of p150(Glued) to microtubule plus ends in organelle transport. J Cell Biol 158: 305-319, 2002.
92. Vilarino-Guell C, Wider C, Soto-Ortolaza AI, Cobb SA, Kachergus JM, Keeling BH, Dachsel JC, Hulihan MM, Dickson DW, Wszolek ZK, Uitti RJ, Graff-Radford NR, Boeve BF, Josephs KA, Miller B, Boylan KB, Gwinn K, Adler CH, Aasly JO, Hentati F, Destee A, Krygowska-Wajs A, Chartier-Harlin MC, Ross OA, Rademakers R, Farrer MJ. Characterization of DCTN1 genetic variability in neurodegeneration. Neurology 72: 2024-2028, 2009.
93. Wagner OI, Ascano J, Tokito M, Leterrier JF, Janmey PA, Holzbaur EL. The interaction of neurofilaments with the microtubule motor cytoplasmic dynein. Mol Biol Cell 15: 5092-5100, 2004.
94. Waterman-Storer CM, Karki S, Holzbaur EL. The p150Glued component of the dynactin complex binds to both microtubules and the actin-related protein centractin (Arp-1). Proc Natl Acad Sci U S A 92: 1634-1638, 1995.
95. Weisbrich A, Honnappa S, Jaussi R, Okhrimenko O, Frey D, Jelesarov I, Akhmanova A, Steinmetz MO. Structure-function relationship of CAP-Gly domains. Nat Struct Mol Biol 14: 959-967, 2007.
96. Wilhelmsen KC, Forman MS, Rosen HJ, Alving LI, Goldman J, Feiger J, Lee JV, Segall SK, Kramer JH, Lomen-Hoerth C, Rankin KP, Johnson J, Feiler HS, Weiner MW, Lee VM, Trojanowski JQ, Miller BL. 17q-linked frontotemporal dementia-amyotrophic lateral sclerosis without tau mutations with tau and alpha-synuclein inclusions. Arch Neurol 61: 398-406, 2004.
97. Wils H, Kleinberger G, Janssens J, Pereson S, Joris G, Cuijt I, Smits V, Ceuterick-de Groote C, Van Broeckhoven C, Kumar-Singh S. TDP-43 transgenic mice develop spastic paralysis and neuronal inclusions characteristic of ALS and frontotemporal lobar degeneration. Proc Natl Acad Sci U S A 107: 3858-3863.

The Acknowledgements were removed because of the obligation of secrecy

The Curriculum vitae was removed because of the obligation of secrecy

Teile dieser Dissertation wurden bereits in folgenden Fachartikeln veröffentlicht:

Stockmann M, Meyer-Ohlendorf M, Achberger K, Putz S, Demestre M, Yin H, Hendrich C, Linta L, Heinrich J, Brunner C, Proepper C,Kuh GF, Baumann B, Langer T, Schwalenstöcker B, Braunstein KE, von Arnim C, Schneuwly S, Meyer T, Wong PC, Boeckers TM,Ludolph AC, Liebau S. The dynactin p150 subunit: cell biology studies of sequence changes found in ALS/MND and Parkinsonian Syndromes. J Neural Transm. : Epub ahaed of print, 2012